早稲田大学大学院 環境・エネルギー研究科

博士学位論文

Analysis and Proposals for Advance of Automobile Air Conditioning System from the Perspective of Energy Saving and Thermal Comfort

車載用パーソナルエアコンの省エネルギー性と快適性側面からの分析と提案

2013 年 12 月

曾	楊
ZENG	YANG

早稲田大学大学院 環境・エネルギー研究科

博士学位論文

Analysis and Proposals for Advance of Automobile Air Conditioning System from the Perspective of Energy Saving and Thermal Comfort

車載用パーソナルエアコンの省エネルギー性と快適性側面からの分析と提案

早稲田大学大学院 環境・エネルギー研究科

環境・新エネルギー研究

2013 年 12 月

曾	楊
ZENG	YANG

ABSTRACT

Automobile has been seen a rapid increase over the past years and has been becoming a necessary transport tool in the modern society. However, the increase of automobiles gives us a lot of problems including energy shortage. Therefore, with the development of technology, the energy saving has been taken into account in the design of automobile. In term of automobile air conditioning system, the low-energy consumption and high comfort has been required increasingly by consumers. This project aims to force the function of air conditioning systems to provide comfortable conditions for the passengers and reduce energy consumption, especially for the electric vehicles. Therefore, a concept of personal air conditioning system is proposed in this study to replace the traditional one. Using the representative car of Honda Company as the model, thermal properties of vehicle cabin are simulated by computational fluid dynamics software and experimental studies are carried out to validate the simulation results. Based on that, this thesis is summarized as the following four parts.

1. The heat flow properties in sealed cabin of automobile are simulated firstly and experimental studies are carried out to validate the simulation results. Using the car STEPWGN as a model, a simplified three-dimensional geometry with real dimensions is established to predict the heat flow distribution of cabin when car is parking in the summer sunshine. The natural convection and radiation heat transfer from environment to cabin are considered and the total heat transfer rate is calculated by software. Transient temperature and velocity distribution at the central and horizontal plane are also analyzed respectively. It is shown that simulation results have good agreement with experimental data. The cabin temperature increases by time and the highest value is

located at the front and both sides cabin after 15 minutes. The air is essentially stagnant with low velocity and the central compartment has much lower velocity than other regions of cabin.

2. Based on the same methods of above, the cooling effect of traditional air conditioning of automobile is studied by numerical simulation and experimental validation. The experimental study has been taken place in a stable environment. The variation of temperature during 15 minutes is tested at different location of cabin and the energy consumption is measured, which makes a comparison with the numerical study. Using the representative car -N box as the model, the numerical study analyzes the air flow and heat transfer characteristics of inner cabin, especially at the place of wind outlet and inlet during cooling period. The results are in good agreement with experimental data. However, under save energy model the traditional air conditioning system cannot make all the passengers feel comfortable. The rear row of cabin still has higher temperature than front row since it is difficult to carry out thermal exchange due to the complex structure of inner cabin.

3. A personal air conditioning system is proposed to instead of the traditional one. This new system is installed inside of each chair of vehicle cabin to provide thermal comfort for each passenger. Experiment validated that this system can make passengers feel comfortable after 4 minutes and all the apparatuses can just only consume electric power 338.8 W, which is less than the consumption of traditional air conditioning. However, this system cannot make all the body feel comfortable. The numerical results have good agreement with experiment research. Except the area of chairs, the temperature of cabin has almost no change during 15 minutes. It indicates that this

personal air conditioning system cannot provide enough cooling wind to cut down the heat from ambient.

4. In order to resolve the problem that personal air conditioning system just can be local action, a new modified personal air conditioning system is proposed by adding more four wind outlets in the front of cabin, which have bigger size and provide much more wind for all passengers. Based on the simulation calculation, the air flow and heat transfer characteristics of cabin are analyzed during 15 minutes. The results show that front wind outlets can work well to bring much cooling and put in motion the heat exchange among the cabin under the assist of wind outlets in chairs. The temperature of cabin can be dropped by about 5 ℃, which is consistent with the expectation of before. Therefore, it demonstrates that this new modified personal air conditioning system can be used well in the future automobile.

Contents

Chapter 1
Introduction

Automobile has been seen a rapid increase of over the past years and has become a necessary transport tool in the modern society. However, the increase of automobiles gives us a lot of problems including the environment pollution and energy shortage. Nowadays the energy shortage is really serious problem and it tends to more serious. Therefore, with the rapid development of the technology, the energy saving has been taken into the account in the design of an automobile to resolve the energy shortage problem. In term of automobile air conditioning system, the low-energy consumption and high thermal comfort have been required increasingly by consumers.

In order to enhance the performance of automobile to satisfy customers and improve the thermal comfort for passengers, there is plenty of necessary information that should be mastered as the basic data. For example, thermal resource of vehicle cabin, heat flow properties and temperature distribution of cabin, work performance of automobile air conditioning system and energy consumption and so on. All these analyses can help to design the high-efficiency air conditioning system to apply in the future vehicle, especially for the electric vehicle.

1.1 Research background

1.1.1 Thermal environment in the cabin

The main reason of thermal environment in the cabin is the effect by a variety of external disturbance and internal interference. Outside interference includes outdoor climate parameters, such as outdoor air temperature and humidity, solar radiation, wind speed, wind direction changes, which can be accessed through the shell to directly affect the indoor environment including passengers, lighting, equipment, etc. Therefore, in order to get a good indoor environment to meet passenger's request, we must understand the car outside the main elements of climate variation and its characteristics. The car has rapid response to the external environment changing as the small thermal inertia. Also, solar radiation is the primary source of heat on the ground and the main factors to determine the climate. Thus, the car air-conditioning load is the most direct affected by solar radiation. The solar radiation intensity can be calculated by the equation [1]:

$$I_x = I_0 \exp(-kx) \tag{1.1}$$

Where

I_x, solar intensity at the distance of x from the atmosphere boundary;

I_0, solar constant, $I_0 = 1353W/m^2$;

k, a constant of proportionality, m^{-1};

x, the distance from the test location to the atmosphere boundary.

The calculation process of solar radiation intensity is shown in Fig.1-1. From this picture, we can see that the greater k the greater the attenuation of radiation intensity, so the value a can be expressed by:

$$a = kL \tag{1.2}$$

Where

a, atmospheric specific extinction;

L, the distance when the sun on the top (solar radiation perpendicular to the ground)

k, atmospheric specific extinction per unit thickness.

When the sun is located not on the top but the angle β, the distance of solar reach at the ground can be expressed as L/sinβ. The solar radiation intensity can be calculated by the equation:

$$I_n = I_0 \exp(-a/\sin\beta) \tag{1.3}$$

Where

I_n, the distances of solar reach at the ground;

β, position angle of sun.

Therefore, according to this equation, the solar intensity can be calculated at any time during a day.

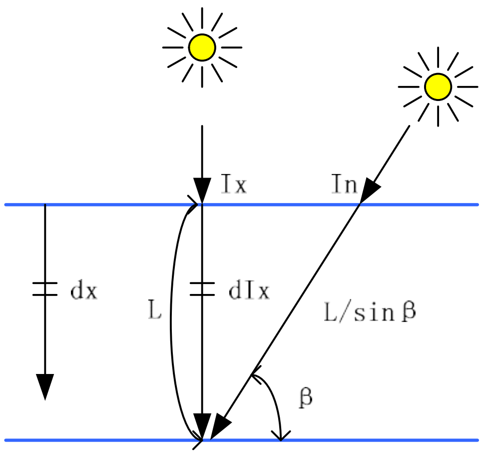

Fig.1-1 Direct solar radiation intensity

Solar radiation getting into the cabin is an unsteady state heat transfer process; the temperature of outdoor is one important factor that cannot be ignored as it is also changing with the time. This hourly temperature is roughly cyclical changes by solar radiation. Thus its specific value has certain randomness, but from the overall trend, the temperature changes by cyclical. Considering from the design perspective of the thermal load, the temperature changes is also assumed to change according to a cyclical continuous rule. When calculating the air-conditioning, especially the heat transfer in the non-transparent car shell, the exterior surface of the shell suffers thermal effect by both solar radiation and the air temperature of outside. Therefore, a synthesis temperature should be considered from both of them. The relationship between outdoor integrated temperature and solar radiation change with a 24-hour cycle is shown in Fig.1-2. Therefore, gain heat also changes according to this rule [2].

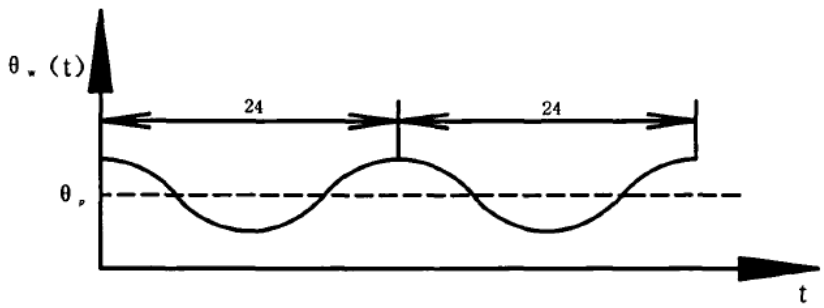

Fig.1-2 Circle change of outside temperature

1.1.2 Traditional automobile air conditioning

Human's tolerance limits to high temperature may be related to his temperature sense, his ability to lose heat by regulatory sweating, and his ability to move heat from his body. There are many interrelating processes involved in heat stress. Pain receptors in man's skin are triggered at a skin surface temperature of 46 ℃. Although direct contact with a metal surface at this temperature is painful and much higher dry air temperatures can be tolerated since the thermal insulation of the air layer around the skin is high. Tolerance times of almost 50 min have been reported at a dry bulb temperature of 82 ℃.

In each case, the dew points were lower than 30 ℃. Many individuals are simulated by exposure to the 82 ℃. Therefore, in high temperature experiment like vehicle cabin, the air conditioning is important to make passengers comfortable. The automobile air conditioning system is a kind of device for refrigeration, heating, ventilation and air purification in the cabin, which is able to provide a comfortable environment for the passengers in any weather and driving conditions. A complete automotive air conditioning system depends on regulating the temperature, humidity, wind speed and ventilation, etc. to create a comfortable environment. The interior temperature is an important indicator of thermal comfort, which is decided by outside temperature, air flow, and solar radiation intensity. When the outside temperature is over 20 ℃, the car can only rely on air conditioning and refrigeration to achieve cooling purposes [3].

Traditional automobile air conditioning system is composed by the compressor, condenser, evaporator, expansion valve, receiver drier, hoses, fans, vacuum electromagnetic valve and so on, which can be seen in the Fig.1-3. Most of car have no independent motor for air conditioning system but depends on the car engine to provide motive power for the compressor. Therefore, the refrigeration performance is greatly influenced by the engine work with poor stability. Generally, the low-grade cars are using the traditional manual air conditioning which has a temperature control knob on the air conditioning control panel. Actually, this knob controls a variable resistance device which composes a series circuit with the resistor of temperature sensor in the evaporator. When the inside temperature changes, the resistance of this group circuit also changes by time, which controls the electromagnetic clutch of compressor depending on manual adjustment through knob. This kind of adjustment method is relatively simple, but the temperature control is not accurate enough. Modern highgrade cars are more and more using the automatic climate control system that is able to automatically adjust the temperature of outlet according to the thermal flow of inside if only pre-set temperature, which can control precision of temperature just only by a simple operation [4].

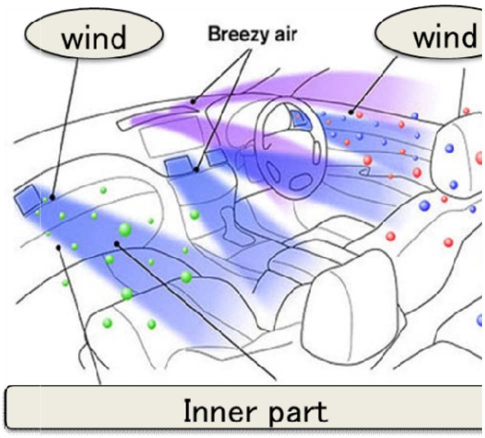

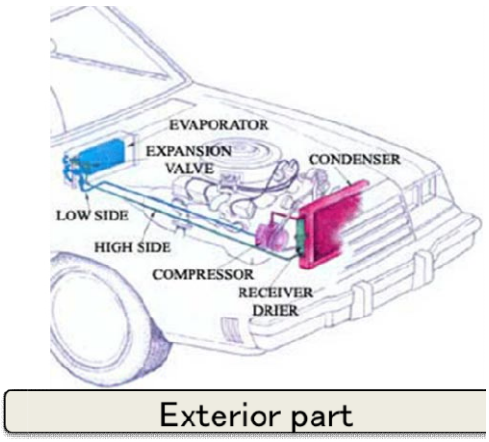

Fig. 1-3 Structure of automobile air conditioning system

Besides conduction and radiation heat, the engine, chassis, motors and other mechanical parts have emitted heat by conduction into the vehicle cabin. Therefore, the effect of automotive air conditioning has closely related to the heat insulation performance of body and window glass. In order to reduce the thermal load of air conditioning, it should pay more attention to the tightness and heat insulation property of vehicle cabin. Car air conditioning systems generally do not need special maintenance, but due to the impact of the external environment, the air purification equipment and air conditioning evaporator require regular cleaning to maintain good regulation of air quality [5].

Up to now, most of automobile are still using the traditional air conditioning system, which is easy to induce temperature gradient between the front row and back row. Another new climate-control system is reported to use in the vehicle cabin to control the inner temperature, which is the most complex and thoughtful air conditioning system at present in the word. This kind of system is able to adjust the cabin temperature according to the outside and even it can divide the cabin into several parts and work for each part individually.

1.1.3 New personal air conditioning system

In recent years, a few companies have come out with a personal portable air conditioning that is light weight, battery-operated, and promises to cool down wherever people are. By means of this idea, a personal air conditioning system applied to automobile is proposal in this study. This system is designed by using the peltier module which has become increasingly popular in the cooling research field. The structure appearance of peltier module is given in the Fig.1-4.

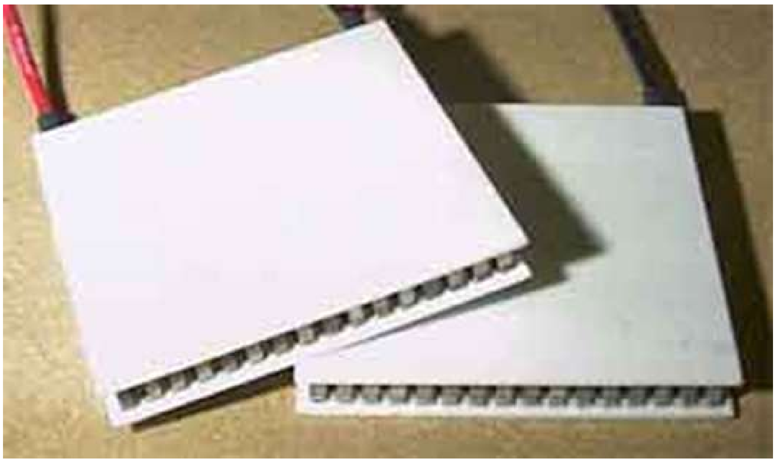

Fig.1-4 Appearance of peltier module

Peltier is also called as semiconductor refrigeration tablets which is a refrigeration technology of generating a negative resistance. Peltier module just utilizes the peltier effect of material to create a heat flux between the junctions of two different types of materials with consumption of electrical energy depending on the direction of the current, which is similar with the heat pump that transfers heat from one side of the device to the other. The Fig.1-5 has described the rising warmer air (the orange part) and falling cooler air (the blue part) on the surface of heat sink of a peltier model. This device has flexible shape with small size and does not need the refrigerant, compressor and some other traditional high-energy consumption device so that it can be used as the personal air conditioning system in the automobile to save energy. Moreover, the cooling capacity of this device is controllable via changing the input current and the temperature control to within fractions of a degree can be maintained. In addition, it has long life with mean time between failure exceeding one million hours [6].

However, there are plenty of restrictions of using a peltier device in terms of efficiency. Currently, the peltier device can typically produce a maximum temperature difference of 70 ℃ between its hot and cold sides. The more heat to be required, the less efficient it becomes since it needs to dissipate both the heat being moved and the heat it generates itself from its own power consumption. Therefore, it has been relegated to application of low heat flux without high efficiency [7].

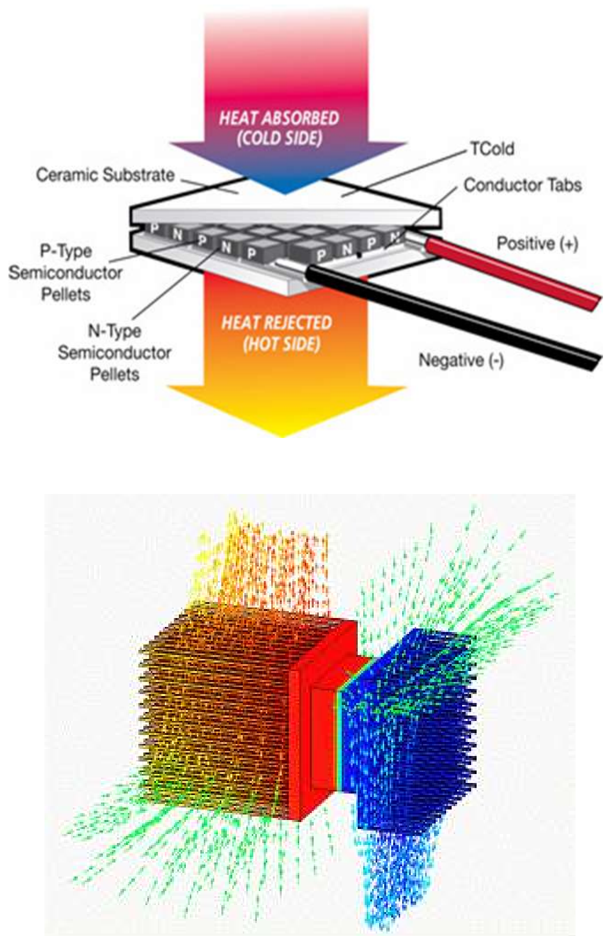

Fig.1-5 Working schematic plot of peltier unit

1.1.4 Current research condition

The performance of air conditioning system plays an important role to decide the comfortable level of an automobile and it has been paid extensive attention by a lot of researchers. For so many years, plenty of researches and experiments on the passengers' thermal comfort have been done in many automobile companies including Nissan, Honda and some other units of car. A brief review is given as the follows. Yamamoto and Hill [8] simulated the flow field in a truck by using a simplified mesh to obtain the air flow distribution. Wan and Kooi [9] used software to simulate the flow and temperature field in a car. They gained the optimal case for the air supply. Lin [10] studied how the parameters affect the amenity, such as the wind volume rate and locations of air inlets. Kihler [11] used the zone calculation method to investigate the temperature field and the corresponding heat flux change with time and simulate the sunshine radiation into the cabin. Ishihara and Hara [12] measured the air flow velocity distribution by visualization and compared to their numerical simulation results. Another analysis by them was the full scale model of a passenger compartment by using a laser light sheet method. Hagino and Hara [13] investigated the factors affecting the thermal comfort of cabin, like air temperature, air flow, and sunlight radiation and proposed a method to forecast passengers' thermal feeling. Currle [14] simulated the temperature field by STAR-CD and considered the passengers' thermal model to discuss the thermal comfort of cabin. Brown and Jones [15] create a thermal comfort model for the Ford Company, which considered the variation of temperature and velocity with time as well as the physiological status of passengers. Ambs made a simulation of the vehicle compartment climatic conditions to improve thermal comfort while reducing vehicle development time and cost [16]. Gokhan and Muhsin added a virtual manikin model to make a three-dimensional transient numerical analysis to determine the air flow and heat transfer characteristics inside the vehicle cabin during a heating period [17]. Huajun Zhang built a numerical model to investigate the air flow and temperature fields inside a passenger compartment for improving thermal comfort and saving energy at the same time [18].

The researches mentioned above are mostly about the effects on passengers' thermal comfort from air flow field, the temperature filed, heat transfer from outside to inside and radiation, etc. Study on the performance improvement of automobile air conditioning system is quite limited and it has suffered little attention by the researchers. Therefore, the manufacture technology of automobile air conditioning system has little change in recent years. Actually, this field occupies more and more important position in the research of future automobile technology. The problems related to this grow more urgent, especially in the energy shortage countries.

1.2 Research purpose and method

1.2.1 Research purpose

This project aims to force the function of air conditioning systems to provide comfortable conditions for the passengers and reduce the energy consumption, especially for the electric vehicles. This kind of vehicle has limited electric power when driving on the road so that the air conditioning system should consume power as little as possible. Actually, the traditional air condition system consumes plenty of electric power. When cooling system turns on, the drive distance could be shortened by one third and this number could be a half when the heating system turns on. In order to solve this problem, the concept of personal air conditioning system is proposed in this study instead of the traditional one. This air conditioning system provides comfortable environment for each passenger individually by installed under each chair of vehicle cabin. By doing this, the energy wasting to cool the space of no person of cabin would be reduced dramatically. In addition, the appliance of this system is produced by Peltier module and fan motor that can only consume lower electric power to drive so that the saved energy can be used to provide vehicle to drive longer.

1.2.2 Research method

In this study, using the representative car of Honda Company as the model, a simplified three-dimensional geometry model with real dimensions and shape is established to analyze the thermal transfer process by the computational fluid dynamics (CFD) software. The analysis of thermal transfer process is essential to deal with the thermal performance of cabin and provide comfortable conditions with high quality air for the passengers [19]. The first step has simulated the effect of solar to the cabin and a simple car model is used without any in-car facility and the computational domain only consists of the inner space of the cabin. Then, the chair and the air conditioning system have been considered in the model to calculate the temperature distribution and wind velocity in different directions, which is based on overall cabin and the air conditioning is operated. The third step has analyzed the thermal characteristics of cabin using the personal air conditioning system to replace the traditional one. To validate the simulation, the experimental studies with the same conditions are carried out to make a comparison. Finally, an optimized personal air conditioning system is proposed to resolve the shortage of previous one.

The numerical simulation process is shown as follows: First, a 3-D model of vehicle cabin is established by AutoCAD software and exported to CFD to generate mesh for numerical analysis, which is very curial to obtain the accurate predicted results. Then, the boundary conditions are set according to the thermal transfer properties and environment situation. Finally, the calculation is carried out by software and the analysis results are obtained [20]. Because of the complicated of the calculation and analysis we simplified the heat transfer process and presumed as follow: All the parts of the cabin are the same temperature at the beginning; just consider the solar radiation at the exterior shell of the car; ignore the radiation of interior wall surface in the cabin as their low temperature [21]. All the analysis is focus on the thermal flux and the simulation site was set at Tokyo Shinjuku, Japan, which can be seen in the Fig.1-6.

Fig.1-6. Parking location of car

1.3 Organization of this thesis

This thesis is organized as follows:

Chapter 1 presents the background of this research including thermal environment of the vehicle cabin, traditional automobile air conditioning system and the application of new personal air conditioning system. Moreover, the current research condition about the automobile thermal comfort and energy saving are introduced briefly from the year 1990 to 2010. In addition, the research purpose and method are given in this chapter.

Chapter 2 analyzes the heat flow distribution in the sealed cabin of automobile. Using the representative car of Honda Company-STEPWGN as a model, a simplified three-dimensional geometry with real dimensions is established to predict the heat flow properties of cabin when car is parking in the summer sunshine by CFD analysis software. The nature convection and radiation heat transfer from environment to cabin are considered and the distribution of transient temperature and velocity at the central and horizontal plane are analyzed respectively. The comparisons between predicted and tested temperature at pointed position of cabin is also presented and the total solar heat transfer is calculated by the software during 15 minutes.

The cooling effect of the traditional air conditioning of automobile is studied by numerical calculation and experimental validation in chapter 3. The experimental study has been taken place in a stable environment condition. The variation of temperature during 15 minutes is tested at different location of cabin and the energy consumption is also recorded, which makes a comparison with the numerical study. Using the representative car of Honda Company-N box as the model, the numerical study analyzes the air flow and heat transfer characteristics of the inner cabin, especially at the place of wind outlet and inlet during the cooling period.

Chapter 4 proposes a new personal air conditioning system to instead of the traditional one. This new system is installed inside of each chair of vehicle cabin to provide thermal comfort for each passenger, which can help to resolve the energy consumption problem, especially for the electric vehicle. Numerical calculation and experimental validation are carried out in this chapter. Thermal transfer properties of vehicle cabin under using this system are predicted and the total heat transfer during 15 minutes is calculated by software. Thermal comfort and temperature experiment are validated to have good agreement with simulation results. In addition, the electrical consumption is tested to prove this system to be lower energy consumption.

In order to resolve the problem that personal air conditioning system just can be local action, a new modified personal air conditioning system is proposed in chapter 5. This modified system adds more four wind outlets in the front of cabin, which have bigger size and provide much more wind for all the passengers. Based on the simplified 3-D vehicle model, a numerical study has analyzed the air flow and heat transfer characteristics of cabin under the cooling action during 15 minutes. The energy consumption is estimated to compare with the traditional air conditioning system.

Chapter 6 concludes this thesis and sets the work in the future.

References

[1] YANG Rongxia, The research on calculation and experiment of the automobile air conditioner’s non-steady load, mater degree thesis of Lanzhou University of Technology, 2007.

[2] Richard C. Farmer, Gary C. Cheng, Yen-Sen Chen, Ralph W. Pike, Computational transport phenomena for engineering analyses, USA, 2009.

[3] Robert Parsons, ASHRAE handbook Fundamentals, 1997.

[4] Lou Kren, The History of Air Conditioning Properties, 2007

[5] A. Mezrhab, M.Bouzidi, Computation of thermal comfort inside a passenger car compartment, applied thermal engineering, 26(14-15): 1697-1704, 2006.

[6] Http://en.wikipedia.org/wiki/Main_Pag

[7] Thermoelectric Coolers Basics, TEC Microsystems, Retrieved 16 March 2013.

[8] K. Yamamoto, W.R. Hill, Interior flow visualization of a small pick-up truck and A/C Feeling Estimate, SAE International Congress and Exposition, ISSN: 0148-7191, SAE, Detroit, MI, USA, 1990.

[9] J.W. Wan, J. van der Kooi, Influence of the position of supply and exhaust openings on comfort in a passenger vehicle, Int. J. Vehicle Des. 12 (5–6): 588–597, 1991.

[10] Chao-Hsin Lin, A. Lelli Michael, Han Taeyoung, J. Niemiec Robert, C. Hammond Dean, Jr., Experimental and computational study of cooling in a simplified GM-10 passenger compartment, International Congress and Exposition, ISSN:0148-7191, SAE, Detroit, MI, USA, 1991.

[11] J. Kohler, Numerical calculation of the distribution of temperature and heat flux in buses under the influence of the vehicle air-conditioning system, ASHRAE Trans. 96(1): 432–446, 1990.

[12] Ishihara Yuji, Shibata Minoru, Hoshino Hiroshi, Hara Junichiro, Kamemoto Kyoji, Analysis of interior airflow in a full-scale passenger-compartment model using a laser-light-sheet method. International Congress and Exposition, ISSN: 0099-5908, SAE, Detroit, MI, USA, 1992.

[13] M. Hagino, J. Hara, Development of a method for predicting comfortable airflow in the passenger compartment. Worldwide Passenger Car Conference and Exposition, ISSN: 0148-7191, SAE, Dearborn, MI, USA, 1992.

[14] J. Currle, Numerical simulation of the flow in a passenger compartment and evaluation of the thermal comfort of the occupants, in: Proceedings of the 1997 International Congress and Exposition, ISSN: 1054–6693, SAE, Detroit, MI, USA, 1997.

[15] J.S. Brown, B.W. Jones, New transient passenger thermal comfort model, in: Proceedings of the 1997 International Congress and Exposition, ISSN: 1054-6693, SAE, Detroit, MI, USA, 1997.

[16] Ambs, R: Improved Passenger Thermal Comfort Prediction in the Preprototype Phase by Transient Interior CFD Analysis Including Mannequins, SAE, 2002.

[17] Gokhan Sevilgen, Muhsin Kilic: Transient Numerical Analysis of Airflow and Heat Transfer in a Vehicle Cabin During Heating Period, Int. J. Vehicle Design, Vol. 52, Nos. 1/2/3/4, 2010.

[18] Huajun Zhang, Lan Dai, Guoquan Xu, Yong Li, Wei Chen, WenQuan Tao: Studies

of Air-flow and Temperature Fields inside a Passenger Compartment for Improving Thermal Comfort and Saving Energy. Part I: Test/ Numerical Model and Validation, Applied Thermal Engineering 29: 2022-2027, 2009.

[19] Massoud Kaviany, Essentials of heat transfer, USA, 2011.

[20] ANSYS Inc. Fluent Manuals.

[21] S. Mostafa Ghiaasiaan, Convective Heat and Mas Transfer, USA, 2011.

Chapter 2
Analysis of Heat Flow in Sealed Vehicle Cabin

2.1 Chapter Introduction

Recently, the parking car under solar radiation has been suffered a wide range of attention by plenty of researchers. There was reported that a baby alone locked in the car by parents had nearly died of heat stroke and exhaust due to the high temperature of cabin. It is well known that the temperature of sealed cabin tends to become increasingly high along with time, which could conduct the terrible comfortableness when passengers enter into the car after long time parking [1]. Especially in the summer, the temperature of cabin can increase rapidly over 50 ℃, which could result in intelligent system device disable (IPAD and IPHONE, etc.) if these items are put inside the cabin. More serious is that the spontaneous combustion could be happened in the car because of the high temperature.

The reason why cabin under sunshine is a so dangerous place can be expressed by the heat flux attributing to the solar radiation [2]. Therefore, in order to improve the performance of vehicle air conditioning system, the thermal distribution of inside of cabin should be analyzed as the first step. In this chapter, the thermal characteristic of a sealed cabin is studied by numerical simulation and experimental validation. The numerical simulation has used the representative car of Honda Company—STEPWGN as model which is shown in the Fig.2-1 [3] and a simplified three-dimensional geometry with real dimensions has been established to analyze the heat flow distribution in a sealed cabin of car [4]. The heat flow distribution of cabin is predicted when car is parking in the summer sunshine by using the CFD analysis software. The natural convection and radiation heat transfer from environment to cabin are considered and the distribution of transient temperature and velocity at the central and horizontal plane are analyzed respectively. The experimental study has been carried out in a stable environment condition which is the same as the boundary conditions of simulation to validate the numerical calculation.

Fig. 2-1 Representative car of Honda Company—STEPWGN

2.2 Solar intensity calculation

The sunshine from environment can conduct energy which is separated into three parts: heat radiation, heat convection and heat conduct. Under the steady state conditions the energy equation from sun to the cabin based on the first law of thermodynamics is expressed as below [5]:

$$Q = Q_{conv} + Q_{rad} + Q_{cond} \tag{2.1}$$

Where

Q, total heat from sun;

Q_{conv}, the part of heat through convection;

Q_{rad}, the part of heat through radiation;

Q_{cond}, the part of heat through conduction.

However, the main energy access to cabin includes the heat radiation and heat convection. The heat conduction can be ignored. Accordingly, the calculation can be summarized in two parts: the radiation and the convection. The heat equation can be represented by the following equation [6]:

$$Q = Q_{conv} + Q_{rad} \tag{2.2}$$

Radiation is one of the basic mechanisms by which energy is transferred between regions of different temperature. It is distinguished from conduction and convection by the fact that it does not depend upon the presence of an intermediate material to act as a carrier of energy. The radiation process can be explained as the consequence of energy-carrying electromagnetic waves. These waves are emitted by atoms and molecules as the result of various changes in their energy content. The amount and characteristics of the radiant energy emitted by a quantity of material depend upon the nature of the materials. Although the rate of emission of energy is not dependent of the surroundings, the energy transfer rate depends upon the temperatures and spatial relationships among the various materials involved. So how to calculate the radiation heat is the most important. The Fig.2-1 shows the thermal behavior of solar radiation through the glass of the car windows. The solar radiation is separated into radiation, glass absorption and penetration, which is defined constant thermal property. In order to calculate each value, we must check the solar thermal property and analyze the ratio of the each part in the entire solar outside. The thermal property of normal glass into the cabin can be discussed by this equation [7]:

$$Q_s = Q_r + Q_a + Q_p \tag{2.3}$$

Where

Q_s, the part of heat from solar radiation;

Q_r, the part of heat through glass reflection;

Q_a, the part of heat through glass absorption;

Q_p, the part of heat through glass penetration.

In this equation, Q_r can be expressed as ρQ_s; Qa can be expressed as αQ_s and Q_p can be expressed as τQ_s. According to the general relationship of thermal radiation:

$$\rho + \alpha + \tau = 1 \tag{2.4}$$

Therefore, the solar radiation also can be expressed by:

$$Q_s = \rho Q_s + \alpha Q_a + \tau Q_p \tag{2.5}$$

Where

ρ, reflection rate;

α, absorption rate;

τ, penetration rate.

About the reflection ratio, we can put the sheet on the exterior of the glass and measure the reflection thermal from the glass.

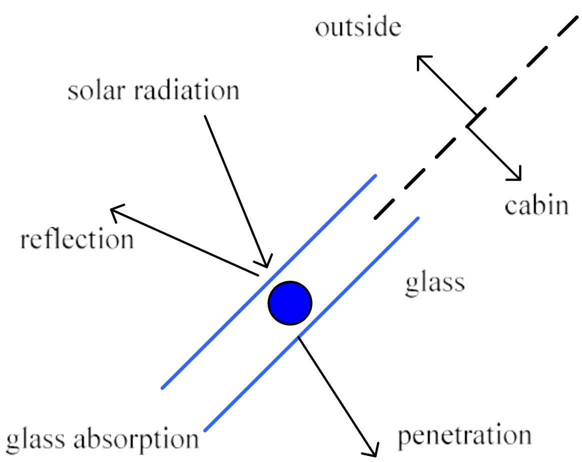

Fig.2-2 Three approaches of sunshine through the glass

Fig.2-2 just shows the phenomena of radiation. Thus the situation is getting more complicated about the radiation and convective heat. We are supposed to take only radiation of each glass surface including the outside and inside into account in the first step. The calculation of thermal flow on the surface is just accorded to the natural property. In this study, all the radiation energy calculation can be done by the software which uses the governing equations to deal with the heat transfer through the boundary setting [8].

2.3 Experimental investigation

This experiment was carried out in the natural convection conditions. Ambient environment was quiescent without any winds. The relative humidity was determined at 60% and the ambient temperature stayed at 30 ℃. In order to avoid the direct sunlight causing too much high temperature, the test car was parking in the shade of trees. Before starting the experiment, the engine of car was flameout to be cooling and all the doors were opened to make the in-car air flow to maintain almost same as that of outside environment. After one hour's ventilation, the temperature of vehicle cabin can be considered the same as the ambient temperature and the car dashboard showed that the temperature was 30.1 ℃.

The experiment measuring time was set for 15 minutes in 5-minute intervals, which can be obtained three sets of data for one test. In order to eliminate accidental errors, the multiple measurements were performed and three sets of test were carried out due to time constraints. The infrared temperature probe was used in this experiment and the five measuring points were picked up to monitor the temperature variation of cabin. Four points were fixed at the position of face when passengers sitting in the car including the front row and rear row. The part of face is very important place to feel if the environment is comfortable or not. Another measuring point is close to the windshield which can help to study the affection of glass to cabin temperature. All the measuring points are given in the Fig.2-3.

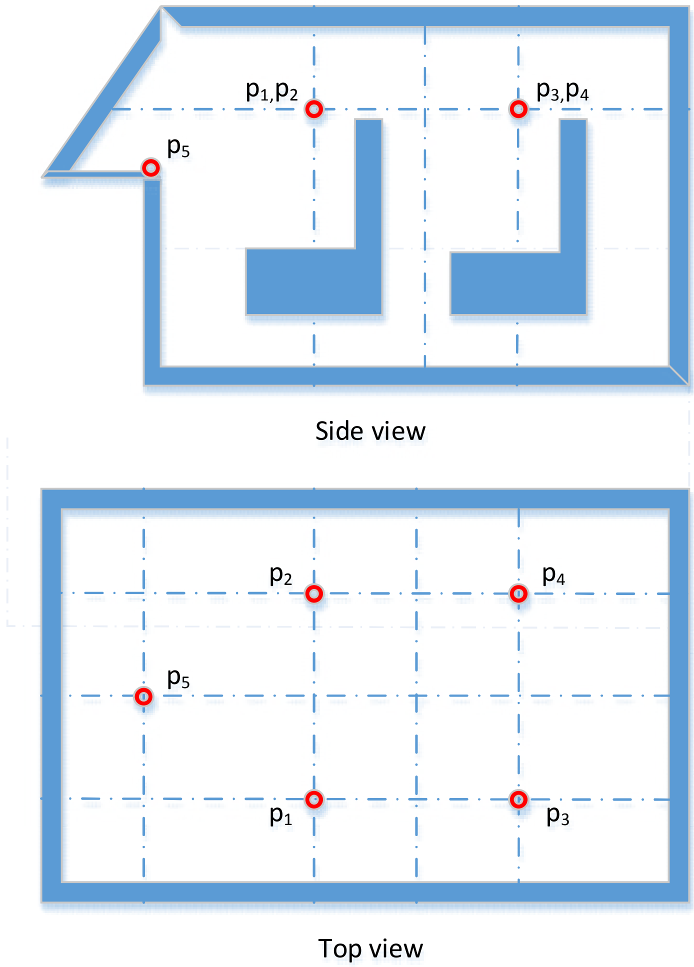

Fig.2-3 Measuring points of temperature in the vehicle cabin

2.4 Numerical simulation

A three-dimensional (3-D) CFD model of a vehicle cabin with real dimensions shape is used to determine heat transfer of solar radiation from environment. The analysis is fully transient and the computed flow and temperature distributions in the vehicle cabin included the interactions from turbulent flow, thermal buoyancy, and the three modes of heat transfer, i.e., radiation. Computed local heat transfer characteristics of the solar radiation and the flow and temperature fields at the different planes are discussed in this study.

2.4.1 Governing equations and basis of algorithm

In the numerical simulation, this software is based on the technique using a control volume theory to convert the governing equations to algebraic equations which can be solved numerically. The control volume technique works through integration of the governing equations about each control volume and generates discretization of the equations which keep each quantity based on control volume [9].

The algorithm for the numerical simulation can be carried out by the calculation equation which is based on the governing equations including the energy conservation equation, momentum conservation equation and mass conservation equation [10]. The energy conservation equation is written as follow:

$$\frac{\partial(\rho E)}{\partial t} + \nabla\cdot\left(\vec{v}(\rho E + p)\right) = \nabla\cdot\left(k_{eff}\nabla T - \left(\sum_j h_j \vec{J_j} + \bar{\bar{\tau}}eff\cdot\vec{v}\right)\right) + S_h$$

(2.6)

Where

h, enthalpy;

p, static pressure;

ρ, density;

v, velocity;

k_{eff}, effective conductivity (k + k_t);

J_j, the diffusion flux of species j;

k_t, turbulent thermal conductivity;

$\bar{\bar{\tau}}$, stress tensor;

S_h, defined volumetric heat sources.

In the equation, the first term on the left hand side represents unsteady energy and the second term represents the part of energy by conduction; the first three terms on the right hand side show the energy of conduction, species diffusion and viscous dissipation, respectively. The E and $\bar{\bar{\tau}}$ can be expressed as:

$$E = h - \frac{p}{\rho} + \frac{v^2}{2}$$

(2.7)

$$\bar{\bar{\tau}} = \mu\left[(\nabla \vec{v} + \nabla\vec{v}T) - \frac{2}{3}\nabla\vec{v}I\right]$$

(2.8)

Where

μ, molecular viscosity;

I, unit tensor.

The second term on the right hand side of the equation (2.8) is the effect of volume dilation. Therefore, the momentum conservation equation is given as follow:

$$\frac{\partial}{\partial t}(\rho\vec{v}) + \nabla\cdot(\rho\vec{v}\vec{v}) = -\nabla p + \nabla\cdot(\bar{\bar{\tau}}) + \rho\vec{g} + \vec{F}$$

(2.9)

Where

$\vec{F}$, gravitational body force and contains other model-dependent source terms;

$\rho\vec{g}$, external body forces.

Therefore, the mass conservation equation can be expressed as follow:

$$\frac{\partial\rho}{\partial t} + \nabla\cdot(\rho\vec{v}) = S_m$$

(2.10)

Where

S_m, the mass added to the continuous phase from the dispersed second phase and any user-defined sources.

This equation is the general form which is valid for incompressible and compressible flows. The realizable k-ε (2εqn) model is chosen for the turbulent modeling in this calculation. This model is different from the standard model which may result in the minus normal stress. According with the physical laws of turbulence, the normal stress should be restrained by some mathematical ways and the realizable turbulent model is just derived from this theory. The turbulence energy equation can be expressed as follow [11]:

$$\frac{\partial(\rho k)}{\partial t}+\frac{\partial(\rho k u_i)}{\partial x_i}=\frac{\partial}{\partial x_j}\left[\left(\mu+\frac{\mu_t}{\sigma_k}\right)\frac{\partial k}{\partial x_j}\right]+G_k+G_b-\rho\varepsilon-Y_M \tag{2.11}$$

$$\mu_t=\rho C_\mu\frac{k^2}{\epsilon} \tag{2.12}$$

$$C_\mu=\frac{1}{A_0+A_s U^{\cdot} k/\epsilon} \tag{2.13}$$

$$A_s=\sqrt{6}\cos\emptyset \tag{2.14}$$

Where

G_k, the turbulence energy caused by the average of velocity gradient;

G_b, the turbulence energy caused by the buoyancy;

Y_M, the effect of total dissipation rating from the compressible turbulence expansion

A_0, empirical constant, in this equation, $A_0 = 4$;

σ_k, Prandtl number of turbulence energy.

2.4.2 Model Geometry

The geometry model of the vehicle was created by the AutoCAD software with real dimensions and shape. The CAD model of the vehicle cabin is given in the Fig.2-4. However, this model was simplified and the computational domain only consists of the inner space of the cabin without the chairs and other in-car facilities, for example, the steering wheel. And then the model was exported to CFD software to generate mesh for numerical analysis, which is very curial to obtain the accurate predicted results. In the process, the hybrid structure grid including the tetrahedral and triangular elements was used in this mesh generation. The computational domain consists of 10199830 elements. The mesh of numerical calculation zone is shown in the Fig.2-5.

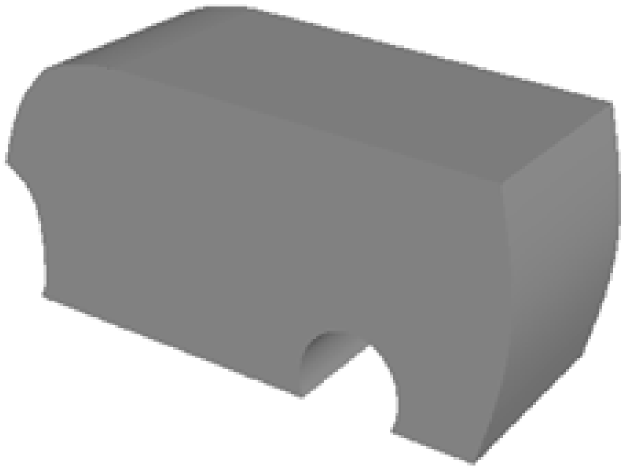

Fig.2-4 CAD model of vehicle cabin

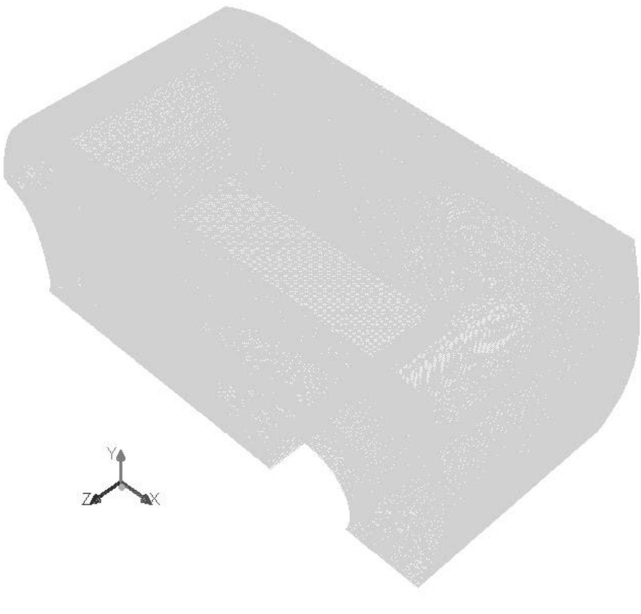

Fig.2-5 Surface mesh of numerical calculation zone

2.4.3 Boundary conditions and problem setup

The boundary condition also is an important factor to obtain the accurate results. In this numerical calculation, the surface boundaries were considered as solid walls including the roof, the bottom, the door and the windows, which were set as the stationary wall and semi-transparent. The outside thermal condition of the wall can be defined as a combination of convection and radiation from solar energy. The inner thermal flow can be considered as only natural convection from car shell.

On the one hand, the heat flux from environment caused the inner air temperature high and the major heat is generated by two major modes of heat transfer including the solar radiation and natural convection [10]. The solar radiation can be calculated by the solar ray tracing model of simulation software. The simulation starting date and time was set at the noon of the 21st in the June of 2012. According to the angle of sun in the sky, radiation heated level to the cabin can be gotten automatically. The direct and diffuse solar irradiations were presumed as constant value respectively. And the inner radiation of car shell was ignored. The heat of ambience transfers to car shell from air through natural convection and the environmental free stream temperature was set at 30 ℃ the same as experimental data. At the beginning of simulation, the boundary layer temperature of wall was equal to the environmental temperature at the outside edge of part close to the air flow. The thickness and heat generation rate of car shell was also considered in the calculation, which was important to predict the temperature variation of inner cabin.

On the other hand, the air flow of cabin moved as an internal circulation type depending on the thermal buoyancy, which was seen as natural convection. Therefore, the Bousinnesq model was used in the calculation of air zone. Natural convection is the major cause for air motion in this sealed cabin and plays an important role in the energy transfer process from solar energy. Natural convection in the cabin can be represented in the type of internal circulation, which depends on the gravitation field to drive the air moving in the cabin [12]. Therefore, the gravity value had been set in the numerical calculation. The Bousinnesq model is appropriate for the analysis object whose temperature has kept within limits without any large change, which assumes the constant value of air density to carry out the iterative calculation [13]. All the setup and the boundary conditions are presented in the Table 2-1.

In the present work, the model domains were calculated using pressure-based solver with transient time and absolute velocity formulation. The energy and transport governing equations were discretized by the finite volume method and the SIMPLE algorithm was adopted for the coupling between pressure and velocity. The standard k-epsilon (2eqn) turbulent model derived from the instantaneous Navier-Stokes equations was chosen as the viscous model in conjunction with the standard wall function for the near wall region treatment in this simulation [14-15].

Table 2-1 Setup and boundary conditions

Category	Parameter	Internal	External
Physical properties	Fluid	Air	Aluminum
	Density [kg/m^3]	1.177	2719
	Cp [J/kg-K]	10046.43	871
	Thermal conductivity (W/m-K)	0.0242	202.4
	Viscosity [kg/m-s]	1.7894e-05	/
	Thermal expansion coefficient [1/K]	3.356e-03	/
Boundary conditions			
Momentum	Wall motion	/	Stationary
	Shear condition	/	No slip
	Wall roughness height (m)	/	0
	Wall roughness constant	/	0.5
Thermal convection	Heat transfer coefficient (W/m^2-K)		4.048
	Free stream temperature (℃)		30
	Wall thickness (m)		0.02
	Heat generation rate (W/m^3)		0.045
Thermal radiation	BC type		Opaque
	Absorptivity of direct visible		0.8
	Absorptivity of direct IR		0.8

2.5.1 Validation of the results

The simulation results are validated by comparison of the predicted temperature values and the measuring data at the points located in the vehicle cabin described in the experimental investigation part, which is displayed in Figure 2-6. It can be seen that the predicted results are in good accordance with the experiment result and both of them present same trend with the time. The temperature shows a rapid increase before 5 minutes with the rate of nearly one degree per minute and it can reach about 35 ℃ after 5 minutes. This increased trend turns to slow down in the following 10 minutes and the final temperature can reach above 40 ℃ after 15 minutes. Especially, the temperature at the location close to the front windshield is measured over 46 ℃ which is very high and far more than the endurable degree of people. The two points located at same row show almost similar experimental and simulated temperature, individually.

In addition, from the figure it can be seen that at the back row (selected points p_3 and p_4), the differences between calculation and experimental temperature are about 1 ℃. At the front row (selected points p_1 and p_2), this value can be seen to stay at 2 ℃ in general. However, the simulation results at the place close to windshield (selected points p_5) show a worse agreement with measuring data, with the maximum deviation of 3 ℃ and the value has an increased trend with the time. Considering the parameters such as heat losses from the outside of cabin and heat transfer coefficient of car shell etc., there are too many factors affecting the numerical simulation. Therefore, such an agreement of a dynamic simulation results can be accepted to satisfy the engineering requirements.

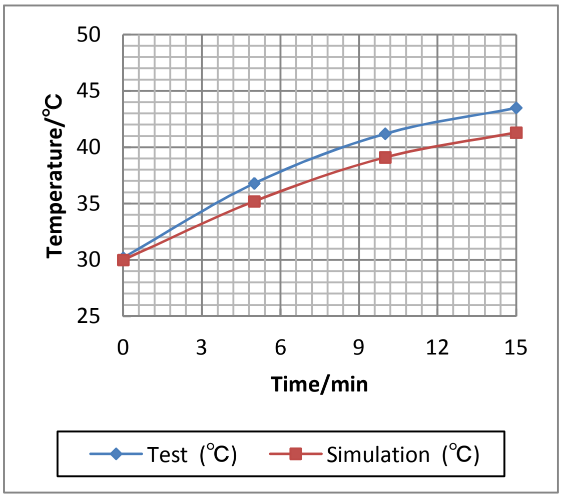

50
45
40
35
30
25
Temperature/℃
0
3
6
9
12
15
Time/min
Test (℃)
Simulation (℃)

(a)

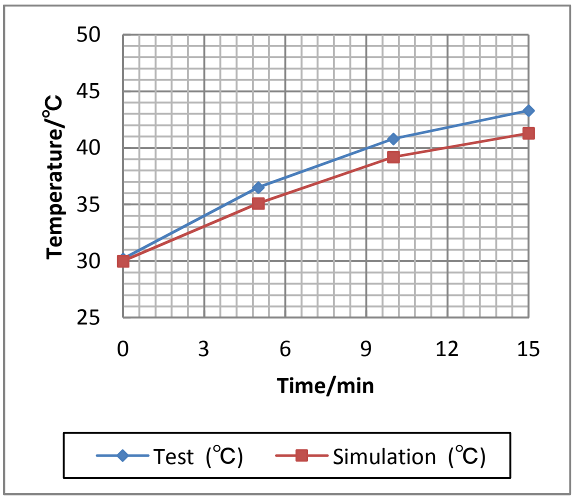

50
45
40
35
30
25
Temperature/℃
0
3
6
9
12
15
Time/min
Test (℃)
Simulation (℃)

(b)

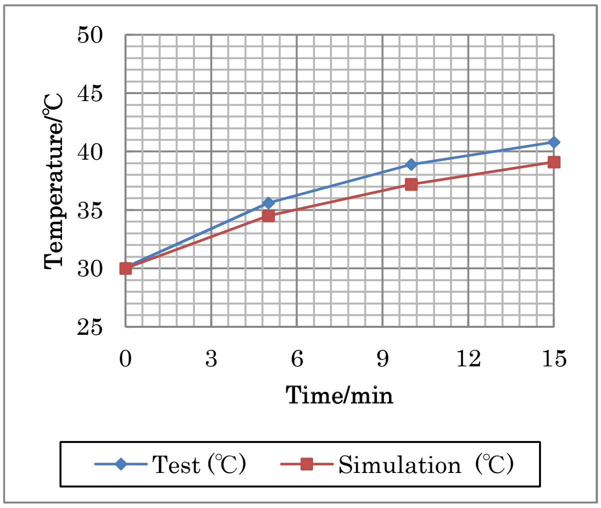

Temperature/℃
50
45
40
35
30
25
0
3
6
9
12
15
Time/min
Test (℃)
Simulation (℃)

(c)

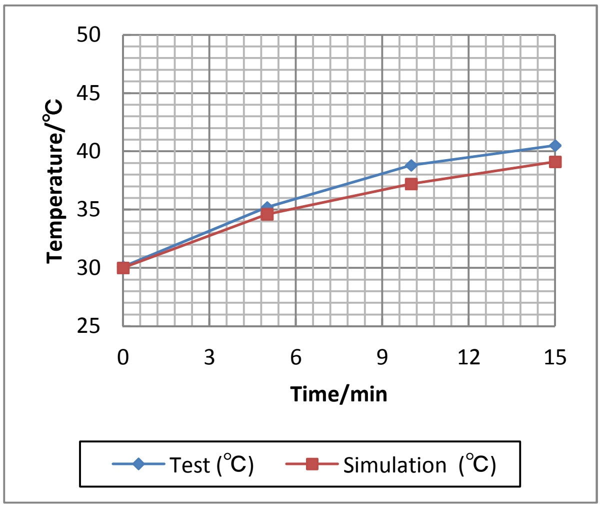

Temperature/℃
50
45
40
35
30
25
0
3
6
9
12
15
Time/min
Test (℃)
Simulation (℃)

(d)

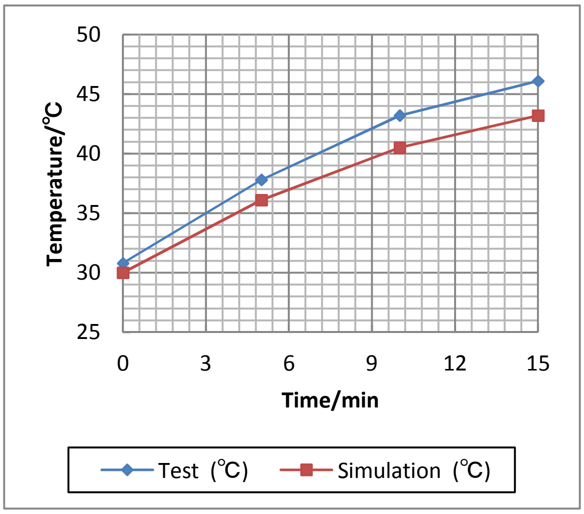

(e)

Fig. 2-6 Temperature comparison of simulation results with experimental data, (a) P_1; (b) P_2; (c) P_3; (d) P_4; (e) P_5

2.5.2 Heat flow characteristics of the central plane of vehicle cabin

The numerical result of the temperature distribution at the central plane of the vehicle cabin model is drawn in Fig.2-7. It can be seen that there is different temperature distribution in the cabin and the difference is simulated in the range of 8 ℃ after 15 minutes. The maximum average temperature stays about 43 ℃ at the location close to the wind glass and car shell including the front, top and bottom of cabin, Which is due to that the air flow around of these places are easy to be influenced by the heat concentrated in car shell from solar energy. The minimum average temperature remains at 35 ℃ at the rear cabin, which just occupies a little area of cabin. The temperature of most space stays at the range from 39 to 41 ℃.The simulation prediction of the velocity vector magnitude at the central plane of the vehicle cabin is shown in the Fig.2-8. It is easy to see that the air is essentially stagnant with low velocities in the cabin. However, the velocity at the central compartment is much lower than other regions. It can be said that the velocity is very important for maximizing heat transfer rate.

2.5.3 Heat flow characteristics of the horizontal plane of vehicle cabin

The heat flow field of the horizontal plane is shown in Fig.2-9. It can be seen that the temperature of horizontal plane stays in the same range with central plane and the minimum temperature region is still distributed at the rear cabin. However, the maximum average temperature occurs at the left and right side vehicle. The simulation result of the velocity vector magnitude at the horizontal plane of the vehicle cabin is presented in Fig.2-10. It is found that the air at the horizontal plane also moves with the low velocity in the cabin. The minimum velocity is calculated at the front cabin with small area. There is a good agreement of region distribution between the temperature and velocity.

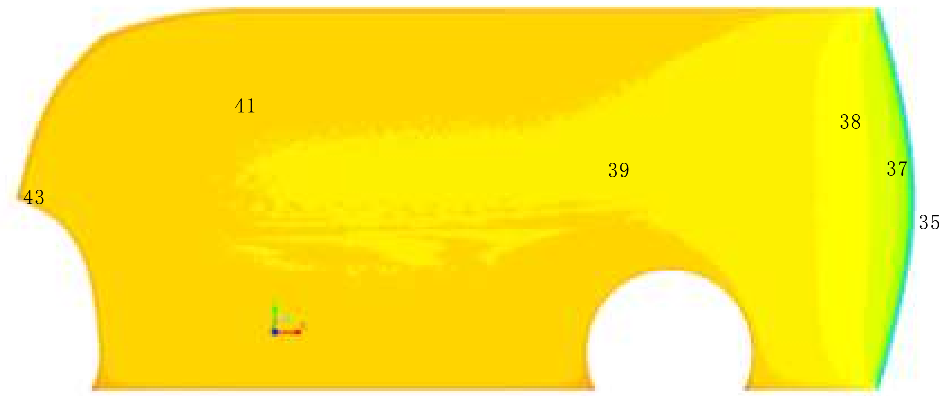

Fig.2-7 Numerical result of the temperature distribution (℃) at the central plane cabin

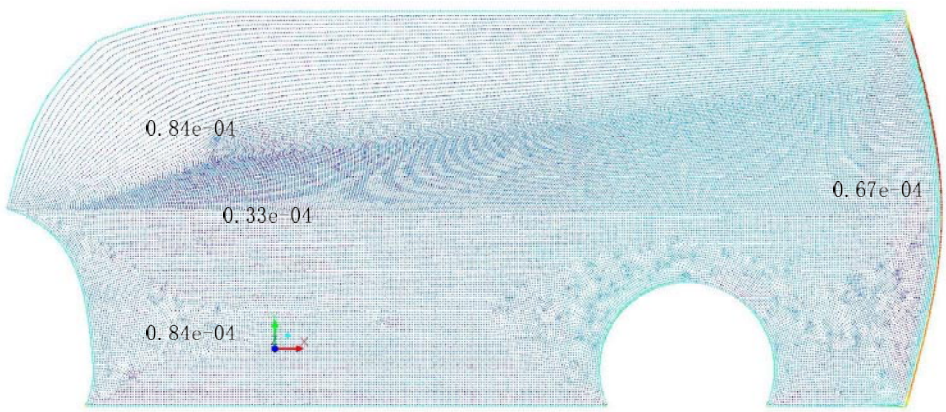

Fig.2-8 Numerical result of the velocity vector magnitude (m/s) at the central plane cabin

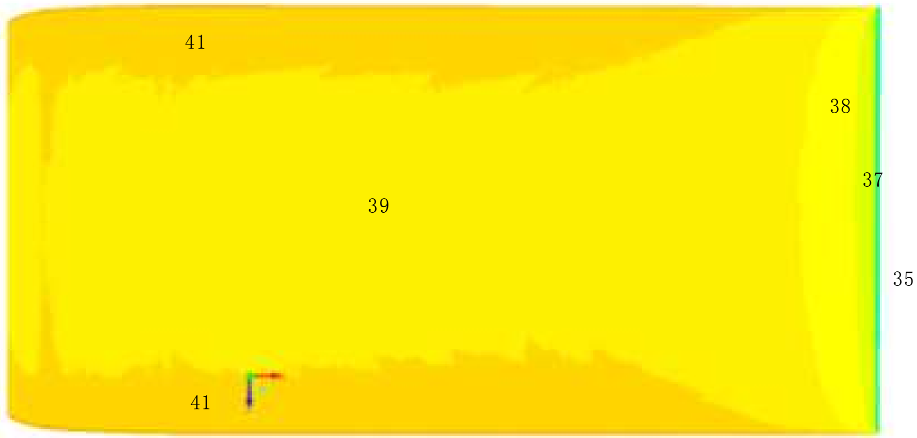

Fig.2-9 Numerical result of the temperature (℃) distribution at the horizontal plane cabin

Fig.2-10 Numerical result of the velocity vector magnitude (m/s) at the horizontal plane cabin

2.5.4 Heat flow characteristics of whole model

The heat flow transferred from the wall surface at a given temperature to the inner of vehicle cabin is obtained by solving the momentum and energy equations, which is derived under the assumption of constant material properties, but in reality the density, pressure and thermal conductivity of air will changes strongly with temperature. After 15 minutes numerical calculation, the reality thermal properties of the whole cabin can be observed directly from the results of the analysis through the graphics and plots. The pressure, density and temperature of the whole cabin are given in the Fig.2-11.

From these pictures, it can be easy to see that the pressure of the vehicle cabin has not any variation in the numerical time. The front row of cabin has higher temperature than other space, which is accorded with the report that the front row is the most dangerous space when the car parking under the sunshine because the radiation can enter into the cabin through the wide area of the front window glass. Also, the turbulent characters of front row are seen to be different from the other space, which is shown in Fig.2-12. The front row has higher turbulent intensity and bigger turbulent dissipation rate which can drive the air flow to move rapidly and cause the heat transfer from high temperature of wall to the low inner space, which can explain the reason why the front row has higher temperature than other space in the vehicle cabin. In addition, the wall fluxes has also shows much higher value in the front row and the solar heat flux shows stronger radiation at the surface of the vehicle, which is also agreement with the analysis about temperature characters before.

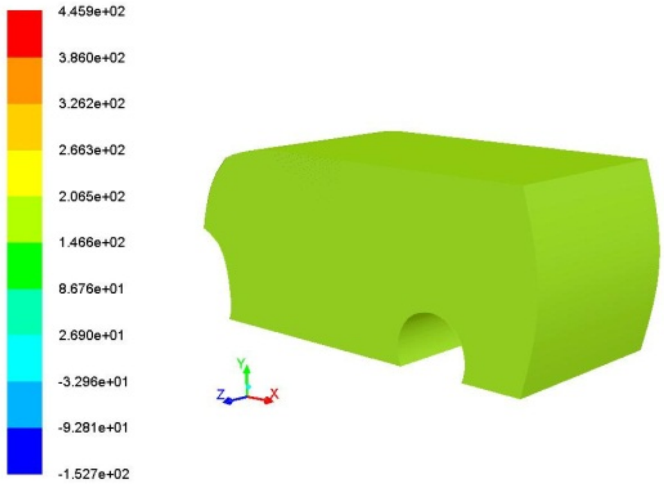

(a)

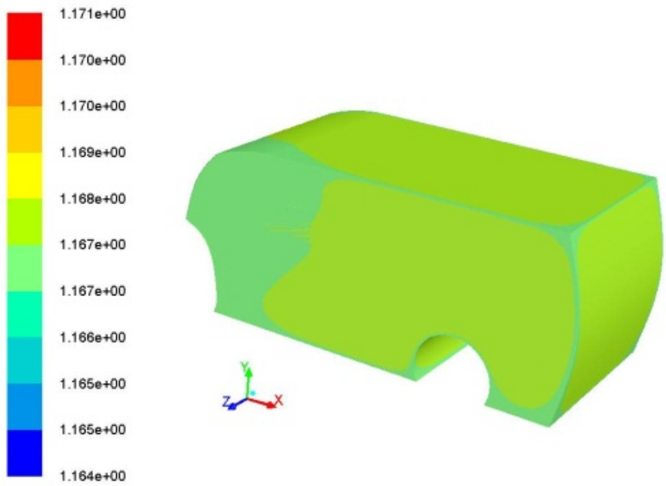

(b)

Fig.2-11 Thermal properties of whole cabin view, (a) Pressure (Pa); (b) Density (kg/m^3)

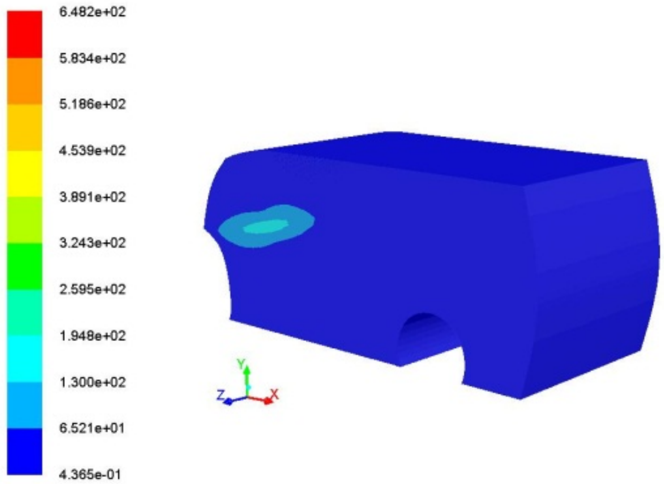
6.482e+02
5.834e+02
5.186e+02
4.539e+02
3.891e+02
3.243e+02
2.595e+02
1.948e+02
1.300e+02
6.521e+01
4.365e-01
Y
Z
X

(a)

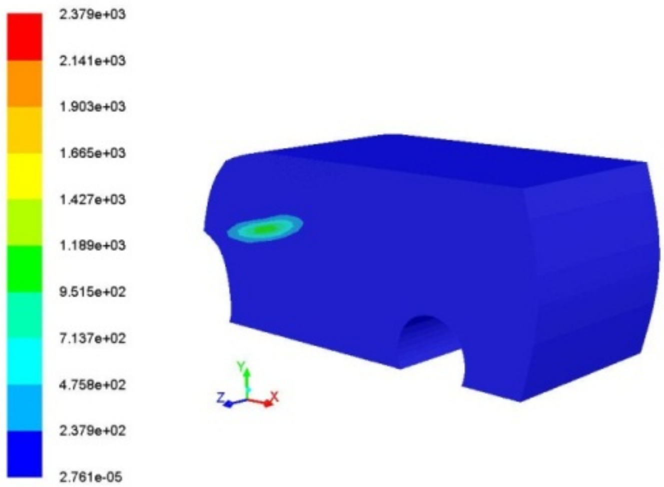
2.379e+03
2.141e+03
1.903e+03
1.665e+03
1.427e+03
1.189e+03
9.515e+02
7.137e+02
4.758e+02
2.379e+02
2.761e-05
Y
Z
X

(b)

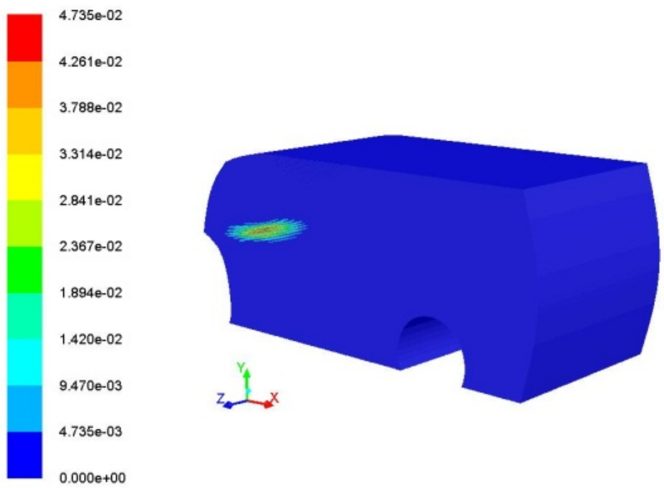

(c)

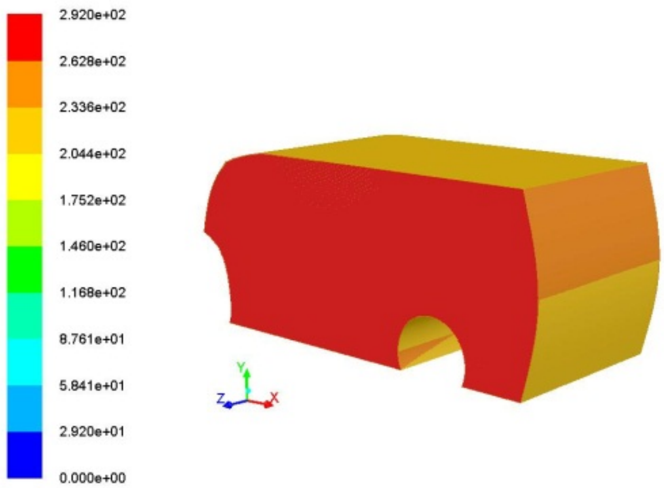

(d)

Fig.2-12 Turbulent properties of whole cabin view, (a) Turbulent intensity (%); (b) Turbulent dissipation rate (m^2/s^3); (c) Wall shear stress (Pa); (d) Solar heat flux (W/m^2)

2.5.5 Heat flow rate calculation

The total heat of cabin obtained from solar heat can be calculated by using the heat flow rate to multiply by the simulation time when car parking under sunshine. The total heat transfer rate of each wall surface of vehicle cabin after 15 minutes is shown in the Table 2-2. The whole cabin has got 112.02 kW heat in the 15 minutes. From this table, it can be easy to see that plenty of heat focuses on the roof of cabin due to the simulation time that is at noon when sun is just located right above of the roof. The bottom surface also has high heat can attribute to the height of bottom from ground is much too small so that the heat cannot flow fast and concentrate together.

Table 2-2 Total heat transfer rate at different direction (W)

Wall surface	Total heat transfer rate
Roof	1652.62
Front	403.68
Back	661.78
Bottom	1628.19
Left side	1579.13
Right side	1542.27
Net	7467.68

2.6 Conclusion

This chapter used CFD analysis software to predict the heat flow distribution in the simplified 3-D STEPWGN vehicle cabin when parking under sunshine. The constant environment boundary conditions were presumed to apply in this simulation. The nature convection and radiation heat transfer from environment to cabin were considered and the distribution of transient temperature and velocity at the central and horizontal plane were analyzed respectively. The experimental test had been carried out in a stable environment the same as the boundary conditions of simulation to validate the numerical calculation. The following results are obtained:

(a). The temperature of vehicle cabin increases by time and the predicted transient temperatures have good agreement with the experimental results, which shows the reliability of models and simulation method. The highest temperature is concentrated at the front side close to the windshield and the region of front row has higher temperature than back row.

(b). The air velocity of vehicle cabin stays at the lower level and the central compartment has much lower velocity than other regions of the cabin.

(c). The region of front row has stronger turbulent motion than back row, which is the reason why front row has higher temperature than back row.

The vehicle model used in this paper is supposed to be a simplified one without any in-car facility. The next work is going to analyze the entire vehicle with chairs and to simulate the heat flow distribution when air conditioning working.

References

[1] Tomohiro Kitagawa, Kiyoshi Kawaguchi, Daisuke Watanabe and Ryota Toyohara: Reducing Temperature in a Parking Automobile under Summer Solar Radiation, 49th Japan Heat Transfer Symposium proceedings, 2012.

[2] William S. Janna, Engineering heat transfer: third edition, Great Britain, 2009.

[3] http://www.honda.co.jp/

[4] Richard C. Farmer, Gary C. Cheng, Yen-Sen Chen, Ralph W. Pike, Computational transport phenomena for engineering analyses, USA, 2009.

[5] Robert Parsons, ASHRAE Handbook Fundamentals, 1997.

[6] Massoud Kaviany, Essentials of heat transfer, USA, 2011.

[7] J. J. Finley, Heat treatment and bending of low-E glass, Thin Solid Films, 351(1-2):264-273, 1999.

[8] A. Mezrhab, M.Bouzidi, Computation of thermal comfort inside a passenger car compartment, applied thermal engineering, 26(14-15):1697-1704, 2006.

[9] ANSYS Inc. Fluent Manuals.

[10] Shinichiro Wakashima: on Developemnt of the Thermal Environment Simulator of an Automobile, 47th Japan Heat Transfer Symposium proceedings, 2010.

[11] Gokhan Sevilgen, Muhsin Kilic: Transient Numerical Analysis of Airflow and Heat Transfer in a Vehicle Cabin During Heating Period, Int. J. Vehicle Design, Vol. 52, Nos. 1/2/3/4, 2010.

[12] J. Kohler, Numerical Calculation of the Distribution of Temperature and Heat Flux

in Buses under the Influence of the Vehicle Air-conditioning System, ASHRAE Trans, 96 (1), 432–446, 1990.

[13] Deyi Shang, Theory of heat transfer with forced convection film flows, springer, 2010.

[14] Massoud Kaviany, Essentials of heat transfer, USA, 2011.

[15] W. K. Chow, Philip C. H. Yu, Simulation on energy use for mechanical ventilation and air-conditioning (MVAC) systems in train compartments, Energy, 25 (1): 1-13, 2000.

Chapter 3
Analysis of Heat flow in Vehicle Cabin with Traditional Air Conditioning System

3.1 Chapter introduction

The heat of vehicle cabin from sunshine can be driven out by the air conditioning and it also can help to adjust the humidity of cabin. To a large extent, air conditioning system determines the thermal comfort of a vehicle. Therefore, the performance of air conditioning has been becoming more and more important to consider when consumers decide to buy a new car. Even though the device of traditional air conditioning system of a car is installed with standard configuration, the performance of various kinds of car is shown differently. Some cars have lower absolute temperature at the air outlet, but the inner temperature still hold at a high level. Moreover, some cars have terrible temperature gradient between the front row and back row because the wind from outlet cannot reach to the rear of cabin quickly. And also, the size and structure of cabin play a role to affect air conditioning working [1-2]. Therefore, this chapter is focus on the traditional air conditioning to analyze the cooling performance of a car by numerical simulation and experimental validation. The representative car of Honda Company—N box is used as the research object which can be seen in Fig.3-1[3]. The numerical study has analyzed the air flow and heat transfer characteristics of inner cabin, especially at the place of wind outlet and inlet. In order to validate the numerical study, the experimental study has taken place in a stable environment as same as the boundary conditions setting of simulation.

Fig.3-1 Representative car of Honda Company—N box

3.2 Experimental investigation

The experiments were performed under the natural convection conditions. Ambient environment was quiescent without any wind since the conditions of natural convection will be requested in this experiment. The relative humidity was determined at about 60% and the ambient temperature stayed at 28.6 ℃. Before the operation of air conditioning, the engine of car was flameout to be cooling and all the doors were opened to make the in-car air flow to maintain almost same as that of outside environment. After one hour`s ventilation, the temperature of vehicle cabin can be considered the same as the ambient temperature and the car dashboard showed that the temperature was 30.1 ℃.

The experiment measuring time was set for 15 minutes in 5-minute intervals, which can be obtained three sets of data for one test. In order to eliminate accidental errors, the multiple measurements were performed and three sets of test were carried out due to time constraints. The internal recirculation of vehicle cabin was used in this experiment as the way of refrigeration. The wind mode was set as only blowing the upper body of passengers and all the vent of wind were directed toward horizontal direction. For the purpose of calculating the energy consumption under the saving model, the air temperature was set at 25 ℃ and the wind was set at the lowest speed. Moreover, the inner temperature will be affected by interior colors, space size and many other factors. Hence, nine measuring points were picked up to monitor the temperature variation at different part of cabin. Four points were fixed at the position of face when passengers sitting in the car including the front row and rear row. In addition, the temperature and velocity of wind at vent can reflect the real absolute cooling capacity of air conditioning of cabin. Therefore, four points were put at four wind outlets individually to measure each temperature of them and another point was selected at the inlet of air conditioning which is located at the front of cabin close to windshield. All the measuring points are given in detail in the Fig.3-2. The infrared temperature probe was used in this experiment and the measuring points were fixed at the position. The anemometer was used in the test to determine the velocity of wind from the outlet of air conditioning in the vehicle cabin. In order to calculate the energy consumption, the fuel tank of car was filled up before and after experiment. The last oil mass added was recorded as the energy consumption of air conditioning system.

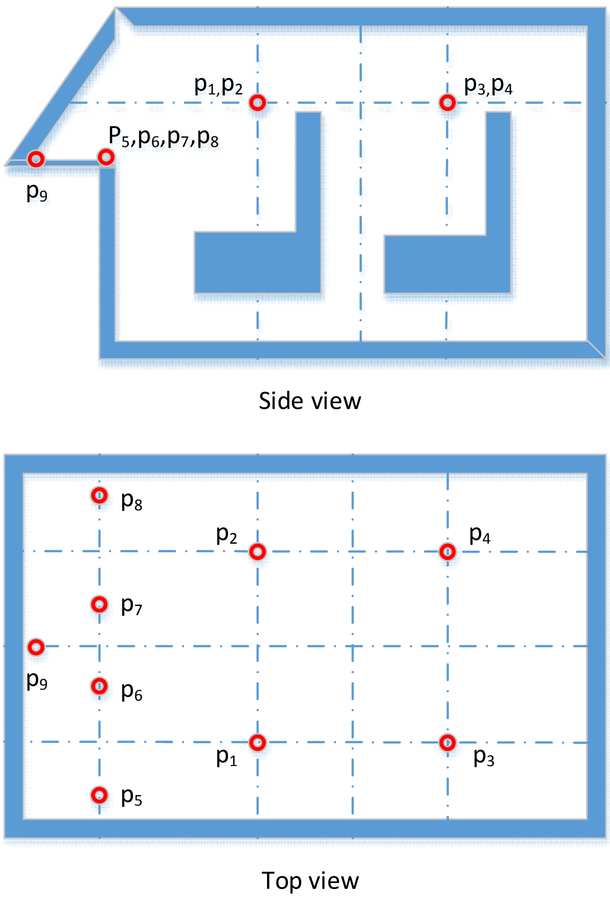

Fig.3-2 Measuring points of temperature in the vehicle cabin

3.3 Numerical simulation

In order to comprehend the thermal motion process in the cabin when air conditioning is operated, the numerical simulation analysis was used in this study. Based on the structure of the objective vehicle, the geometry model profile with real dimensions was drawing by the AutoCAD software and the mesh was created by Gambit which can be input to the CFD analysis software to carry out the numerical simulation. And then, the boundary conditions including the wind outlet and inlet of the vehicle air conditioning system were set according to the data obtained from the experiment before [4-5].

3.3.1 Model geometry

The geometry model of vehicle cabin was created by the AutoCAD software with real dimensions and shape. However, this model was simplified and the computational domain only consists of the inner space of the cabin and the chairs without any other in-car facilities, for example, the steering wheel. And then the model was exported to Gambit software to generate mesh for numerical analysis. In the process, this mesh generation consisted of 19840275 hexahedral elements. The space under the seat was not included in the computational domain. The wind outlet of air conditioning system was marked using blue parts including four outlets on the front of surface of the cabin and the wind inlet was marked using red parts, which can be seen in the Fig.3-3. The shape of wind outlet had been made a little change compared to the original. It had been simplified as a square since the original roundness had difficult to mesh and simulate accurately.

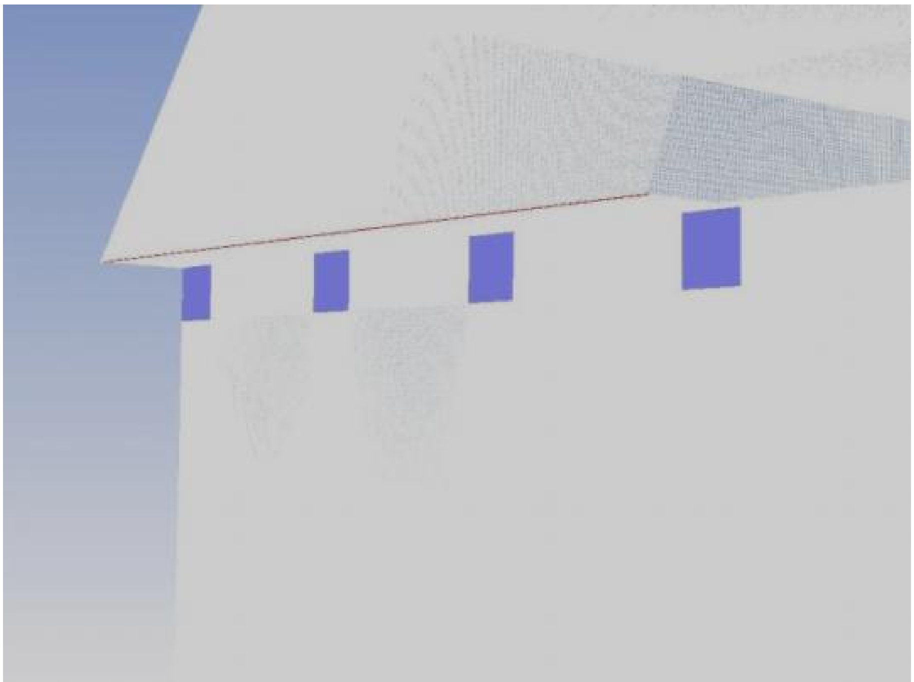

Fig.3-3 Wind outlet and inlet model of air conditioning in the vehicle cabin

3.3.2 Boundary conditions and problem setup

In this simulation, the physical properties of analysis objects were set as same conditions as the last chapter. The surface boundaries of cabin were regarded as solid walls including the roof, the bottom, the door and the windows, which were defined as the stationary wall and semi-transparent. However, the thermal boundary conditions of wall had a little change compared with last chapter. In order to simplify algorithm and accelerate convergence, the heat from solar energy had not been considered in the calculation and a fixed wall temperature was set as the thermal condition, which was equal to the ambient temperature due to the short calculation time. According to the empirically determined data, the wall setup and boundary conditions are presented in Table 3-1.

Table 3-1 Wall setup and boundary conditions

Category	Parameter	Internal	External
Physical properties	Fluid	Air	Aluminum
	Density [kg/m^3]	1.177	2719
	Cp [J/kg-K]	10046.43	871
	Thermal conductivity (W/m-K)	0.0242	202.4
	Viscosity [kg/m-s]	1.7894e-05	/
	Thermal expansion coefficient [1/K]	3.356e-03	/
Boundary conditions			
Momentum	Wall motion	/	Stationary
	Shear condition	/	No slip
	Wall roughness height (m)	/	0
	Wall roughness constant	/	0.5
Thermal conditions	Temperature (℃)		30
	Wall thickness (m)		0.02
	Heat generation rate (W/m^3)		0

On the other hand, the air flow of inner cabin can be driven by the wind velocity of air conditioning. Hence, the wind outlet can be defined as a mass flow inlet [6].

Conversely, the wind inlet of air conditioning was regarded as an outlet of this model. The detail setup of momentum and thermal conditions are given in the Table 3-2.

Table 3-2 Mass flow inlet setup

Category	Parameter	Value
Momentum	V(mass flow rate) [kg/s]	0.0085
	Turbulent Intensity [%]	10
	D (Hydraulic Diameter) [m]	0.1
	Gauge pressure [Pa]	0

According to the recording data obtained from the experiment before, the temperature mass flow inlet that is wind outlet of air conditioning system changed by time. The temperature variation of the four wind outlets with time is shown in Fig.3-4. A user-defined function was carried out to improve the function of numerical calculation. Hence, the mass flow inlet temperature became an equation of time [7].

In this simulation, the air flow motion in cabin can be regarded as an internal circulation and the model domain was calculated by using the pressure-based solver with the transient time and absolute velocity formulation. The energy and transport governing equations were discretized by the finite volume method and SIMPLE algorithm was adopted for the coupling between pressure and velocity. The k-ε (2εqn) turbulent model derived from the instantaneous Navier-Stokes equations was chosen in this simulation in conjunction with the standard wall function for the near wall region treatment [8]. The time step of this numerical calculation was taken as one second.

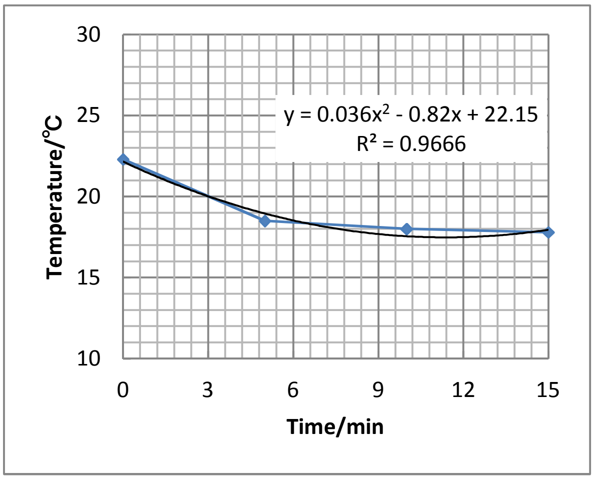
30
25
20
15
10
Temperature/°C
y = 0.036x² - 0.82x + 22.15
R² = 0.9666
0
3
6
9
12
15
Time/min

(a)

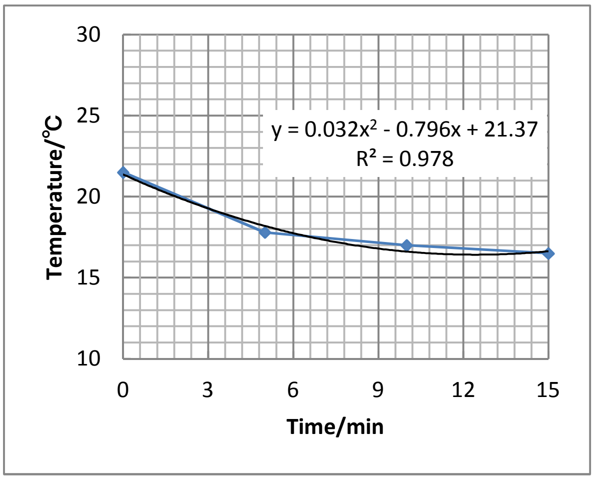
30
25
20
15
10
Temperature/°C
y = 0.032x² - 0.796x + 21.37
R² = 0.978
0
3
6
9
12
15
Time/min

(b)

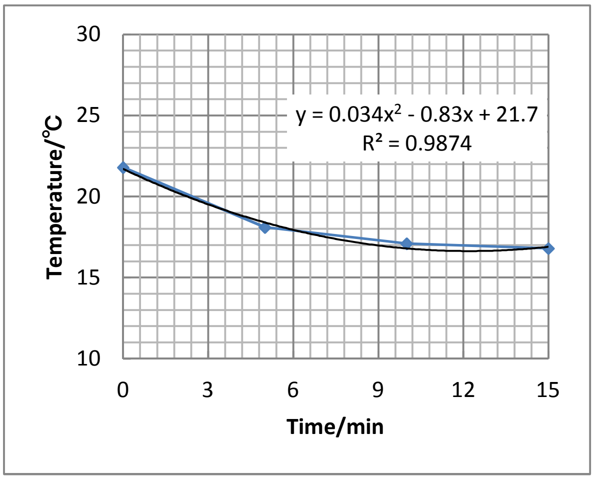

(c)

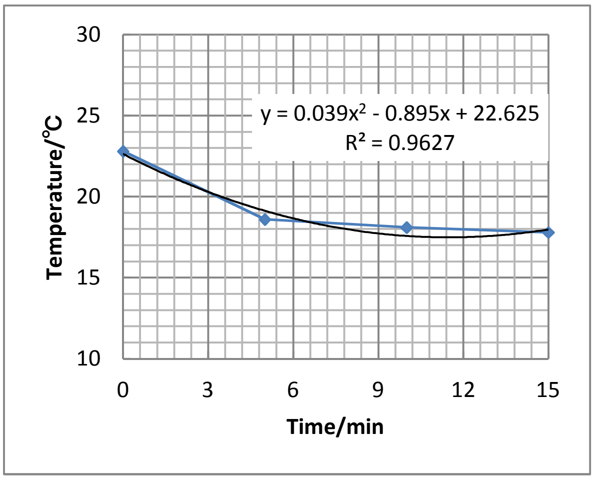

(d)

Fig.3-4 Temperature variation of wind outlets with time, (a) P5; (b) P6; (c) P7; (d) P8

3.4 Results and discussion

3.4.1 Validation of the results

On the basis of experimental data of three times gathered, the simulation results are validated by comparison of the predicted temperature values and the measuring data at the points located at the front and back seats, which is displayed in Figure 3-5. It can be easy to see that the predicted results are in good accordance with the experiment result and both of them present same trend with the time. The temperature shows a rapid decrease before five minutes and it has turned to stable conditions in the following 10 minutes. However, the front row has much stronger downtrend than rear row. In the initial 5 minutes, the temperature of front seat can drop to 25 ℃ which is the set value of experiment and back seat remains over 28 ℃, which shows a big temperature gradient of 3 ℃. The two points located at same row show almost similar experimental and simulated temperature, individually. In addition, from the figure it can be seen that at the back row (selected points p_3 and p_4), the differences between calculation and experimental temperature are about 1 ℃. However, at the front row (selected points p_1 and p_2), this value rises to 2 ℃ in general and it has an increased trend with the time, which shows a worse deviation with the measuring data.

At the wind outlet and inlet of air conditioning, the comparisons of experimental data and simulation results are shown in Figure 3-6. On the one hand, it can be seen that the simulation values of wind outlet (selected points p_5-p_8) have good agreement with the experimental value. In order to save energy, the cabin temperature was set at 22 ℃. In the initial 5 minutes, the temperature of outlet was measured to drop to 18 ℃ which is lower than the set value. In the following 10 minutes, the downtrend of four wind outlets has turned to slow down and the temperature keeps at about 17 ℃. On the other hand, the predicted results of wind inlet (selected point p_9) are also in good agreement with the experiment result and the differences of temperature between of both are below 1 ℃. Also, both of them present the same trend with the time. The rapid decrease is shown in the initial 5 minutes and then the temperature keeps a slow downtrend in the following 10 minutes.

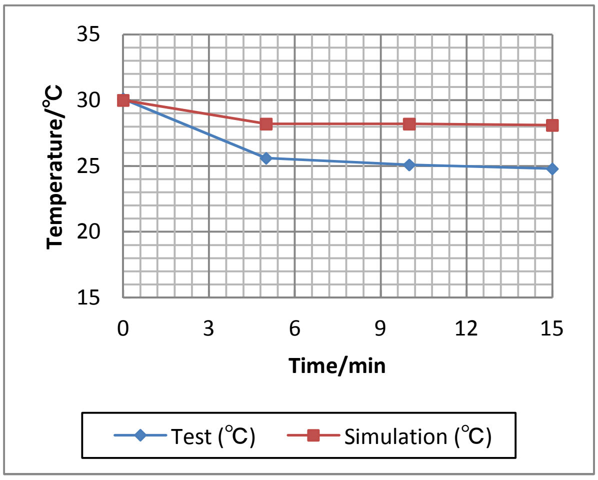
Temperature/℃
35
30
25
20
15
0
3
6
9
12
15
Time/min
Test (℃)
Simulation (℃)

(a)

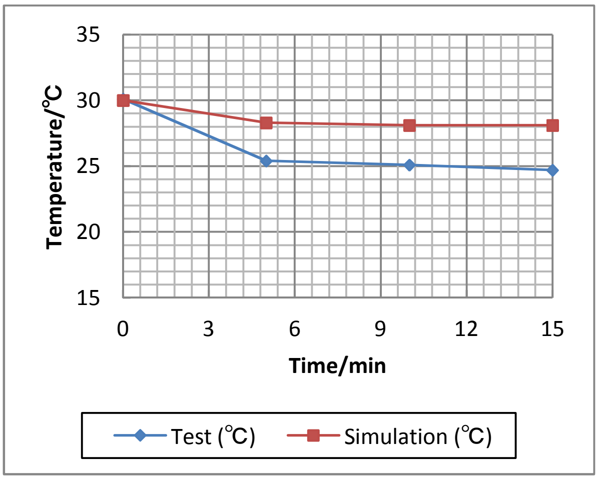
Temperature/℃
35
30
25
20
15
0
3
6
9
12
15
Time/min
Test (℃)
Simulation (℃)

(b)

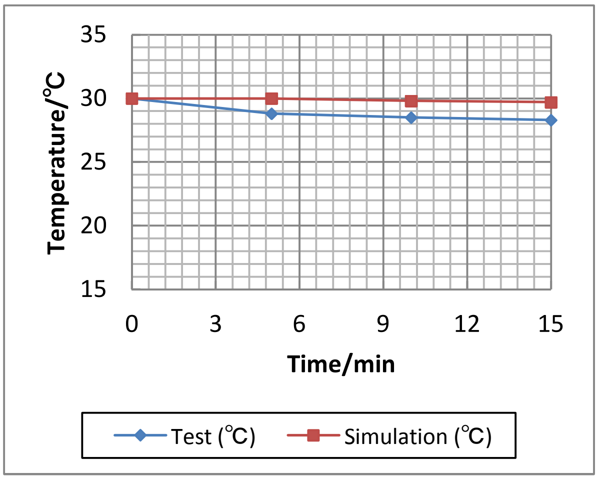

(c)

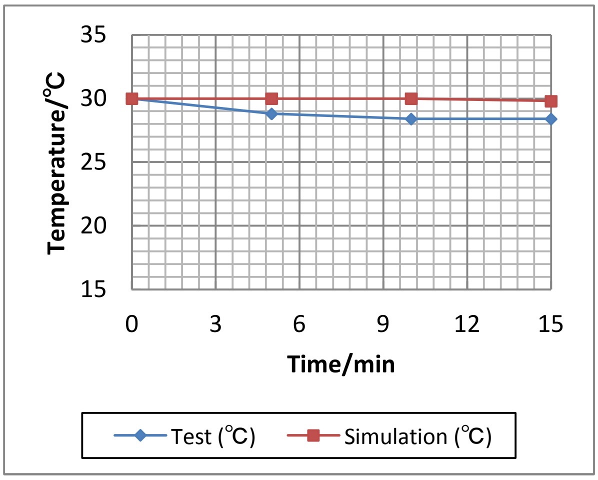

(d)

Fig.3-5 Temperature comparison of simulation results with experimental data, (a) P_1; (b) P_2; (c) P_3; (d) P_4

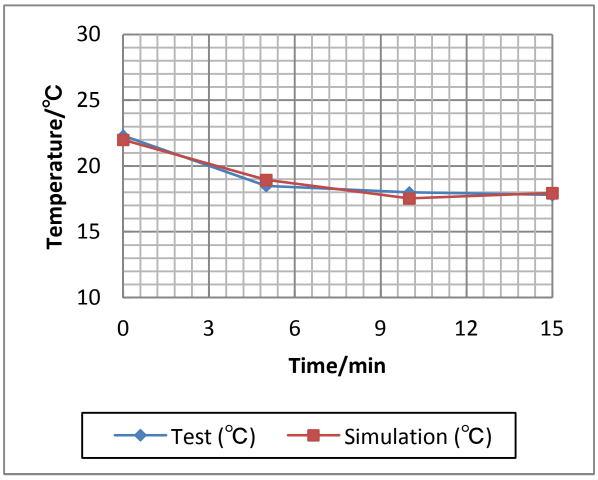
30
25
20
15
10
Temperature/℃
0
3
6
9
12
15
Time/min
Test (℃)
Simulation (℃)

(a)

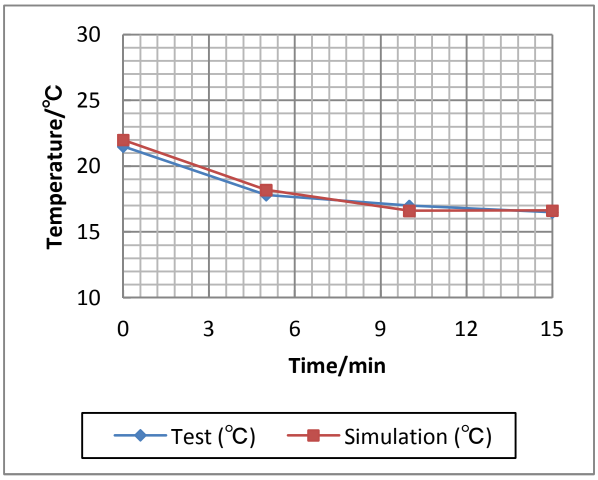
30
25
20
15
10
Temperature/℃
0
3
6
9
12
15
Time/min
Test (℃)
Simulation (℃)

(b)

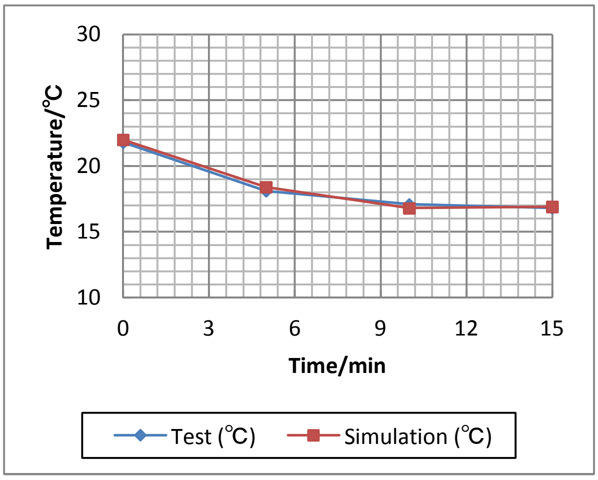
30
25
20
15
10
Temperature/℃
0
3
6
9
12
15
Time/min
Test (℃)
Simulation (℃)

(c)

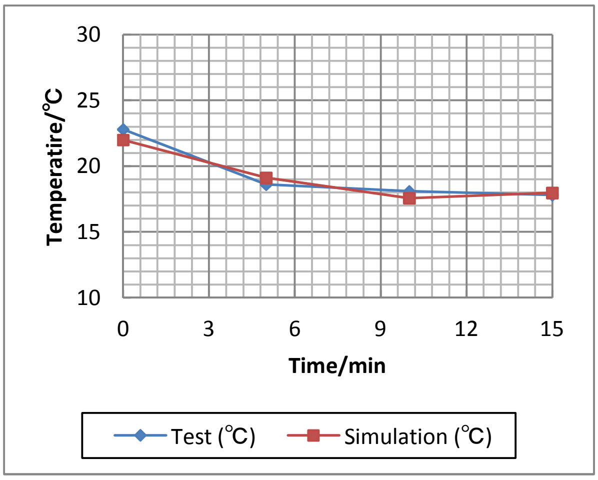
30
25
20
15
10
Temperatire/℃
0
3
6
9
12
15
Time/min
Test (℃)
Simulation (℃)

(d)

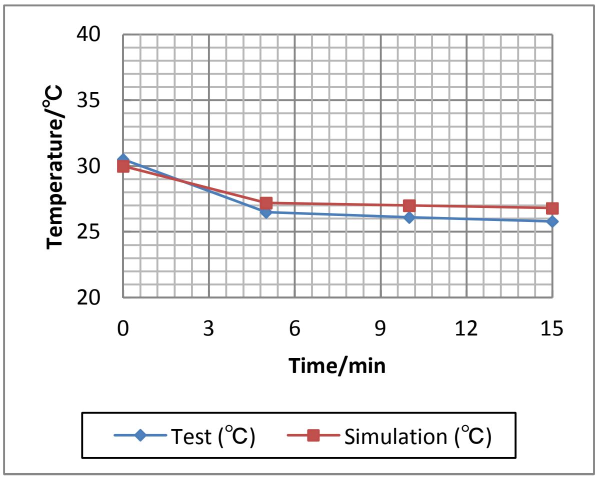

(e)

Fig.3-6 Temperature comparison of simulation results with experimental data, (a) P_5; (b) P_6; (c) P_7; (d) P_8; (e) P_9

3.4.2 Heat flow characteristics of whole cabin

The stable numerical results of thermal characteristics are obtained after calculating for 15 minutes. By solving the momentum and energy equations, the heat flow characteristics of the whole cabin including pressure and turbulent property of air are shown through the following graphics and plots.

Actually, thermal performance of air conditioning can be optimized by the appropriate wind outlet. If it is open at the right place the wind outlet can provide suitable wind to make the passengers feel more comfortable in a relatively short working time [9], which can help vehicle to save more energy. Therefore, the heat flow characteristics analysis of cabin plays a significant role because it can help to find out the right place where the wind outlet should be open.

The heat flow characteristics of whole vehicle cabin including wind outlet and inlet of air conditioning system are given in the Fig.3-7. It can be easy to see that the density of air in the cabin has no change during the test time. But the pressure of wind outlet and inlet are quite different from other location because the wind drives the air flow moving and causes the pressure change. Also, it can be obvious to see the front row of cabin has lower temperature than the rear row. The same reason is due to the wind of front row which is difficult to blow to the rear row since the structure of cabin. Obviously, traditional air conditioning can just reduce the temperature of rear row to 28 ℃ (301K) which is still not comfortable for passengers. Therefore, this cooling model cannot satisfy all the passengers of the cabin, which is consistent with the experimental results.

In addition, the turbulent characteristics of front row are seen to be different from the other space in the cabin, which is shown in Fig.3-8. From the picture, it can be easy to see that the front row has quite stronger turbulent intensity and turbulent dissipation rate than other region. These factors can drive the air flow of cabin to move rapidly and conduct the heat transfer from high to low, which is the reason why front row has lower temperature than the rear row [10].

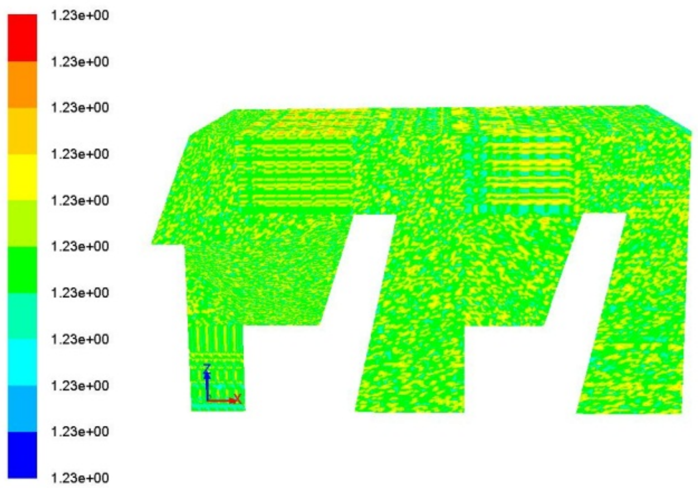
1.23e+00
1.23e+00
1.23e+00
1.23e+00
1.23e+00
1.23e+00
1.23e+00
1.23e+00
1.23e+00
1.23e+00
1.23e+00

(a)

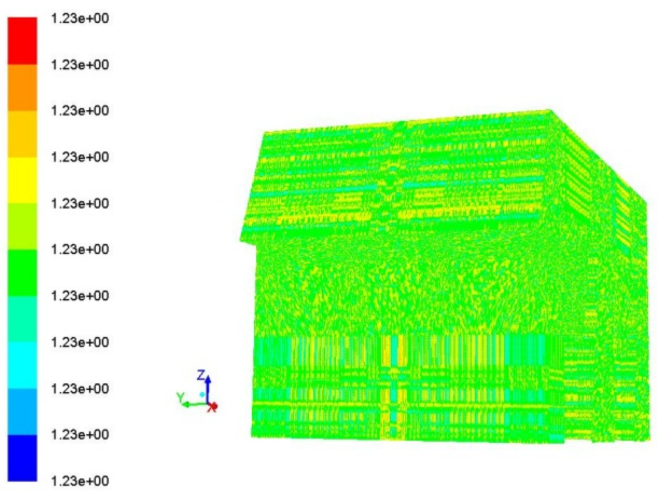
1.23e+00
1.23e+00
1.23e+00
1.23e+00
1.23e+00
1.23e+00
1.23e+00
1.23e+00
1.23e+00
1.23e+00
1.23e+00

(b)

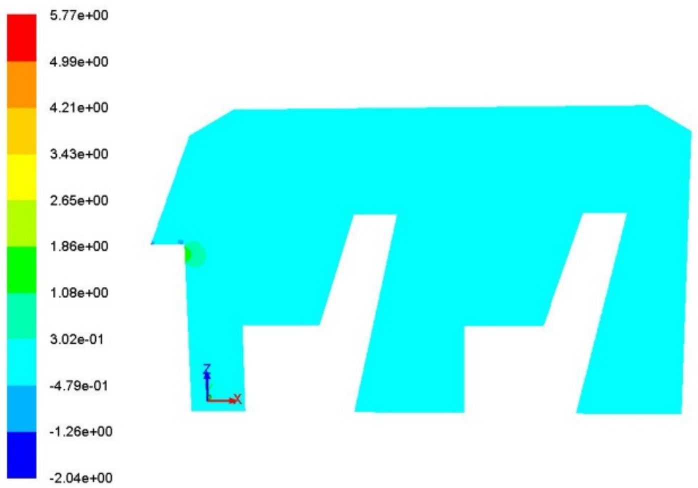
5.77e+00
4.99e+00
4.21e+00
3.43e+00
2.65e+00
1.86e+00
1.08e+00
3.02e-01
-4.79e-01
-1.26e+00
-2.04e+00

(c)

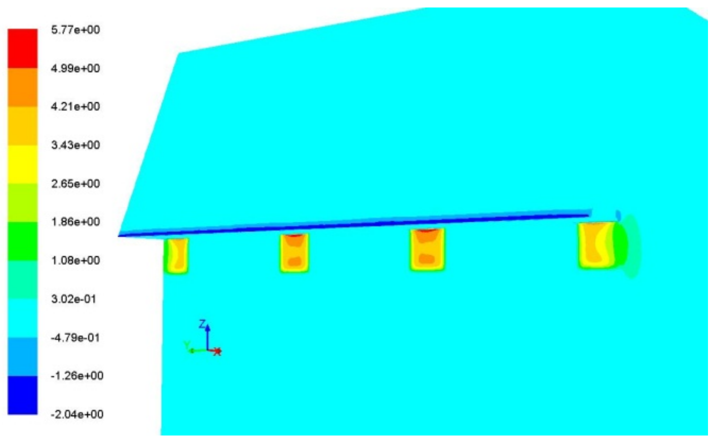
5.77e+00
4.99e+00
4.21e+00
3.43e+00
2.65e+00
1.86e+00
1.08e+00
3.02e-01
-4.79e-01
-1.26e+00
-2.04e+00

(d)

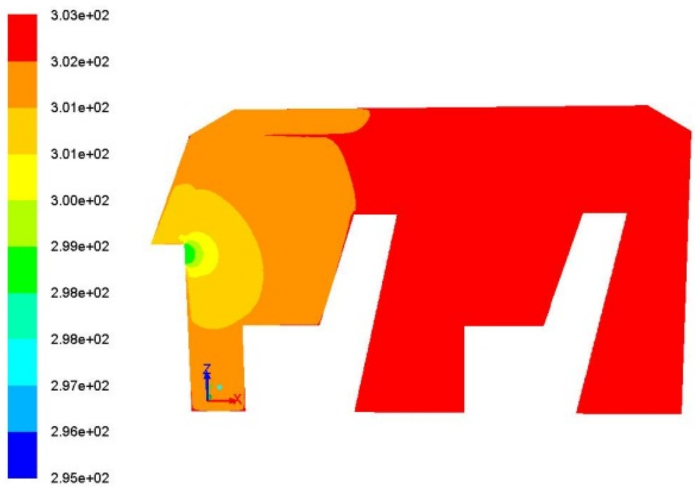

(e)

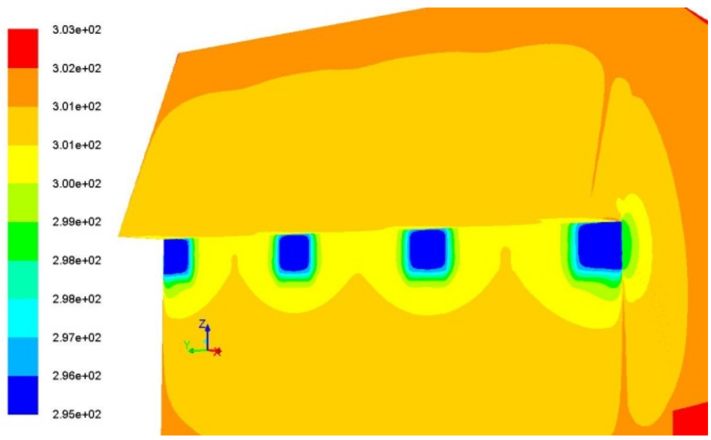

(f)

Fig.3-7 (a)(b) Density (kg/m^3) view of whole cabin; (c)(d) Pressure (Pa) view of whole cabin; (e)(f) Temperature (K) view of whole cabin.

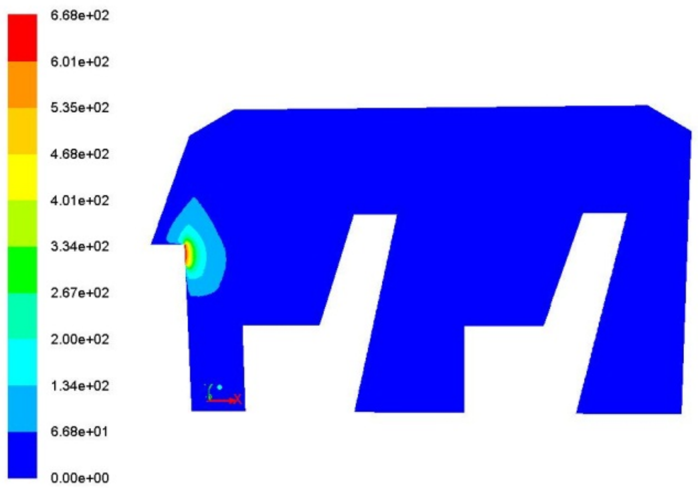
6.68e+02
6.01e+02
5.35e+02
4.68e+02
4.01e+02
3.34e+02
2.67e+02
2.00e+02
1.34e+02
6.68e+01
0.00e+00

(a)

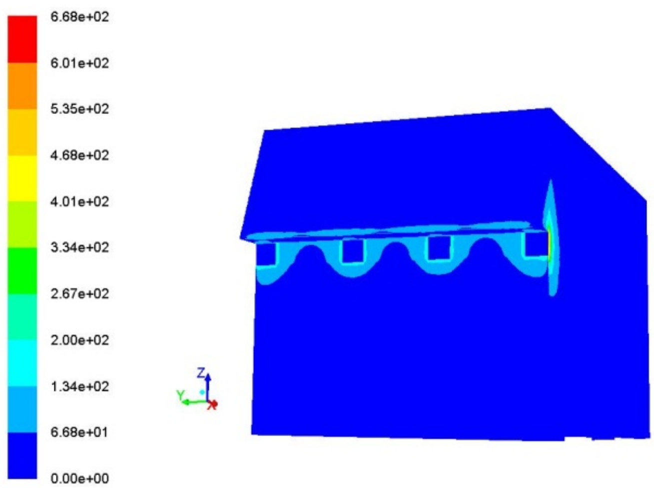
6.68e+02
6.01e+02
5.35e+02
4.68e+02
4.01e+02
3.34e+02
2.67e+02
2.00e+02
1.34e+02
6.68e+01
0.00e+00

(b)

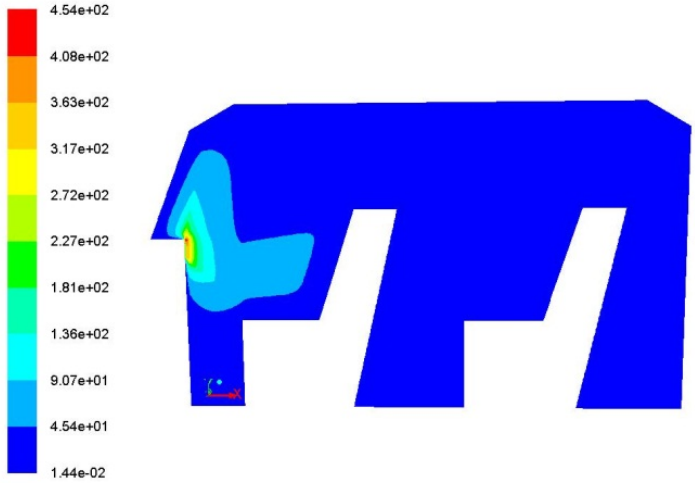
4.54e+02
4.08e+02
3.63e+02
3.17e+02
2.72e+02
2.27e+02
1.81e+02
1.36e+02
9.07e+01
4.54e+01
1.44e-02

(c)

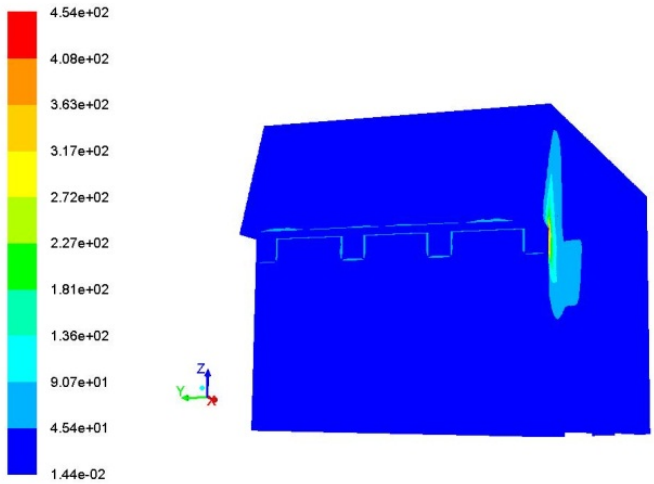
4.54e+02
4.08e+02
3.63e+02
3.17e+02
2.72e+02
2.27e+02
1.81e+02
1.36e+02
9.07e+01
4.54e+01
1.44e-02

(d)

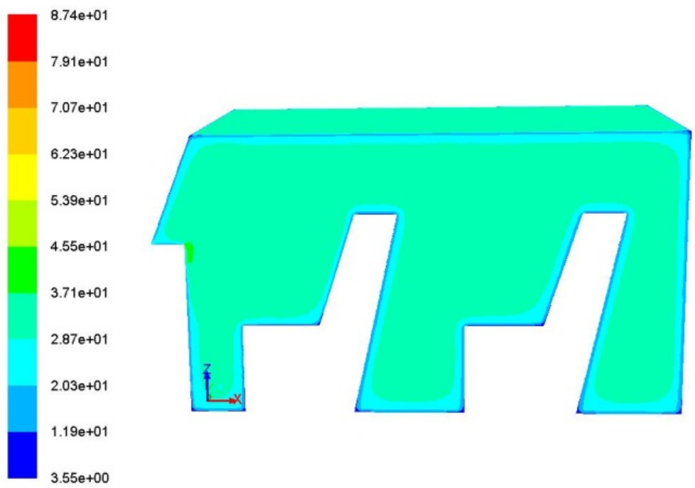
8.74e+01
7.91e+01
7.07e+01
6.23e+01
5.39e+01
4.55e+01
3.71e+01
2.87e+01
2.03e+01
1.19e+01
3.55e+00

(e)

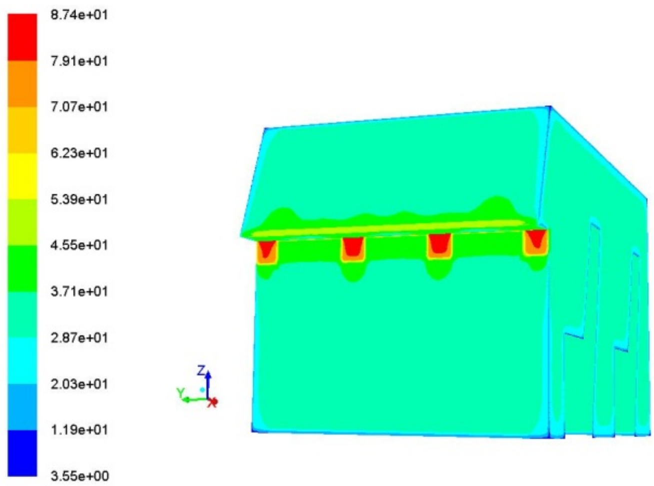
8.74e+01
7.91e+01
7.07e+01
6.23e+01
5.39e+01
4.55e+01
3.71e+01
2.87e+01
2.03e+01
1.19e+01
3.55e+00

(f)

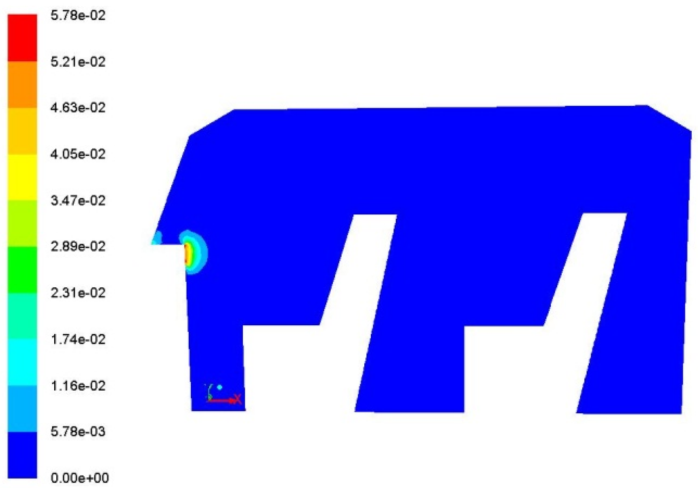

(g)

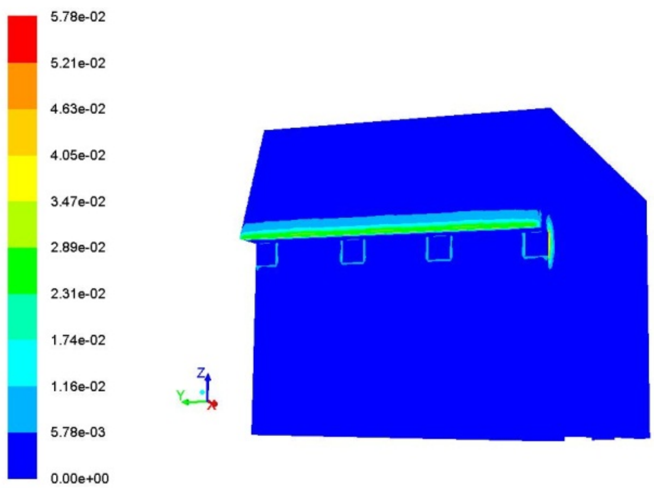

(h)

Fig.3-8 (a)(b) Total heat surface flux (W/m^2) of whole cabin. (c)(d) Turbulent dissipation rate (m^2/s^3) of whole cabin. (e)(f) Turbulent intensity (%) of whole cabin. (g)(h) Wall shell stress (Pa) of whole cabin.

3.4.3 Heat flow calculation

The total heat of cabin obtained from environment of outside can be calculated by using the heat flow rate to multiply by the simulation time when air conditioning is working. According to the heat flow reports of simulation results, the total heat transfer rate at each wall surface between ambient and vehicle cabin can be seen in the Table 3-3. Through the calculation, the whole cabin has got heat 2333.55 W after 15 minutes. When temperature of cabin is adjusted to the normal room temperature, the energy consumption of air conditioning would be calculated according to this basic data. From this table, it can be easy to see that the heat transfer rate turns to decrease by time. There is much more heat getting into the cabin through the front wind glass than other surface and the minus value of total energy shows the heat transfer from cabin to ambient by air conditioning.

The mass flow rate is given in the Table 3-4. According to the boundary setting, the mass flow rate keeps in a stable condition. Hence, these values remain the set value without any variation in the simulation time of 15 minutes.

Table 3-3 Total heat transfer rate at different direction (W)

Time / Wall surface	5 minutes	10 minutes	15 minutes
Back	15.37	12.23	10.56
Bottom	16.10	11.55	9.79
Chair1	79.61	69.23	61.13
Chair2	24.90	19.51	17.42
Front	101.53	88.87	78.04
Inlet1	-74.27	-58.56	-49.04
Inlet2	-103.13	-87.61	-77.51
Inlet3	-103.11	-87.59	-77.50
Inlet4	-74.36	-58.62	-49.08
Left side	57.44	49.60	44.63
Outlet	90.41	94.44	98.35
Right side	57.41	49.58	44.62
Roof	54.59	49.02	44.17
Net	142.49	151.64	155.57

Table 3-4 Mass flow rates at different direction (kg/s)

Wall surface	Mass flow rate
Back	0
Bottom	0
Chair1	0
Chair2	0
Front	0
Inlet1	0.0085
Inlet2	0.0085
Inlet3	0.0085
Inlet4	0.0085
Left side	0
Outlet	-0.034
Right side	0
Roof	0
Net	-2.51E-08

3.4.4 Energy consumption calculation

As an economically affordable vehicle, the experimental car has a low-emission engine with cylinder of 0.66 L working volume, which can enhance the efficiency of fuel oil. It has been well known that the vehicle air conditioning is driven by the engine of vehicle. Hence, the air conditioning system has affected the dynamic property and economic efficiency of vehicle. In terms of motor, when it accelerates from a static standing to a certain speed, the car using air conditioned always has lag response without any refreshing. In terms of the economy, it is manifested that the air conditioning has made the fuel oil consumption significant increase compared with no using. In this experiment, the single energy consumption of air conditioning system was measured under the non-driving condition. Based on the average value of three times, the car consumed fuel oil 0.3 L in 15 minutes, this means that the waste fuel oil of air conditioning system can drive about more 2 km distance per hour (according to the JC08 model fuel fee of N box).

3.5 Conclusion

This chapter studied the cooling effect of traditional air conditioning system of automobile by numerical simulation and experimental validation. Using the CFD software, a simplified 3-D N box vehicle cabin model was created to analyze the air flow and heat transfer characteristics of inner cabin, especially at the place of wind outlet and inlet during cooling period. The experimental study took place in a stable environment under the same condition with the simulation. Temperature variation during 15 minutes was tested at different location of cabin and the energy consumption was also measured, which makes a comparison with the numerical study. The following results are obtained:

(a). The temperature of vehicle cabin decreases by time and the predicted transient temperatures have good agreement with the experimental results, which shows the reliability of models and simulation method. The back row of cabin has higher temperature than the front row.

(b). The cabin turns to thermal stable after 5 minutes and the oil consumed by air conditioning can help car to drive more 2 km in one hour.

(c). Under save energy model, the temperature gradient is terrible and the back row still has high temperature. The traditional air conditioning system cannot make all the passengers feel comfortable.

The new air conditioning system has been considered to improve the efficiency and enhance thermal comfort for the passengers instead of the traditional one in the next step.

References

[1] Richard C. Farmer, Gary C. Cheng, Yen-Sen Chen, Ralph W. Pike, Computational transport phenomena for engineering analyses, USA, 2009.

[2] Thoma Lund Madsen, Thermal effects of ventilated car seats, International journal of industrial ergonomics, 13(3):253-258, 1994.

[3] Http://www.honda.co.jp/

[4] ANSYS Inc. Fluent Manuals.

[5] A. Mezrhab, M.Bouzidi, Computation of thermal comfort inside a passenger car compartment, applied thermal engineering, 26(14-15):1697-1704, 2006.

[6] Ambs, R: Improved Passenger Thermal Comfort Prediction in the Pre-prototype Phase by Transient Interior CFD Analysis Including Mannequins, SAE Paper, 2002.

[7] Huajun Zhang, Lan Dai, Guoquan Xu, Yong Li, Wei Chen, WenQuan Tao: Studies of Air-flow and Temperature Fields inside a Passenger Compartment for Improving Thermal Comfort and Saving Energy. Part I: Test/ Numerical Model and Validation, Applied Thermal Engineering, 29: 2022-2027, 2009.

[8] Gokhan Sevilgen, Muhsin Kilic: Transient Numerical Analysis of Airflow and Heat Transfer in a Vehicle Cabin During Heating Period, Int. J. Vehicle Design, Vol. 52, Nos. 1/2/3/4, 2010.

[9] P.Ole Fanger, Human requirements in future air-conditioned environments, International journal of refrigeration, 24(2):148-153, 2001.

[10] Robert Parsons, ASHRAE handbook Fundamentals, 1997.

Chapter 4
Analysis of Heat Flow in Vehicle Cabin with Personal Air Conditioning System

4.1 Chapter introduction

Currently, traditional automobile has been bringing a lot of problems including the environment pollution and energy shortage. In order to resolve these problems, the electric vehicle has been developing and had a rapid increase in recent years. However, the driving distance of battery capacity has been the main problem to perplex the consumers. According to the current electric vehicle, the driving range varies about from 180 to 200 km for one charge. Nonetheless this driving range will be reduced by one third to a half when the air conditioning system is operated. Therefore, energy consumption as little as possible has been taken into account in the design of air conditioning system of electric vehicle. In this chapter, a concept of personal air conditioning system is proposed to replace the traditional one in vehicle. This system can provide comfortable thermal environment for each passenger individually by installed inside of chairs, which could reduce the waste energy at the space of no person in the cabin. In addition, this system is produced by Peltier module and fan motor that can only consume lower electric power to drive so that the saved energy can be used to provide vehicle to drive longer [1-5].

In this study, the car—N box was also used as the model to simulate the thermal characteristics of cabin when using personal air conditioning system. To validate the simulation, thermal comfort and temperature measure was carried out under the same conditions. Also, the energy consumption of the whole system was calculated to make a comparison with traditional one.

4.2 Evaluation of thermal comfort

Generally, thermal comfort is affected by heat conduction, convection, radiation, and evaporative heat loss. Thermal comfort is maintained when the heat generated by human metabolism is allowed to dissipate, thus maintaining thermal equilibrium with the surroundings. It has been long recognized that the sensation of feeling hot or cold is not just dependent on air temperature alone. Since there are large variations from ambient to person in terms of physiological and psychological satisfaction, it is hard to find an optimal temperature for everyone in a given space. Laboratory and field data have been collected to define conditions that will be found comfortable for a specified percentage of occupants [6].

Thermal comfort is the condition of mind that expresses satisfaction with the thermal environment and is assessed by subjective evaluation. Maintaining this thermal comfortable standard for occupants of buildings or other enclosures is one of the important goals of air conditioning system design engineers. The Predicted Mean Vote (PMV) is proposed out and it stands among the most recognized thermal comfortable models [7]. It was developed using principles of heat balance and experimental data collected in a controlled climate chamber under steady state conditions. Because the PMV model was derived from data collected in a controlled climate, it is not suitable for applications in naturally ventilated spaces which often have high levels of air movement. This shortcoming motivated the development of a family of empirical statistical models of thermal comfort in naturally ventilated spaces known as adaptive models. Adaptive models of thermal comfort consider occupants as dynamically interacting with their environment, and controlling their thermal comfort by means of clothing or windowopening and closing. This is in contrast to thermal comfort in sealed cabin, in which occupants experience the environment passively. Researcher Fanger [8] proposed a set of correlations giving the PMV as a function of the thermal load, L, on the body, defined as the difference between the rate of metabolic heat generation and the calculated heat loss from the body to the actual environmental conditions assuming these optimal comfortable conditions. The convection and radiation heat transfer are functions of clothing temperature, which is affected by skin temperature. The evaporative losses are directly influenced by skin temperature. Therefore, L can be expressed by the following equation:

$$L = M - w - f_{cl}h_c (T_{cl} - T_a) - f_{cl}h_r (T_{cl}-T_r) - 156 (W_{sk} - W_a) - 0.42 (M - w - 18.43) - 0.00077M (93.2 - T_a) - 2.78M (0.0365 - W_a) \quad (4.1)$$

Where

L, thermal load;

M, rate of metabolic generation per unit DuBois surface area, Btu/h ft^2;

w, human work per unit DuBois surface area, Btu/h ft^2;

T_{cl}, average surface temperature of clothed body, °F;

f_{cl}, ratio of clothed surface areato DuBois surface area(A_{cl}/A_D);

T_a, air temperature, °F;

h_c, convection heat transfer coefficient, Btu/h ft^2 °F;

T_r, mean radiant temperature, °F or °R;

h_r, radiative heat transfer coefficient, Btu/h ft^2 °F;

W_a, air humidity ratio;

W_{sk}, saturated humidity ratio at the skin temperature.

In this equation, the clothing temperature can be easily calculated from the skin temperature, the air temperature, mean radiant temperature, and the thermal resistances.

$$\frac{T_{sk} - T_{cl}}{R_{cl}} = f_{cl} h_c (T_{cl} - T_a) + f_{cl} h_r (T_{cl} - T_r) \tag{4.2}$$

$$T_{cl} = \frac{T_{sk} + R_{cl} f_{cl} (h_c T_a + h_r T_r)}{1 + R_{cl} f_{cl} (h_c + h_r)} \tag{4.3}$$

Where

R_{cl}, effective thermal resistance (R-value) of clothing, ft^2°F h/Btu.

In this equation there is no definitive set of values for all applications. Fanger [8] used the following approximations as these parameters to develop his original correlation:

$$f_{cl} = \begin{Bmatrix} 1.0 + 0.2 I_{cl} \\ 1.05 + 0.1 I_{cl} \end{Bmatrix} \qquad I_{cl} < 0.5\ clo \tag{4.4}$$

$$h_c = max \begin{Bmatrix} 0.361 (T_{cl} - T_a)^{0.25} \\ 0.151 \sqrt{v} \end{Bmatrix} \tag{4.5}$$

$$h_r = 0.7$$

(4.6)

Therefore, the final correlation between PMV and the thermal load can be expressed by the following equation:

$$\mathrm{PMV} = 3.155(0.303e^{-0.114M} + 0.028)\mathrm{L}$$

(4.7)

According to the calculation results, the evaluation index of comfort can be introduced by the value of PMV. This index value has seven levels and is in the range of -3 to +3. -3 means hot and +3 means cold, which can help to predict the thermal comfort for passengers. The thermal comfortable degree that number represents is shown in Table 4-1. In the summer, the comfortable sensation should be a little bit cold or neutral which can be expressed by the PMV index that ranges from 0 to -1.

Table 4-1 PMV index

Sensation	Hot	Warm	A little bit warm	Neutral	A little bit cold	Cool	Cold
PMV	+3	+2	+1	0	-1	-2	-3

Thermal comfort is a combination of body feeling which can influenced by a lot of factors like air velocity. According to the calculation results made by previous researchers, the relationship between PMV index and air velocity is given in Fig.4-1. From this picture, it can be easy to understand that the black frame shows the thermal comfortable region. When temperature varies from 20 to 24 ℃, thermal comfortable region is maximum focus on the wind velocity from 2 to 3 m/s.

In this study, the temperature of wind outlet of air conditioning system is set as 22 ℃.Therefore, according to this relationship, thermal comfortable region is located at the wind velocity range from 1 to 4 m/s and the optimum value is 2.5 m/s.

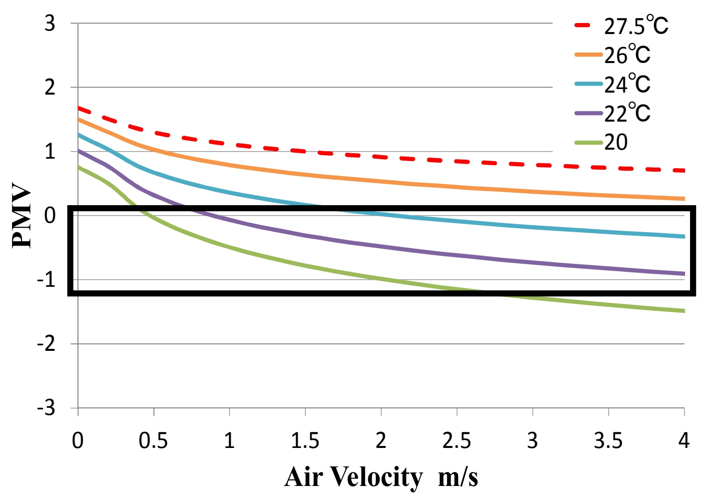

Fig.4-1 Relationship between PMV and air velocity at different temperature conditions

4.3 Experimental investigation

4.3.1 Peltier module seat

In this experiment, the personal air conditioning system is installed inside of the vehicle chair and it is conducted by the Peltier module and fan motor. Outside of the seat, there are two wind outlet vents with the dimension of 45 mm × 45 mm on the back of cushion and on the top of the seat back, which can provide wind for the back and neck of passenger, respectively. The outside view of the chair is given in Fig.4-2. The two wind outlets are marked by the red circle in the picture.

Inside of the seat, this personal air conditioning system is working by temperature regulation equipment which is installed under the cushion. This temperature regulation equipment is made by peltier module, heat sink, cooling fin and DC fan motor. 4 pieces of peltier modules (2 sets of 2 pieces overlap) are used in this system and they are fixed on the heat sink. The cooling fin is settled on the peltier modules and behind cooling fin there is a fan motor to produce wind for heat dissipation. The structure of inner chair is shown in Fig.4-3.

Fig.4-2 Outside view of the chair with personal air conditioning system

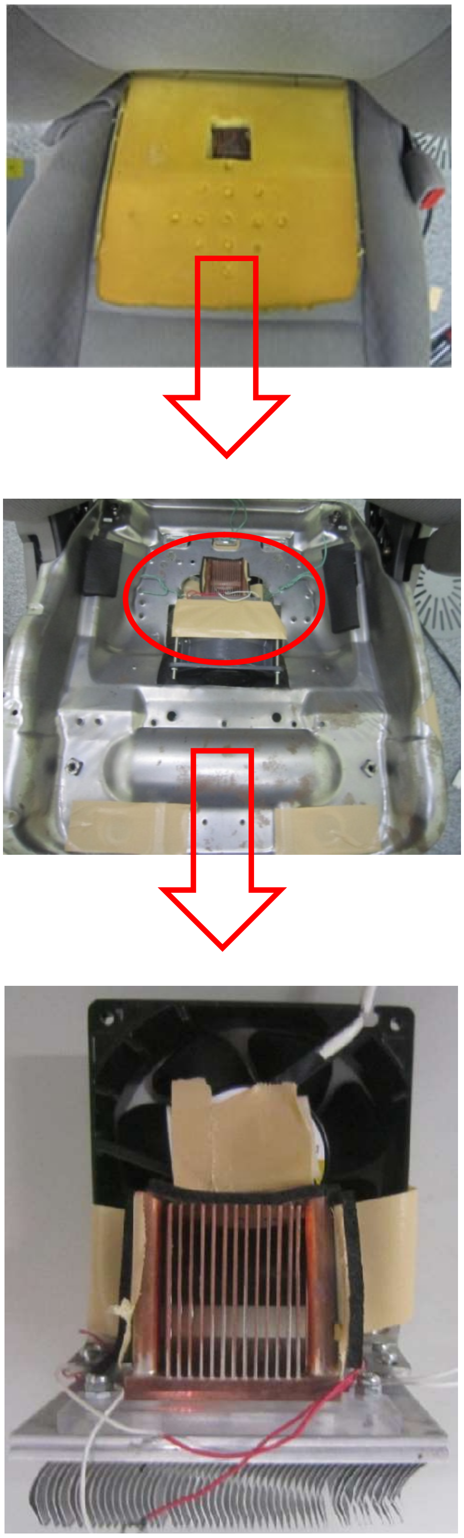

Fig.4-3 Inside view of the chair with personal air conditioning system

4.3.2 Specification of instrument

1. Peltier module

Company：AISIN SEIKI Co., Ltd

Type：U-11G236F-S401

Rated voltage：DC12V

Maximum electric current：4.2A

Maximum unit of heat：37.8W

Size：(L)115mm×(W)80mm×(H)47mm

Weight：390g

2. Heat sink

Company：SAKAGUCHI E. H VOC CORP

Size：(L)115mm×(W)80mm×(H)28mm

3. Cooling fin

Company：Takagi Mfg. Co., Ltd

Size：(L)120mm×(W)120mm×(H)120mm

4. DC fan motor for heat dissipation

Company：ORIENTAL MOTOR Co. , Ltd

Type：MDE1451-24L2

Rated voltage：DC24V

Maximum electric current ： 0.7A

Rotating speed： 3150 r/min

Maximum wind velocity： 5.8 m^3/min

Maximum static pressure： 130Pa

Noise level： 49dB

Size： 140mm×51mm

5. DC fan motor for ventilation

Company： SANYO DENKI CO., LTD

Type： 9WG1224F101-E

Rated voltage： 24V

Maximum electric current： 0.16A

Rotating speed： 2280r/min

Maximum wind velocity： 2.45 m3/min

Maximum static pressure： 54.2Pa

Noise level： 36db

Size： 120mm×38mm

6. Acrylic plate

Company： Sugawara Co., Ltd

Thickness： 3mm

7. Power unit①

Company：Agilent Technologies, Inc.

Type：U8002A

Maximum main voltage：30V

Maximum main electric current：5A

Ripple voltage：1.0mVrms

8. Power unit②

Company：KIKUSUI ELECTRONICS CORPORATION

Type：PAS80-4.5

Maximum main voltage：80V

Maximum main electric current：4.5A

9. Power unit③

Company：AND CORPORATION

Type：AD-8724D

Maximum main voltage：30V

Maximum main electric current：2.5A

10. Data logger

Company：ADVANTEST CORPORATION

Type：R7326B

4.3.3 Experimental method

In this experiment, ambient environment was quiescent and the temperature was 29 ℃ with relative humidity 60%. Before the operation of air conditioning system, the engine of car was flameout to be cooling and all the doors were opened to make the in-car air flow to maintain almost same as that of outside environment. After one hour's ventilation, the temperature of vehicle cabin can be considered the same as the ambient temperature and the car dashboard showed that the temperature was 29 ℃. During the experimental process, the environment can be seen to stay in a constant condition due to the short test time of 15 minutes.

The temperature measuring time was set for 15 minutes in 5-minute intervals, which can be obtained three sets of data for a test. In order to eliminate accidental errors, the multiple measurements were performed and three sets of test were carried out due to time constraints. In this test, the wind velocity of personal air conditioning is set as 2.5 m/s and the temperature is set as 22 ℃. The infrared temperature probe was used in this experiment and the eight measuring points were picked up to monitor the temperature variation of cabin. Four points were fixed at the position of neck when passengers sitting in the car including the front row and rear row. The part of face is very important place to feel if the environment is comfortable or not. Another four points were fixed at position of passengers' waist. These eight places are located close to the wind outlet where the temperature is easy to be influenced by the air conditioning system and turn to change. All the measuring points are given in Fig.4-4.

Another thermal comfort test started after the vehicle standing in the setting environment for 120 minutes and reaching steady situation. The examinees went into the cabin and sat on the temperature regulation seat for 10 minutes to get used to the cabin environment. Then, the personal air conditioning turned on and examinees started to feel the thermal comfort. According to the PMV index, examinees' feeling was turned to the related number and made recording. The total test time is 15 minutes and the data is recorded per minute.

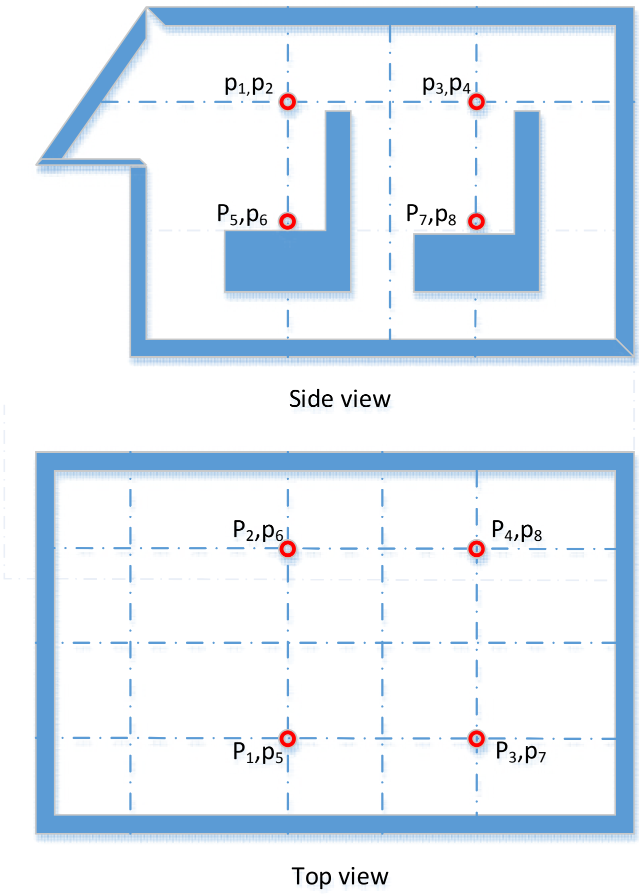

Fig.4-4 Measuring points of temperature

4.4 Numerical simulation

In order to comprehend the motion process of heat flow in the cabin when this personal air conditioning system is operated, the numerical simulation analysis is used in the study. Based on the objective vehicle, the geometry model profile with real dimensions is drawing by the AutoCAD software and the mesh is created by Gambit which can be input to the CFD analysis software to carry out the numerical simulation. And then, the boundary conditions including the wind outlet of the vehicle air conditioning system are set according to the data obtained from the experiment before [9-10].

4.4.1 Model Geometry

The geometry model of the vehicle is created by the AutoCAD software with real dimensions and shape. However, this model is simplified and the computational domain only consists of the inner space of the cabin and the chairs without any other in-car facilities, for example, the steering wheel. And then the model is exported to CFD software to generate mesh for numerical analysis. In the process, this mesh generation consists of 6077670 hexahedral elements. The space under the seat is not included in the computational domain. The outlet of personal air conditioning system is marked as red parts including four outlets on the back of surface of the cushion and four outlets on the top of the seat back, which can be seen in Fig.4-5.

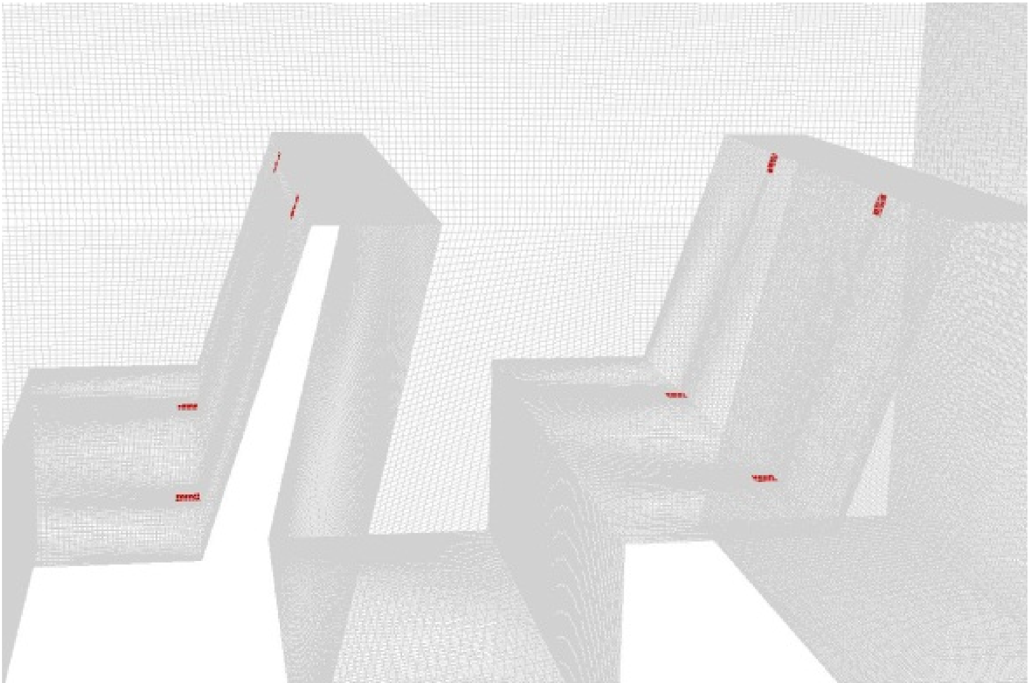

Fig.4-5 Section mesh of the chair in the cabin

4.4.2 Boundary conditions and problem setup

In this numerical calculation, in order to make a comparison with the traditional vehicle air conditioning system, the wall setup and boundary conditions were set as same as the last chapter, which can be seen in the Table 4-2. The model domain is also calculated by using the pressure-based solver with the transient time and absolute velocity formulation. The energy and transport governing equations are discretized by the finite volume method and SIMPLE algorithm is adopted for the coupling between pressure and velocity. The k-ε (2εqn) turbulent model derived from the instantaneous Navier-Stokes equations is chosen in this simulation in conjunction with the standard wall function for the near wall region treatment. The time step of this numerical calculation is taken as one second [11-13].

On the other hand, the eight wind outlets are also defined as mass flow inlet. According to the empirically determined data, the detail setup of momentum and thermal conditions are given in Table 4-3. In order to simplify algorithm and accelerate convergence, the wind outlet of air conditioning is presumed to keep in a stable condition with constant temperature.

Table 4-2 Wall setup and boundary conditions

Category	Parameter	Internal	External
Physical properties	Fluid	Air	Aluminum
	Density [kg/m^3]	1.177	2719
	Cp [J/kg-K]	10046.43	871
	Thermal conductivity (W/m-K)	0.0242	202.4
	Viscosity [kg/m-s]	1.7894e-05	/
	Thermal expansion coefficient [1/K]	3.356e-03	/
Boundary conditions			
Momentum	Wall motion	/	Stationary
	Shear condition	/	No slip
	Wall roughness height (m)	/	0
	Wall roughness constant	/	0.5
Thermal conditions	Temperature (℃)		29
	Wall thickness (m)		0.02
	Heat generation rate (W/m^3)		0

Table 4-3 Mass flow inlet setup

Category	Parameter	Value
Momentum	V(velocity magnitude) [m/s]	2.5
	Turbulent Intensity [%]	10
	D (Hydraulic Diameter) [m]	0.045
	Gauge pressure [Pa]	0
Thermal conditions	Total temperature [℃]	22

4.5 Results and discussion

The stable numerical results of thermal characteristics are obtained after calculating for 15 minutes. By solving the momentum and energy equations, the heat flow characteristics of the whole cabin including pressure and turbulent property of air are shown through the following graphics and plots.

4.5.1 Validation of the results

Based on the experimental data, the simulation results are validated by the comparison of predicted temperature values and experimental data at the points located in the cabin described in the experimental investigation part of this chapter. The temperature comparison results at neck and at waist are shown in the Fig.4-6 and Fig.4-7, individually.

From the Fig.4-6, it can be easy to see that the temperature at neck has good agreement between predicted and experimental results. Both of them show a decrease trend in the test time and the temperature can drop to about 22 ℃ which is the set value of cabin. The four points almost show similar experimental and simulated temperature, individually due to the similar location in the cabin.

However, at the waist showing in Fig.4-7, the temperature difference between calculation and experiment rises to a peak value of about 3 ℃ when the test takes on to 5 minutes, which shows a worst deviation. After 5 minutes, test temperature has maintained a stable value of about 20 ℃ and the predicted temperature goes on decreasing to set value of 22 ℃. The deviation between these turns to weaken and finally keeps at approximate 1.5 ℃. It can be easy to see that the final temperature of test is lower than the set value of 22 ℃, which can be due to the temperature controller system of experimental appliance. It is hard to make a control accurately, even rough by the traditional air conditioning system.

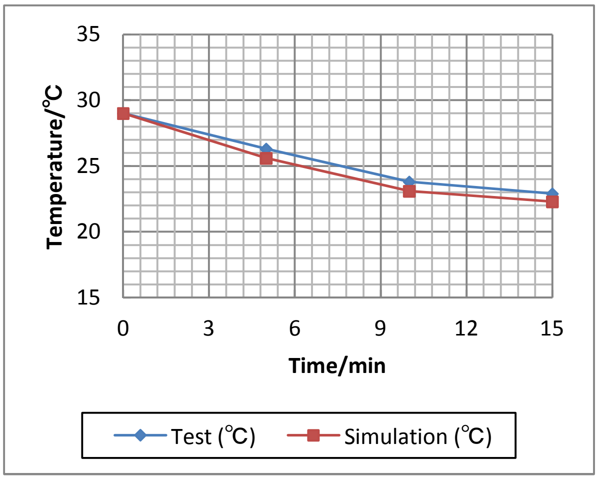
35
30
25
20
15
Temperature/℃
0
3
6
9
12
15
Time/min
Test (℃)
Simulation (℃)

(a)

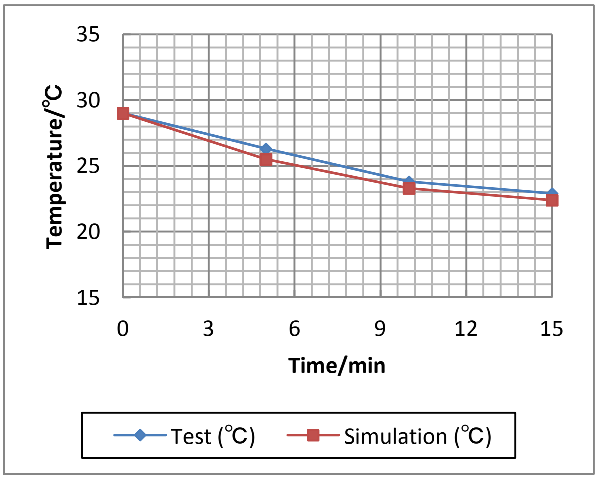
35
30
25
20
15
Temperature/℃
0
3
6
9
12
15
Time/min
Test (℃)
Simulation (℃)

(b)

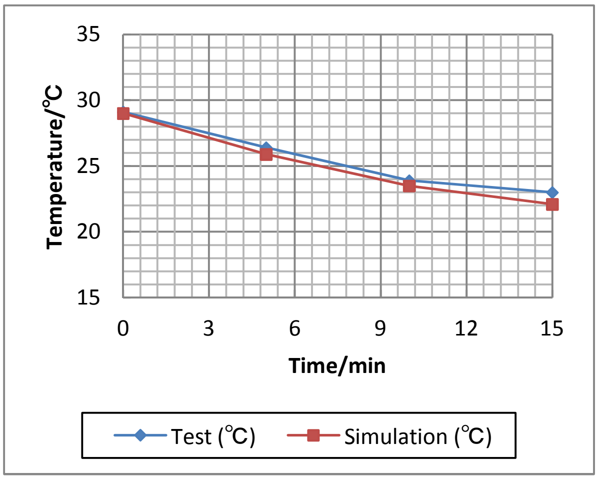

(c)

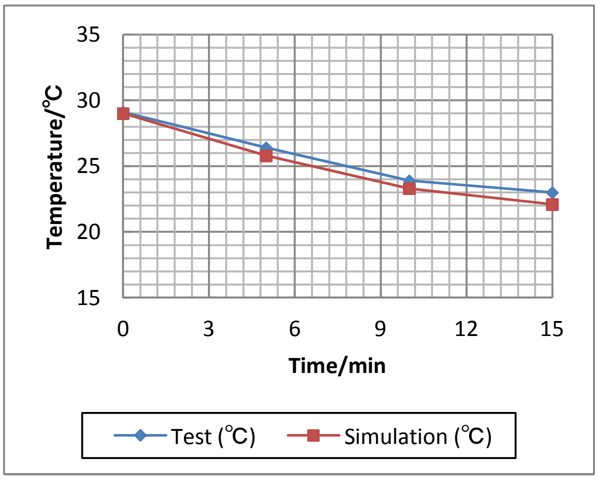

(d)

Fig.4-6 Temperature comparison of simulation results and experimental data at neck, (a) P_1; (b) P_2; (c) P_3; (d) P_4

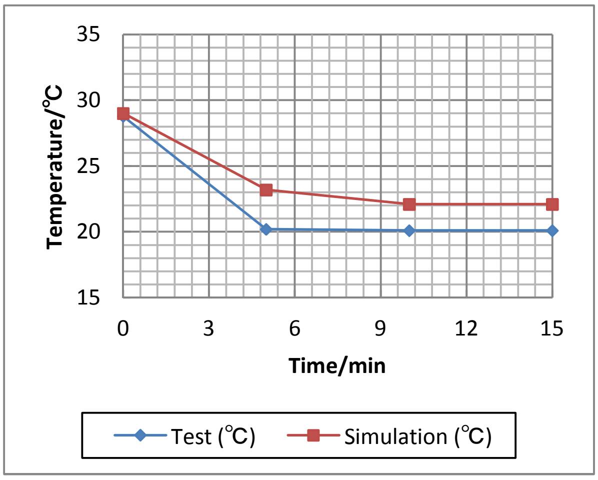
35
30
25
20
15
Temperature/℃
0
3
6
9
12
15
Time/min
Test (℃)
Simulation (℃)

(a)

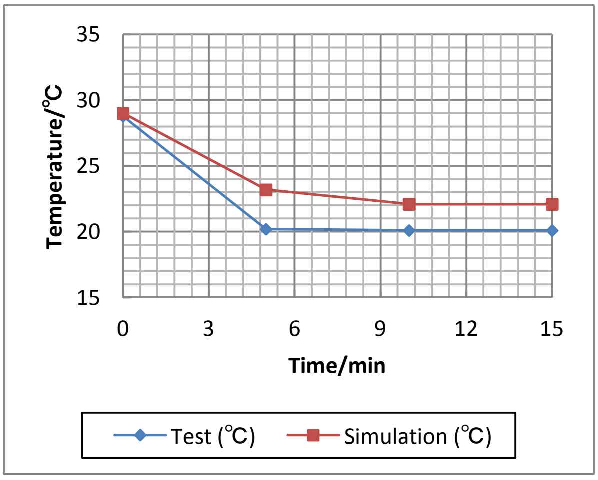
35
30
25
20
15
Temperature/℃
0
3
6
9
12
15
Time/min
Test (℃)
Simulation (℃)

(b)

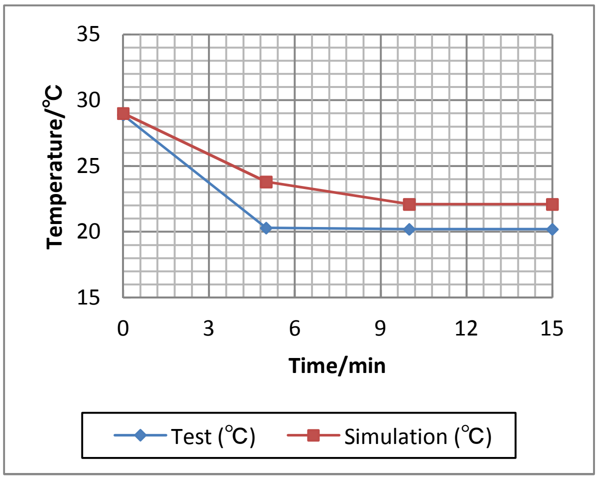

(c)

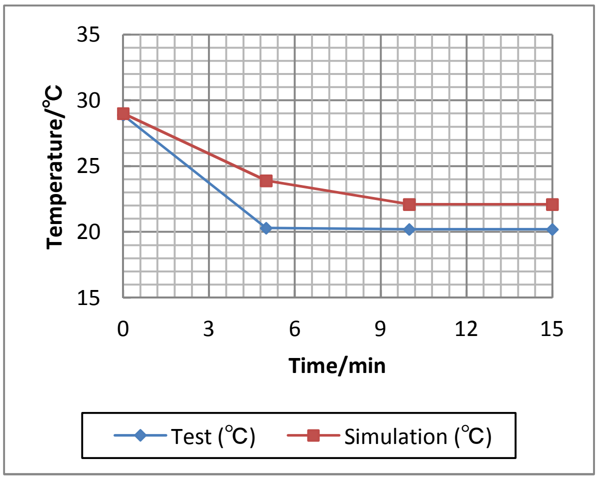

(d)

Fig.4-8 Temperature comparison of simulation results and experimental data at waist, (a) P_5*; (b)* P_6*; (c)* P_7*; (d)* P_8

4.5.2 Heat flow characteristics of chair

The stability numerical results of thermal characteristics are obtained after calculating for 15 minutes. The phenomenon in the chair around the wind inlet vents surface is more important and complicated than other part of solution domain. Hence, a virtual circle of chair surface is picked up to show the temperature distribution.

The temperature of chair is shown in the Fig.4-9 (a). From this picture, it is seen that the seat area around the inlet vents has lower temperature than the rest parts since the cooling wind blows from here and the variation of the value is simulated in the range of 6 ℃ after 15 minutes. It means that the temperature in the back of passengers can decline to under 24 ℃ (297K) that is the normal room temperature and passengers could feel comfortable under this situation, which has good agreement with the experimental results. However, the other part of vehicle cabin has high temperature. This is the reason why examinee feels uncomfortable at the part of face and head.

The temperature distribution in the place where the passengers could feel including the chair and wind outlet vents is drew in Fig.4-9 (b). X axis shows the length of the vehicle and position. From this picture, it can be easy to see that the area near the chair2 (the chair of back row) has the lowest temperature which is 24 ℃ (297K). On the other hand, the front row chair stays at about 26 ℃ (299K). The same personal air conditioning system is used in both of two chairs and the variation of the temperature of two chairs should be similar. Obviously, the inner structure of cabin conducts this result. The front of cabin has more huge space compared to the rear zone. Also, the backboard of front chair has become a factor to affect the heat flow motion.

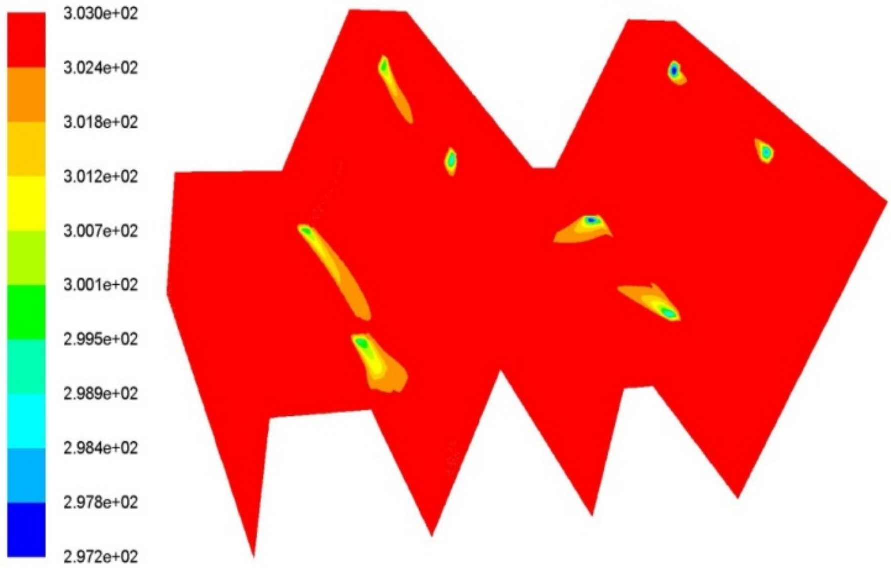

(a)

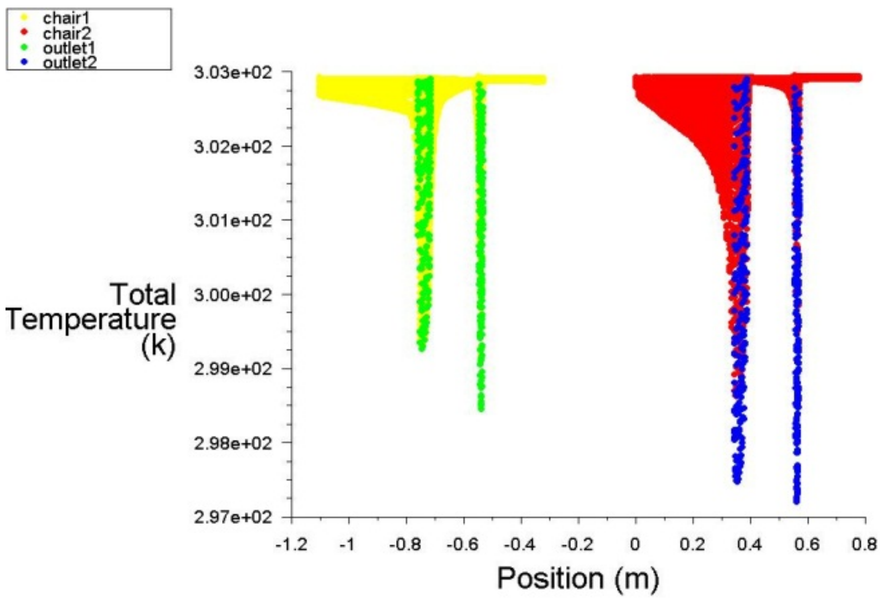

(b)

Fig.4-9 Temperature (K) distribution with the position

4.5.3 Turbulence characteristics of chair

The turbulence characteristics of heat flow of the chairs including the eight wind outlets of personal air conditioning system of vehicle cabin are given in the following picture from Fig.4-10 to Fig.4-15. It directly shows the turbulent properties at different location of the cabin, which can visually explain the results why the vehicle cabin has such complex thermal distribution finally.

From Fig.4-10 and Fig.4-11, it can be easy to see that the front row has higher total pressure and total surface heat flux compared with the rear row during the experimental time. That is the reason why front row has higher temperature than the rear row. The total surface heat flux is also an important factor to affect the temperature of cabin.

From Fig.4-12 and Fig.4-13, it can be obvious to see that the front row has strong turbulent intensity and turbulent energy, especially at the position of wind outlets, which is quite different from other place. The reason can be explained by wind velocity which drives the air flow to move fast and causes the turbulence change. In addition, the structure of cabin also reduces the difference between front and back.

From Fig.4-14 and Fig.4-15, the pictures show the characters of skin friction coefficient and wall shear stress. It also can be seen that the front row has much higher level than back row. The same reason is due to the wind velocity.

Therefore, it is obvious to see that this personal air conditioning cannot keep a balance between front row and back row in the vehicle cabin. The cooling from wind outlet is still not enough and cannot satisfy all the passengers, which is consistent with the experimental results.

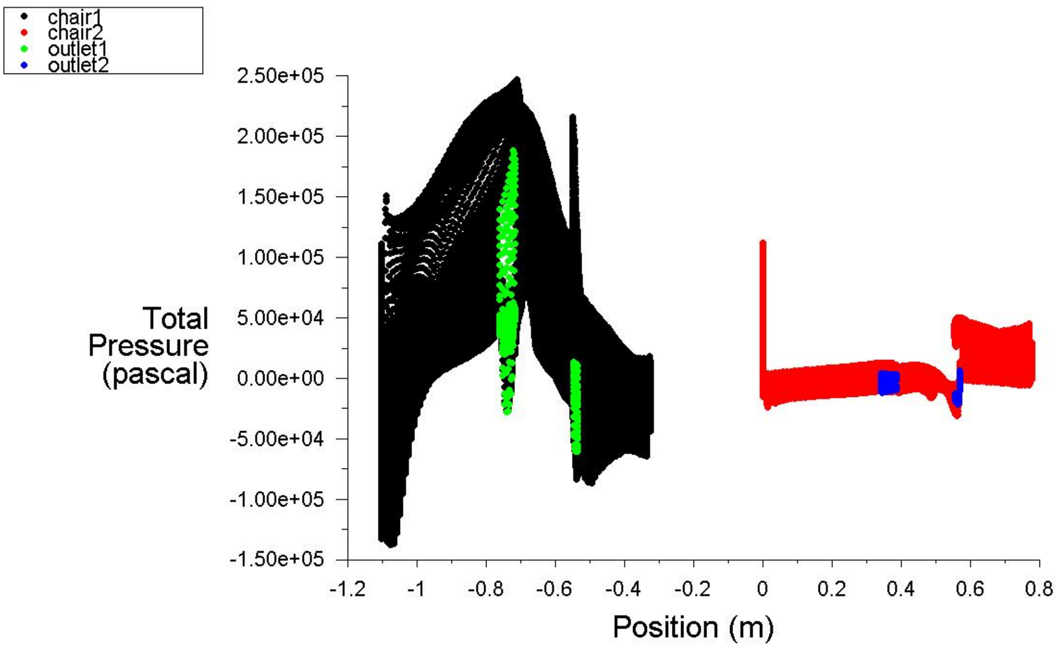

Fig.4-10 Total pressure (Pa) in the different location

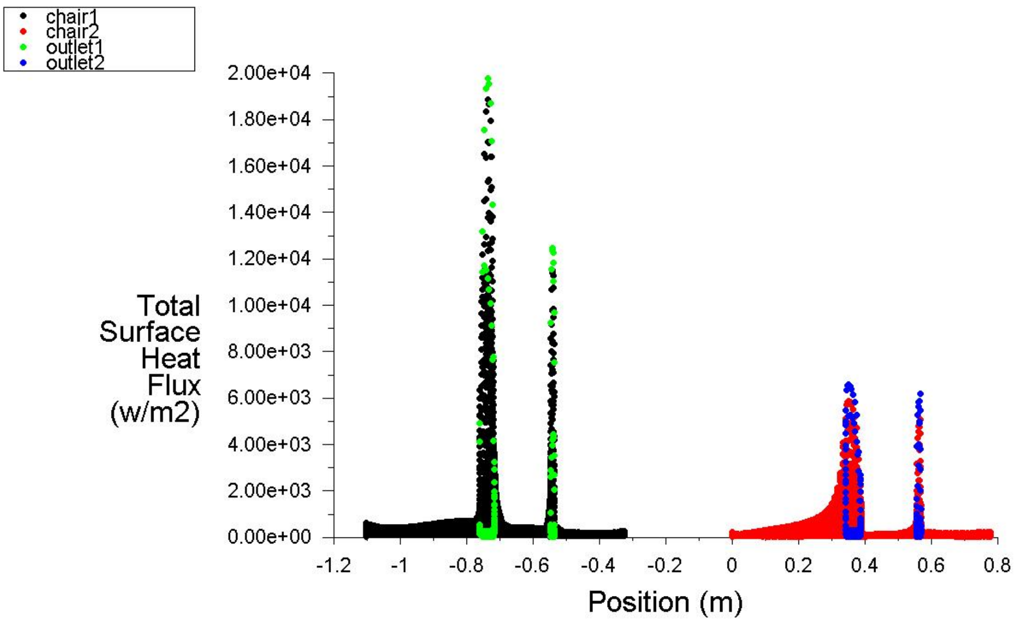

Fig.4-11 Total surface heat flux (W/m^2) in the different location

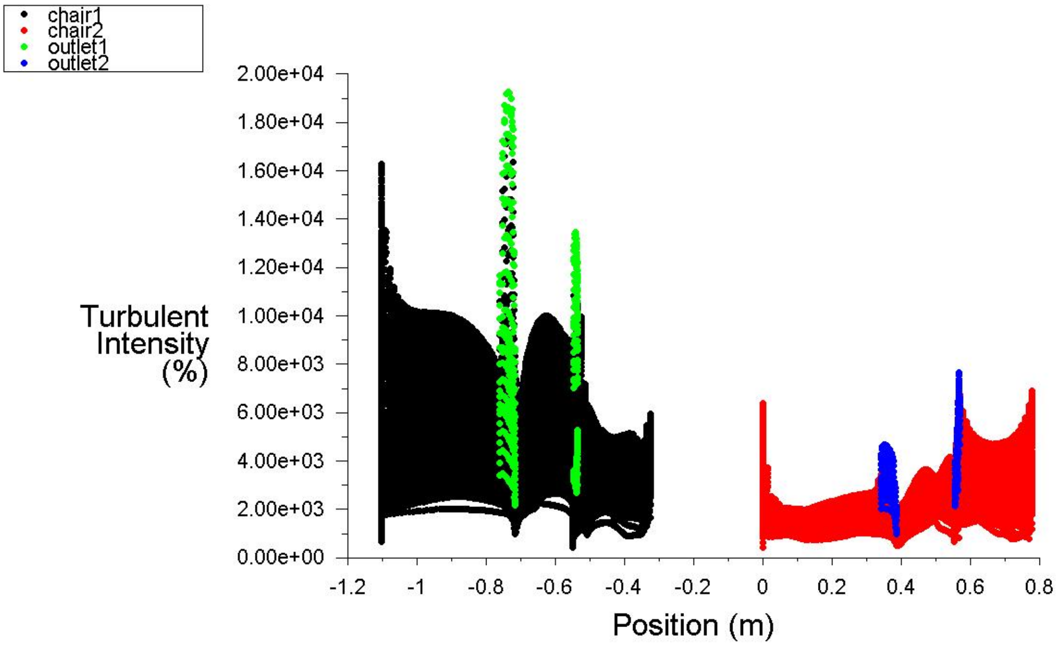

Fig.4-12 Turbulent intensity (%) in the different location

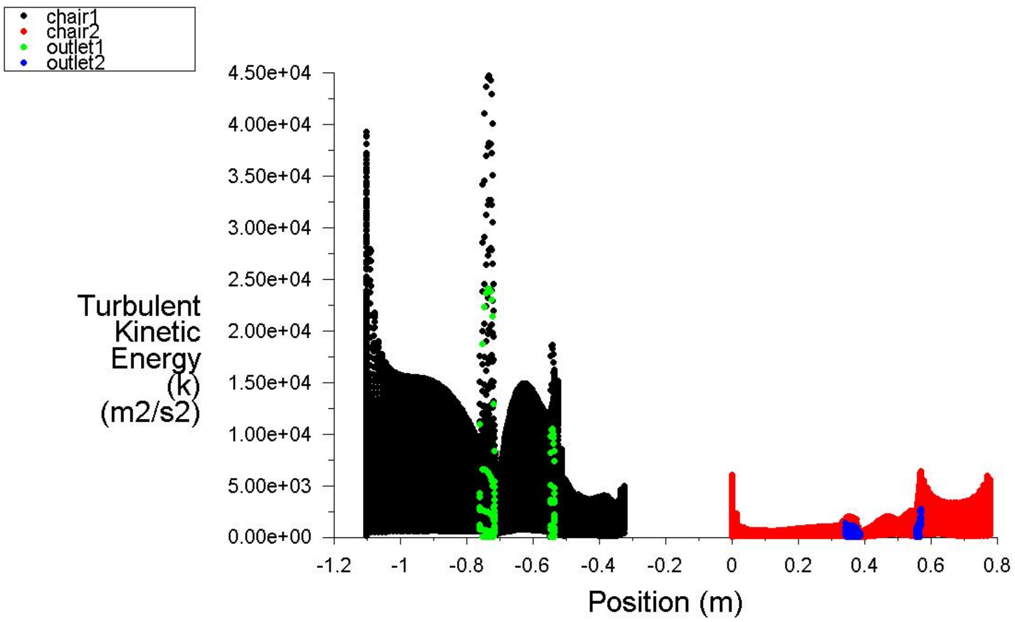

Fig.4-13 Turbulent energy (m^2/s^2) in the different location

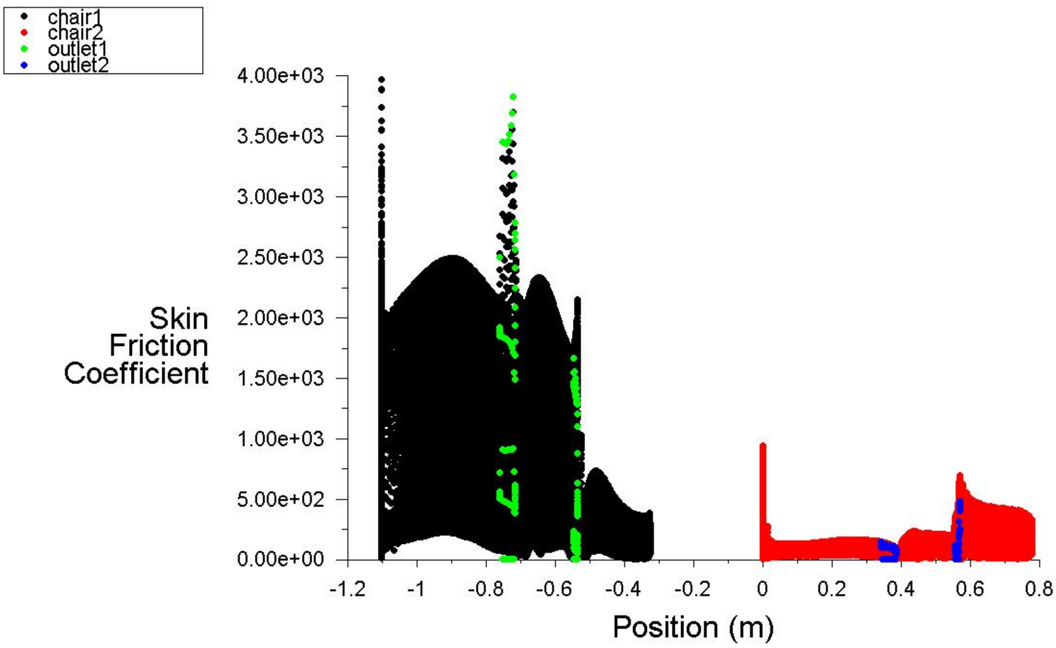

Fig.4-14 Skin friction coefficient in the different location

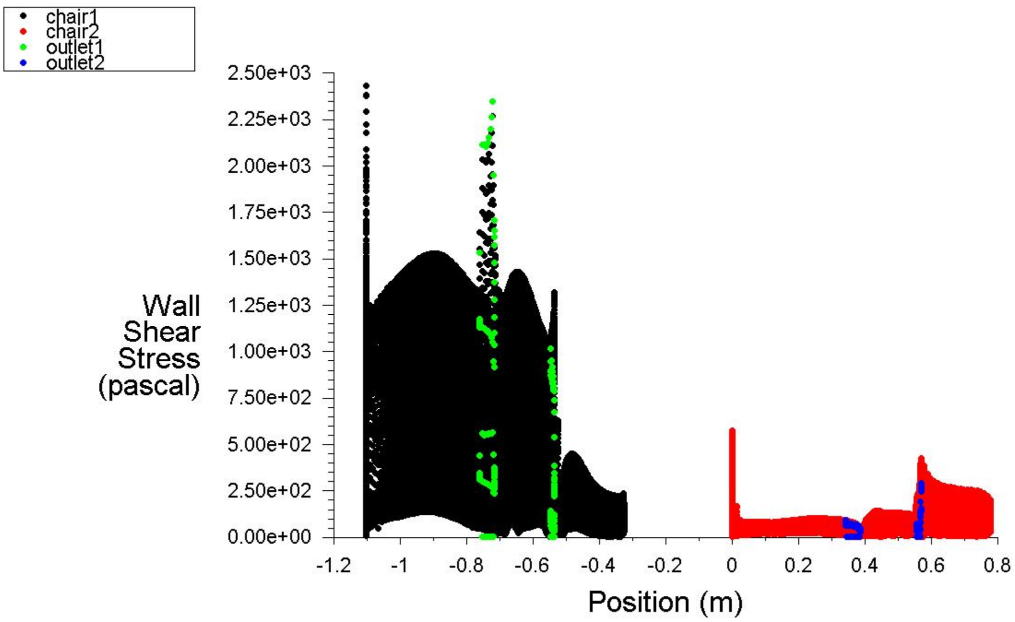

Fig.4-15 Wall shear stress (Pa) in the different location

4.5.4 Heat flow calculation

The total heat of cabin obtained from environment of outside can be calculated by using the heat flow rate to multiply by the simulation time when the personal air conditioning is working. According to the heat flow reports of simulation results, the total heat transfer rate at each surface between ambient and vehicle cabin can be seen in the Table 4-4. Through the calculation, the whole cabin has got 4232.1W heat after 15 minutes. When temperature of cabin is adjusted to the normal room temperature, the energy consumption of air conditioning system would be calculated according to this basic data.

Table 4-4 Total heat transfer rate at different direction (W)

Time / Wall surface	5 minutes	10 minutes	15 minutes
Back	129.03	130.55	130.21
Bottom	186.01	185.23	185.12
Chair1	728.05	729.35	730.67
Chair2	388.01	388.78	387.05
Front	950.23	949.05	949.87
Left side	438.36	435.14	440.48
Outlet1	-2210.02	-2210.95	-2208.64
Outlet2	-1189.05	-1189.87	-1189.25
Right side	385.65	385.96	387.23
Roof	468.21	469.54	469.41
Net	274.48	272.78	282.15

From this table, it can be easy to see that the heat transfer rate almost has no obvious change during the simulation time. There is much more heat getting into the cabin through the front wind glass than other surface. The minus value of total energy shows the heat transfer from cabin to ambient by air conditioning and it is obvious to see that the outlet1 of the front row moves more heat than the outlet2 of the rear row.

The mass flow rate is given in the Table 4-5. According to the boundary setting, the mass flow rate keeps in a stable condition. Hence, these values remain the set value without any variation in the simulation time of 15 minutes.

Table 4-5 Mass flow rate at different direction (kg/s)

Wall surface	Mass flow rate
Back	0
Bottom	0
Chair1	0
Chair2	0
Front	0
Left	0
Outlet1	0.024
Outlet2	0.024
Right	0
Roof	0
Net	0.048

4.5.5 Energy consumption calculation

According to the ampere meter, each personal air conditioning system consumes electric power 84.7 W shown in Table 4-6. This test vehicle is installed for four systems and the overall consumption for a car of four passengers only takes electric power 338.8 W after 15 minutes of working time, which is much less than the traditional one.

Table 4-6 Electric power consumption of each device of personal air conditioning system

Device	Electric power (W)
Peltier device	72.7
DC fan motor for heat dissipation	2
DC fan motor for ventilation	10
Total system	84.7

4.5.6 Evaluation of thermal comfort

The results of thermal comfort evaluation through experiments are given in Fig.4-16. It can be seen that the examinee could feel neutral after 4 minutes and this comfortable feeling can continue in the later 15 minutes of test time. However, according to the examinee, the face and the head still feel uncomfortable because the wind from chair just can reach to the back of passenger straightly not the whole body.

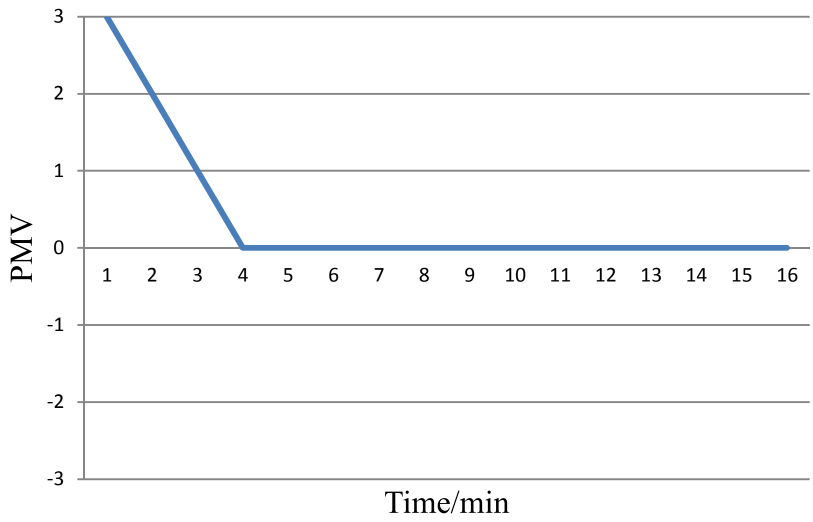

Fig.4-16 Experimental results of PMV

4.6 Conclusion

This chapter used the personal air conditioning system instead of the traditional one to provide thermal comfort for the passengers. A simplified 3-D N box vehicle cabin model was created to simulate the air flow and heat transfer characteristics of inner cabin and under the same condition thermal comfort and temperature experiment was taken place to make a comparison. Also, the electronic power consumption of this system was calculated by recorder. The following results are obtained:

(a). The predict temperature has good agreement with the experimental results, which shows the reliability of models and simulation method. Both of them decrease by time and turn to stable after 5 minutes.

(b). This personal air conditioning system can make passengers feel comfortable after 4 minutes and all the apparatuses can just only consume electric power 338.8, which is less than traditional air conditioning of cabin.

(c). This personal air conditioning system has been validated to be used in electric vehicle instead of traditional one. But it cannot make all the body feel comfortable. Except the area of chairs, temperature of entire cabin has almost no change during 15 minutes

Therefore, the next work is considering adding more wind outlet in the cabin to provide more wind for the passengers.

References

[1] Tomohiro Kitagawa, Kiyoshi Kawaguchi, Daisuke Watanabe and Ryota Toyohara: Reducing Temperature in a Parking Automobile under Summer Solar Radiation, 49th Japan Heat Transfer Symposium proceedings, 2012.

[2] K. Yamamoto, W.R. Hill, Interior Flow Visualization of a Small Pick-up Truck and A/C Feeling Estimate, SAE International Congress and Exposition, ISSN: 0148-7191, SAE, Detroit, MI, USA, 1990.

[3] Chao-Hsin Lin, A. Lelli Michael, Han Taeyoung, J. Niemiec Robert, C. Hammond Dean, Jr., Experimental and Computational Study of Cooling in a Simplified GM-10 Passenger Compartment, International Congress and Exposition, ISSN:0148-7191, SAE, Detroit, MI, USA, 1991.

[4] Ambs, R: Improved Passenger Thermal Comfort Prediction in the Preprototype Phase by Transient Interior CFD Analysis Including Mannequins, SAE Paper, 2002.

[5] Gokhan Sevilgen, Muhsin Kilic: Transient Numerical Analysis of Airflow and Heat Transfer in a Vehicle Cabin During Heating Period, Int. J. Vehicle Design, Vol. 52, Nos. 1/2/3/4, 2010.

[6] Robert Parsons, ASHRAE handbook Fundamentals, 1997.

[7] P.Ole Fanger, Human requirements in future air-conditioned environments, International journal of refrigeration, 24(2):148-153, 2001.

[8] Http://ceae.colorado.edu/~brandem/aren3050/docs/ThermalComfort.pdf.

[9] ANSYS Inc. Fluent Manuals.

[10] Richard C. Farmer, Gary C.Cheng, Yen-Sen Chen, Ralph W. Pike: Computational Transport Phenomena for Engineering Analyses, USA, 2009.

[11] S. Mostafa Ghiaasiaan: Convective Heat and Mas Transfer, USA, 2011.

[12] J.S. Brown, B.W. Jones, New transient passenger thermal comfort model, in: Proceedings of the 1997 International Congress and Exposition, ISSN: 1054-6693, SAE, Detroit, MI, USA, 1997.

[13] Ishihara Yuji, Shibata Minoru, Hoshino Hiroshi, Hara Junichiro, Kamemoto Kyoji, Analysis of interior airflow in a full-scale passenger-compartment model using a laser-light-sheet method. International Congress and Exposition, ISSN: 0099-5908, SAE, Detroit, MI, USA, 1992.

Chapter 5
Proposal of Modified Personal Air Conditioning System

5.1 Chapter introduction

The personal air conditioning system can be considered as an efficient appliance to cut the energy consumption of a car from the study of chapter 4. However, this system cannot cool the front side of passengers and it shows that the whole temperature of cabin still stays at a high level since this system just can be local action. In order to further improve the refrigeration capacity and thermal comfort, a modified personal air conditioning system is proposed in this chapter. Based on the old one, the new system has added four more wind outlets in the front of cabin. These four outlets have bigger size than the original vents on the chairs so that they can provide much more cooling wind for all the passengers. In order to validate the feasibility if this system can apply in vehicle, taking the same car of chapter 4 as the mode, the thermal distribution and heat transfer characteristics of cabin are simulated by CFD software under the cooling action during 15 minutes. Also, the energy consumption is estimated to make a comparison with the traditional air conditioning system.

5.2 Numerical simulation

In this chapter, the numerical simulation process is carried out as same as that of previous chapter. First, the 3-D model of the vehicle is established by AutoCAD and meshed by CFD analysis software. Then, the boundary conditions are set according to the environment situation. Finally, the calculation is carried out by software and the analysis results are obtained [1-3].

5.2.1 Model geometry

The geometry model of the vehicle is created by the AutoCAD software with real dimensions and shape of the N box car. This model is also simplified and the computational domain only consists of the inner space of the cabin and the chairs with personal air conditioning system as same as that of chapter 4. The difference is that this model adds four more wind outlets in the front of the cabin, which can be seen in the Fig.5-1. The four outlets are marked out using red. And then the model is exported to CFD software to generate mesh for numerical analysis. In this process, the mesh generation consists of 6234831 hexahedral elements. The space under the seat is not included in the computational domain.

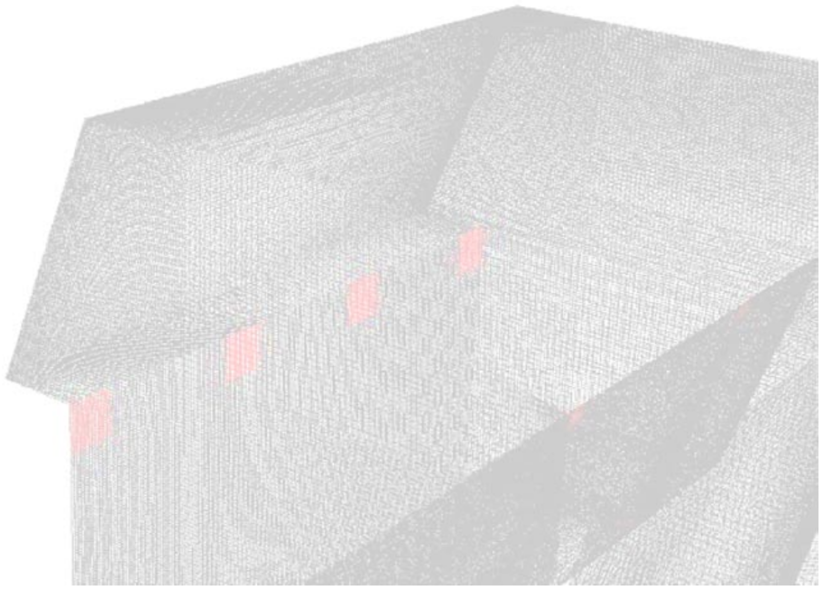

Fig.5-1 Section mesh of four outlets in the front of cabin

5.2.2 Boundary conditions and problem setup

The boundary condition is also set as the same as that of chapter 4. The original boundary temperature of the inner cabin joined to wall is regarded as equal to the ambient temperature of outside which is set to 29 ℃. About the momentum equation, the wind velocity of outlets on the chair still keeps the previous setting that is 2.5 m/s in the chapter 4. But the new four outlets are speeded up to 3 m/s and the size of the outlets is set as 0.1 m which is bigger than the ones on the chair, which will not bring discomfort feeling to the passengers because of the long distance between the two. Also, this velocity is in the range of the thermal comfortable region (1-4 m/s when set temperature is 22 ℃), which is given in the chapter 4.2. The detail of boundary conditions is presented in the Table 5-1. On the other hand, 12 wind outlets are also defined as mass flow inlet. The detail setup of momentum and thermal conditions are shown in Table 5-2. In order to simplify algorithm and accelerate convergence, the environmental temperature is set as a constant value due to the short calculation time and the wind outlet of air conditioning is also presumed to keep in a stable condition with constant temperature.

The calculation setup also uses the same algorithm as that of previous chapter. The air flow motion in cabin can be regarded as an internal circulation and the model domain is calculated by using the pressure-based solver with the transient time and absolute velocity formulation. The energy and transport governing equations are discretized by the finite volume method and SIMPLE algorithm is adopted for the coupling between pressure and velocity. The k-ε (2εqn) turbulent model derived from the instantaneous Navier-Stokes equations is chosen in this simulation in conjunction with the standard wall function for the near wall region treatment [4-6]. The time step of this numerical calculation is taken as one second.

Table 5-1 Setup and boundary conditions

Category	Parameter	Internal	External
Physical properties	Fluid	Air	Aluminum
	Density [kg/m^3]	1.177	2719
	Cp [J/kg-K]	10046.43	871
	Thermal conductivity (W/m-K)	0.0242	202.4
	Viscosity [kg/m-s]	1.7894e-05	/
	Thermal expansion coefficient [1/K]	3.356e-03	/
Boundary conditions			
Momentum	Wall motion	/	Stationary
	Shear condition	/	No slip
	Wall roughness height (m)	/	0
	Wall roughness constant	/	0.5
Thermal conditions	Temperature (℃)		29
	Wall thickness (m)		0.02
	Heat generation rate (W/m^3)		0

Table 5-2 Mass flow inlet setup

Momentum	Outlet1 and outlet2	Outlet3
V(velocity magnitude) [m/s]	2.5	3
Turbulent Intensity [%]	10	10
D (Hydraulic Diameter) [m]	0.045	0.1
Gauge pressure [Pa]	0	0
Inlet vents temperature [℃]	22	22

5.3 Results and discussion

The stable numerical results of thermal characteristics of the cabin are obtained after calculating for 15 minutes. By solving the momentum and energy equations, the heat flow characteristics of the whole cabin including pressure and turbulent property of air are shown through the following graphics and plots.

5.3.1 Heat flow characteristics of whole cabin

The heat flow characteristics of the whole vehicle cabin including the wind outlets of this modified personal air conditioning system are given clearly in the following pictures from Fig.5-2 to Fig.5-5.

The Fig.5-2 shows the thermal characteristic of whole cabin. It can be easy to see that the pressure of cabin has no obvious change except the area of wind outlets. But the temperature of whole cabin has changed dramatically in the 15 minutes of test. The most place of cabin can keep the temperature to stay at 24 ℃ (297K), which means that the temperature of cabin has dropped by 5 ℃ from 29 ℃ (302K) of the beginning of test in 15 minutes. More, the lowest temperature of cabin can reach to 22 ℃ (295K), which is located close to wind outlets. Obviously, the temperature of whole cabin has been cooled by this modified air conditioning system compared with the previous experiments due to the existing of front four wind outlets. These wind outlets can work well to bring much cooling and put in motion the heat exchange among the vehicle cabin under the assist of wind outlets in chairs. In addition, the total heat surface flux and surface heat transfer coefficient also show similar characteristics with the temperature.

The Fig.5-3 displays the turbulent characteristics of whole cabin. It can be easy to see that the space close to wind outlets has stronger turbulent intensity and turbulent dissipation rate than other region of cabin. These factors can drive the air flow to move rapidly and conduct the heat transfer from high to low, which is the reason why the temperature of cabin can drop much more than previous one.

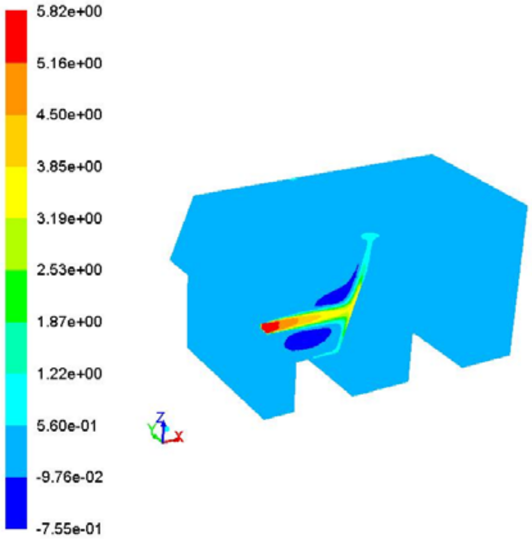
5.82e+00
5.16e+00
4.50e+00
3.85e+00
3.19e+00
2.53e+00
1.87e+00
1.22e+00
5.60e-01
-9.76e-02
-7.55e-01

(a)

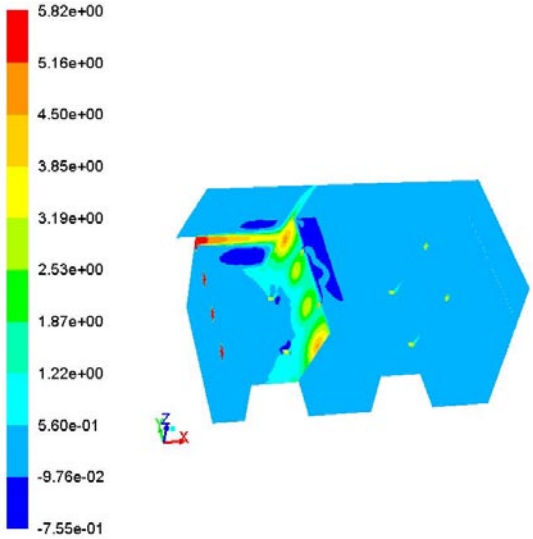
5.82e+00
5.16e+00
4.50e+00
3.85e+00
3.19e+00
2.53e+00
1.87e+00
1.22e+00
5.60e-01
-9.76e-02
-7.55e-01

(b)

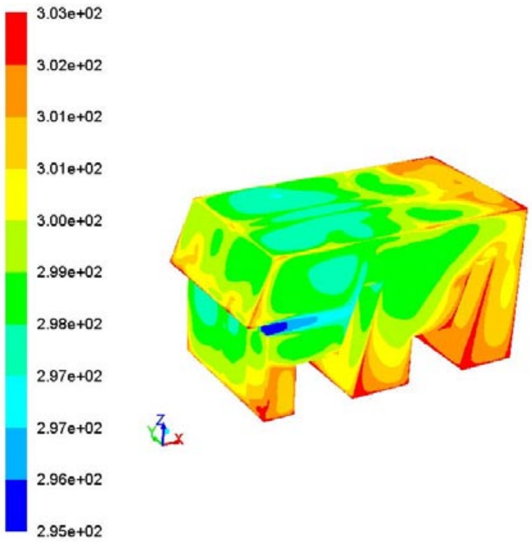
3.03e+02
3.02e+02
3.01e+02
3.01e+02
3.00e+02
2.99e+02
2.98e+02
2.97e+02
2.97e+02
2.96e+02
2.95e+02

(c)

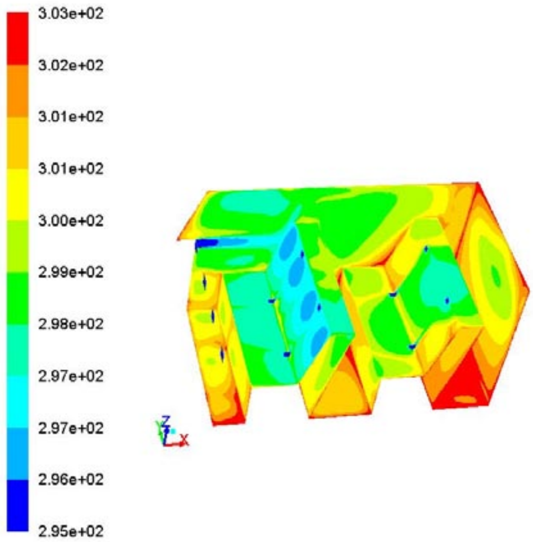
3.03e+02
3.02e+02
3.01e+02
3.01e+02
3.00e+02
2.99e+02
2.98e+02
2.97e+02
2.97e+02
2.96e+02
2.95e+02

(d)

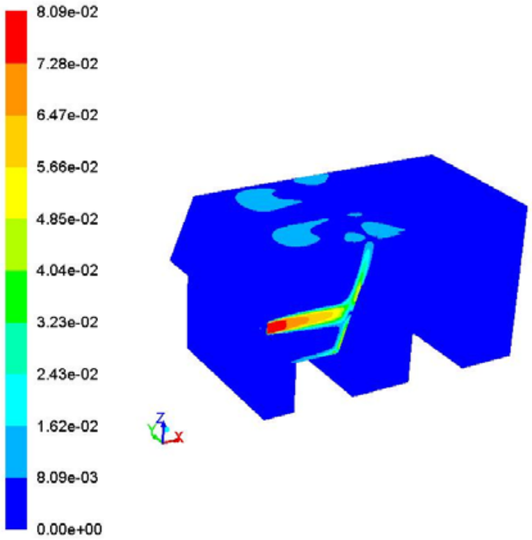

(e)

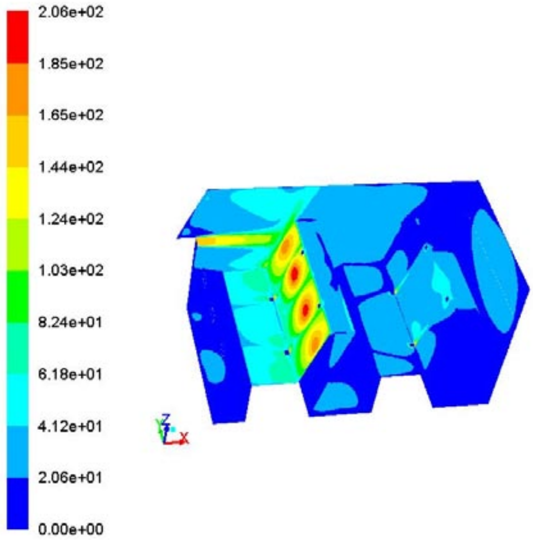

(f)

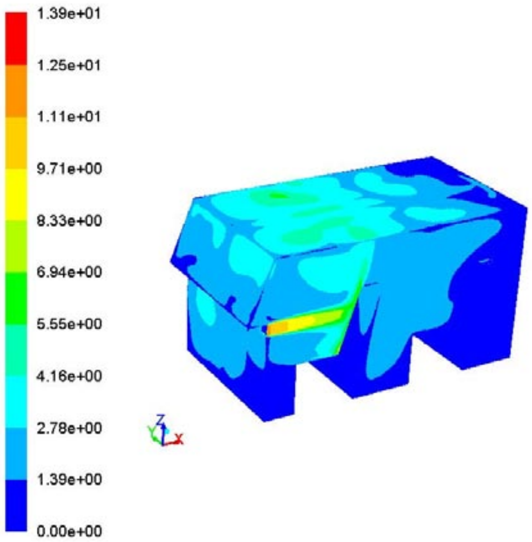

(g)

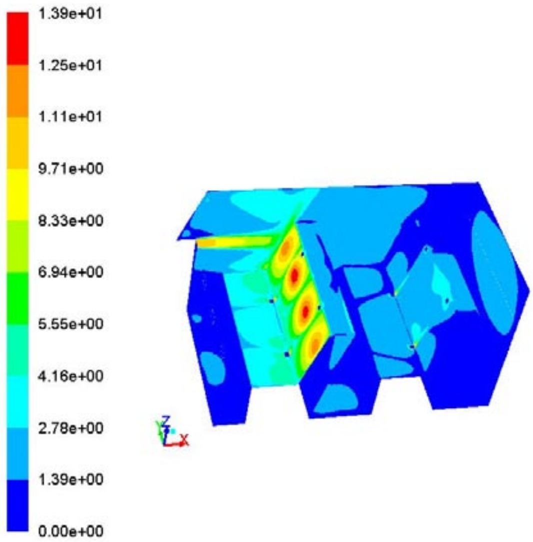

(h)

Fig.5-2 (a)(b) Pressure (Pa) view of whole cabin; (c)(d) Temperature (K) view of whole cabin; (e)(f) Total heat surface flux (W/m^2) of whole cabin; (g)(h) Surface heat transfer coefficient (W/m^2-K) of whole cabin

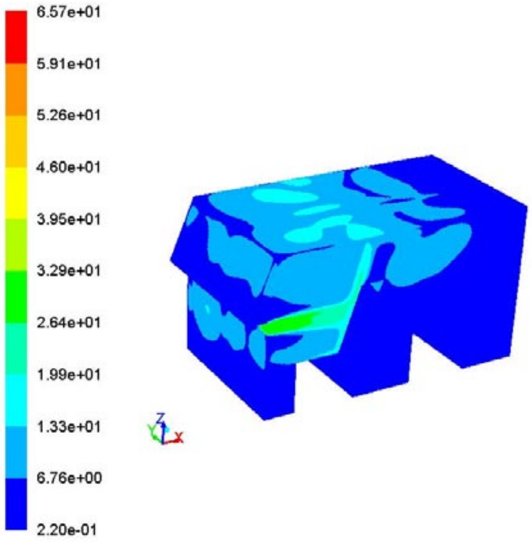
6.57e+01
5.91e+01
5.26e+01
4.60e+01
3.95e+01
3.29e+01
2.64e+01
1.99e+01
1.33e+01
6.76e+00
2.20e-01

(a)

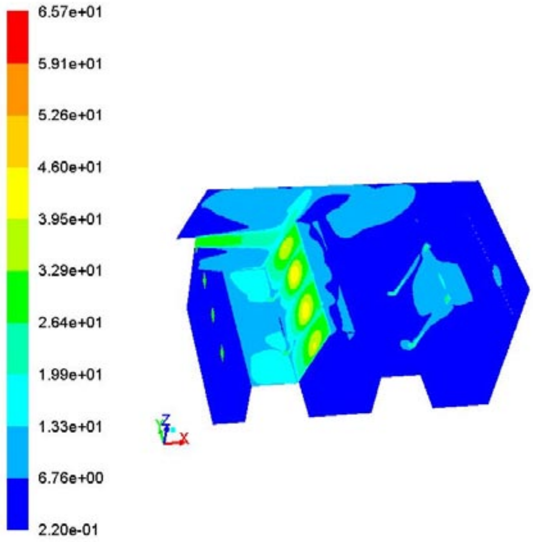
6.57e+01
5.91e+01
5.26e+01
4.60e+01
3.95e+01
3.29e+01
2.64e+01
1.99e+01
1.33e+01
6.76e+00
2.20e-01

(b)

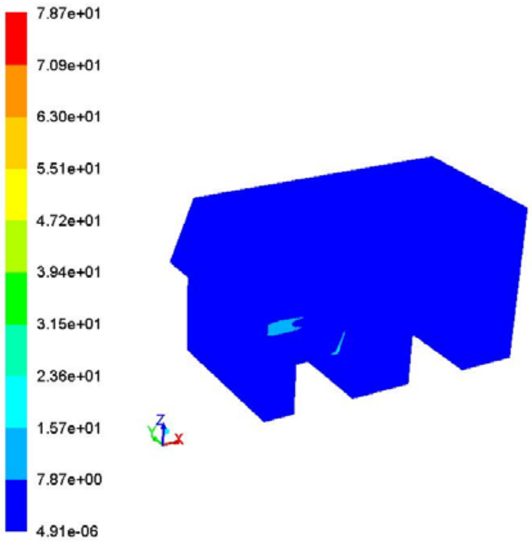
7.87e+01
7.09e+01
6.30e+01
5.51e+01
4.72e+01
3.94e+01
3.15e+01
2.36e+01
1.57e+01
7.87e+00
4.91e-06

(c)

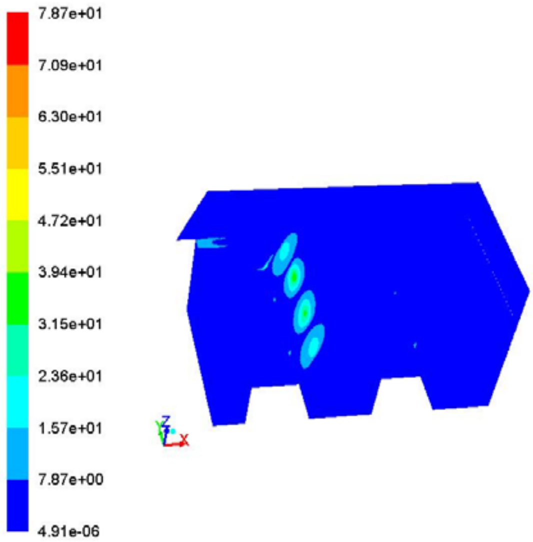
7.87e+01
7.09e+01
6.30e+01
5.51e+01
4.72e+01
3.94e+01
3.15e+01
2.36e+01
1.57e+01
7.87e+00
4.91e-06

(d)

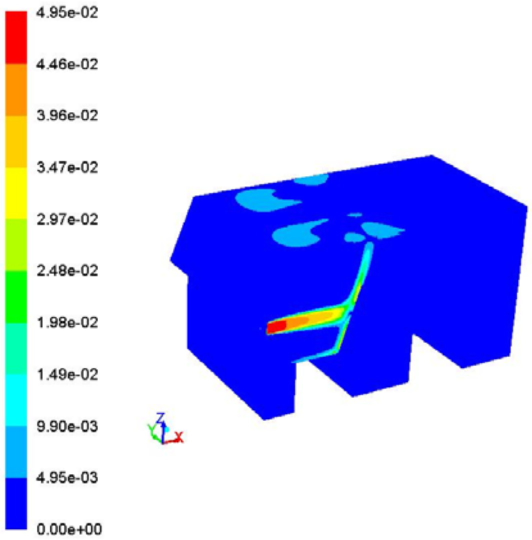

(e)

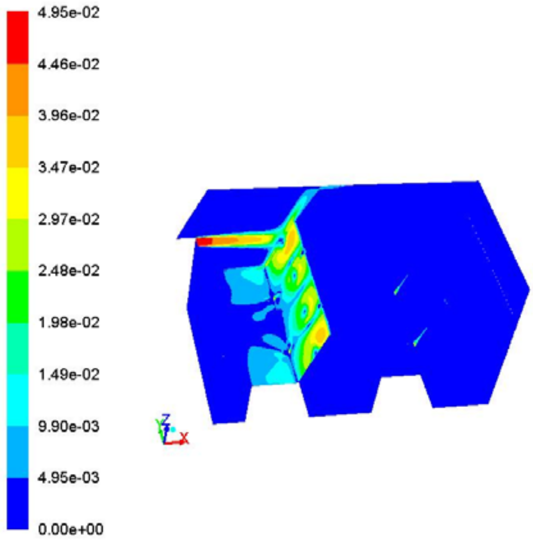

(f)

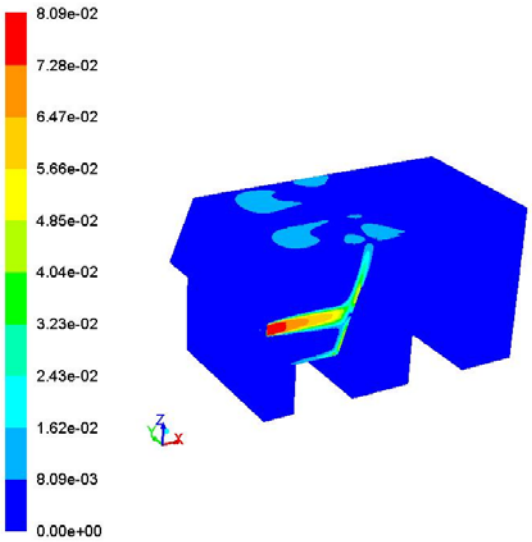

(g)

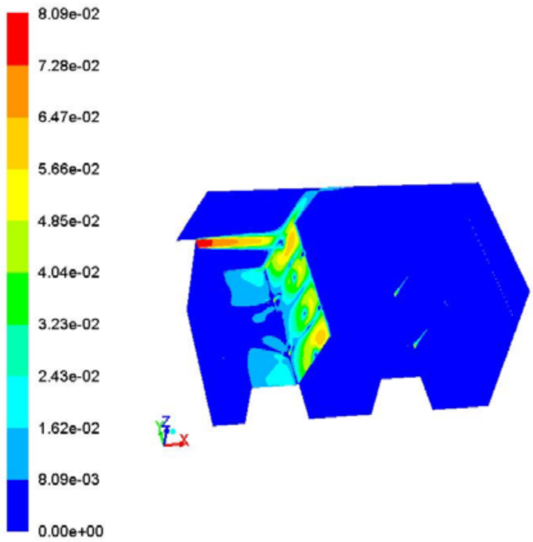

(h)

Fig.5-3 (a)(b) Turbulent intensity (%) of whole cabin; (c)(d) Turbulent dissipation rate (m^2/s^3) of whole cabin ; (e)(f) Wall shell stress (Pa) of whole cabin; (g)(h) Skin friction coefficient of whole cabin

5.3.2 Heat flow calculation

The total heat of cabin obtained from environment of outside can be calculated by using the heat flow rate to multiply by the simulation time when this modified personal air conditioning is working. According to the heat flow reports of simulation results, the total heat transfer rate at each wall surface between ambient and vehicle cabin can be seen in the Table 5-3. Through the calculation, the whole cabin has got heat 97.8 W after 15 minutes, which is much smaller than last chapter. When temperature of cabin is adjusted to the normal room temperature, the energy consumption of air conditioning would be calculated according to this basic data.

From this table, it can be easy to see that the heat transfer rate almost has no obvious change during the simulation time. The minus value of total energy shows the heat transfer from cabin to ambient by air conditioning. It is obvious to see that there is much more heat moving out from cabin through the surface of outlet3 than other surface because there outlet has bigger size and higher wind velocity than other two.

The mass flow rate is given in the Table 3. According to the boundary setting, the mass flow rate keeps in a stable condition. Therefore, these values almost remain as the set temperature without any variation in the simulation time of 15 minutes.

Table 5-3 Total heat transfer rate at different direction (W)

Time / Wall surface	5 minutes	10 minutes	15 minutes
Back	31.27	31.98	32.84
Bottom	19.02	21.05	20.28
Chair1	161.79	160.60	161.31
Chair2	61.74	62.15	61.04
Front	63.53	63.27	63.12
Left	77.52	76.57	76.87
Outlet1	-78.47	-78.47	-78.47
Outlet2	-78.47	-78.47	-78.47
Outlet3	-466.48	-466.48	-466.48
Right	78.27	78.10	77.72
Roof	136.18	136.45	136.75
Net	5.89	6.76	6.52

Table 5-4 Mass flow rate at different direction (kg/s)

Wall surface	Mass flow rate
Back	0
Bottom	0
Chair1	0
Chair2	0
Front	0
Left	0
Outlet1	0.025
Outlet2	0.025
Outlet3	0.15
Right	0
Roof	0
Net	0.20

5.3.3 Energy consumption calculation

The energy consumption of this modified air conditioning system can be evaluated by the experiment results of last chapter. In this chapter, the simulation defines 6 personal air conditioning systems in the vehicle cabin. Therefore, according to the electric power consumption of 84.7 W for one system, the overall energy consumption for a car can be calculated and it only takes 508.2 W after 15 minutes of working time.

Compared with the traditional one, this modified air conditioning system has obvious improvement in the term of saving energy. However, this simulation has been just carried on in 15 minutes so that the value is not accurate enough to predict the energy consumption in longer time.

5.4 Conclusion

Based on the old system, a new modified personal air conditioning system was proposed and demonstrated by numerical simulation in this chapter. The new system added four more wind outlets in the front of vehicle. These four outlets have bigger size than the original vents on the chairs so that they can provide cooling wind for all the passengers. Based on the simplified 3-D vehicle model, a numerical study was carried on to analyze the air flow and heat transfer characteristics of cabin under the cooling action of this new type system during 15 minutes. Also, the energy consumption of this system was evaluated according to the previous experimental data. The following results are obtained:

(a). The simulation results show that the front wind outlets can work well to bring much cooling and put in motion the heat exchange among the cabin under the assist of wind outlets in chairs.

(b). Under the condition of low energy-consumption, the temperature of cabin can be dropped by about 5 ℃ and it just consumed electronic power about 508.2 W for the whole vehicle in 15 minutes.

(c). The results of numerical calculation are consistent with the anticipation of before and it indicates that this new personal air conditioning system can be used well in the future electric vehicle.

References

[1] ANSYS Inc. Fluent Manuals.

[2] Richard C. Farmer, Gary C.Cheng, Yen-Sen Chen, Ralph W. Pike: Computational Transport Phenomena for Engineering Analyses, USA, 2009.

[3] Massoud Kaviany: Essentials of Heat Heat Transfer, USA, 2011.

[4] J. Kohler, Numerical Calculation of the Distribution of Temperature and Heat Flux in Buses under the Influence of the Vehicle Air-conditioning System, ASHRAE Trans, 96 (1): 432–446, 1990.

[5] S. Mostafa Ghiaasiaan: Convective Heat and Mas Transfer, USA, 2011.

[6] J.S. Brown, B.W. Jones, New transient passenger thermal comfort model, in: Proceedings of the 1997 International Congress and Exposition, ISSN: 1054-6693, SAE, Detroit, MI, USA, 1997.

Chapter 6
Conclusions and Further Work

6.1 Conclusions

This thesis has presented a new personal air conditioning system applied to the automobile instead of the traditional air conditioning to resolve the high energy consumption problem. This new system has used the Peltier module and fan motor as a temperature regulation device which is installed under the chair to provide thermal comfort for each passenger individually. Based on this new air conditioning system, using the representative car of Honda Company as the model, the thermal properties of vehicle cabin have been analyzed and energy consumption has been calculated through the ways of experiment and numerical simulation, the following conclusions can be obtained:

1. The temperature of the sealed cabin tends to increase and becomes high along with time when parking under the sunshine. But the inner temperature has little difference. The highest value is concentrated at the front side close to the windshield and the region of front row has higher temperature than back row after 15 minutes. The air is essentially stagnant with low velocity and the central compartment has much lower air velocity than other regions of the cabin.

2. Under the save energy model, the traditional air conditioning system can make the cabin temperature turn to stable after 5 minutes and the oil consumed by air conditioning can help car to drive more 2 km in one hour. But the temperature gradient is terrible and the rear row has higher temperature than front row. Therefore, it cannot make all the passengers feel comfortable in the vehicle.

3. The personal air conditioning system has been validated that it can be used in the electric vehicle instead of the traditional one. This system can make passengers feel comfortable after 4 minutes and the cabin temperature turns to stable after 5 minutes. All apparatuses can just only consume electric power 338.8 W. However, this system cannot make all the body feel comfortable. Except the area of chairs, the temperature of entire cabin has almost no change during 15 minutes. It indicates that this personal air conditioning system cannot be just only installed in the chair because it cannot provide enough cooling wind to cut down the heat flow from ambient.

4. The modified personal air conditioning system has been validated that it can refrigerate the most area of cabin not only local action. The front wind outlets can work well to bring much cooling and put in motion the heat exchange among the cabin under the assist of wind outlets in chairs. Under the condition of low energy-consumption, the temperature of cabin can be dropped by about 5 ℃ and it just consumed electronic power about 508.2 W for the whole vehicle in 15 minutes. The results of numerical calculation are consistent with the anticipation of before and it indicates that this new personal air conditioning system can be used well in the future electric vehicle.

6.2 Further Work

There are plenty of works worth a further consideration including the calculating of cooling load at each part of cabin, experimental validation using real car and engine exhaust heat recovery.

6.2.1 Cooling load calculation of cabin

Cooling load calculation at each part of cabin plays an important role in the design of air conditioning system, which can help to control the cooling quantity to make passengers feel more comfort. The cooling load calculation includes the heat transfer through the non-transparent car shell, glass window, engine room, passengers themselves and inner car facilities.

Non-transparent car shell includes car side, car roof and floor. The solar first reaches at the shell and is easy to be absorbed by them. Therefore, the material characteristic of shell and equipment of the cabin are important for thermal calculation. Glass windows have poor heat storage performance and the heat gain can be easy to be obtained directly from the temperature difference between cabin and outside. The engine of driving car will emit out plenty of heat, which can conduct the temperature difference up to 30 ℃ between engine room and cabin. This temperature difference can be calculated by the steady-state heat transfer formula of multi-wall. The heat caused by passenger has related with the sex, ages, dress, labor intensity and environmental conditions (temperature and humidity) and some other factors. Different people have different heat dissipation. But it can be simplified by considering the ratio of various types of passengers. The heat gain from interior lighting and devices stays a stabilized situation and it can be set as a constant value, which is easy to be calculated [1-3].

6.2.2 Experimental validation

In this thesis, the modified air conditioning system was proposed and analyzed by numerical simulation. However, for practical application, the experimental validation is necessary.

The experiment can be done by using a real vehicle with this modified personal air condition system like chapter 2 to chapter 4. Under the same condition with simulation, the variation of temperature during 15 minutes is tested at different location of cabin to make a comparison with simulation results. Also, the energy consumption is measured to make a comparison with traditional air conditioning system.

6.2.3 Engine exhaust heat recovery

When car driving the engine will emit out a lot of heat, which can be recycle to conduct the air conditioning system.

The exhaust heat from engine is a terrible problem, which can make the cabin temperature rise up to 60 ℃. If it can be recycle for the vehicle the problem could be resolved. Also, the modified air conditioning system just need lower electronic power to work, which means the low energy of exhaust heat from engine is enough to drive it.

Combined the exhaust heat recovery, this air conditioning system will not need any other power to work, which will be a great improvement for automobile [4].

References

[1] K. Yamamoto, W.R. Hill, Interior flow visualization of a small pick-up truck and A/C Feeling Estimate, SAE International Congress and Exposition, ISSN: 0148-7191, SAE, Detroit, MI, USA, 1990.

[2] Chao-Hsin Lin, A. Lelli Michael, Han Taeyoung, J. Niemiec Robert, C. Hammond Dean, Jr., Experimental and computational study of cooling in a simplified GM-10 passenger compartment, International Congress and Exposition, ISSN:0148-7191, SAE, Detroit, MI, USA, 1991.

[3] J. Kohler, Numerical calculation of the distribution of temperature and heat flux in buses under the influence of the vehicle air-conditioning system, ASHRAE Trans. 96 (1): 432–446, 1990.

[4] M. Hagino, J. Hara, Development of a method for predicting comfortable airflow in the passenger compartment. Worldwide Passenger Car Conference and Exposition, ISSN: 0148-7191, SAE, Dearborn, MI, USA, 1992.

Acknowledge

At the finish of this thesis, I am very sincerely to express my deepest gratitude to all those who have lent me hands in the course of my writing this thesis.

First of all, I am heartily thankful to Professor Katsuta, my supervisor of my Ph.D. study, who guided me throughout my writing of this thesis. He carefully revised the whole draft and offered great and precious criticism. His academic standards have made me extremely admire.

And, I would like to express my sincere gratitude to Professor Kusaka, Professor Sekiya and Professor Onoda, who have given me so much useful advices in the process of paper review.

Then, I am deeply indebted to Master students Anamizu tomohiro and Ishimine shotaro, who offered me experimental data and information on time and help me to resolve plenty of problems.

Also, I would like to thank those teachers and working staff especially those in the School of Environment and Energy Engineering. Without their help, it is hard to finish my study and this thesis.

Finally, my thanks would go to my parents, little sister and friends. Their sustained encouragements gave me a long-term power to persist in my study and carrying out this thesis.

ZENG YANG

Tokyo 2013.11

List of publication

[1] Yang Zeng, Masafumi Katsuta. "Numerical Simulation of Heat Flow in a Vehicle Cabin", *Advanced Materials Research*, Vols. 602-604, pp. 1769-1774. (2013)

[2] Yang Zeng, Masafumi Katsuta, Tomohiro Anamizu. "Numerical Simulation of Heat Flow in a Vehicle Cabin Using the Personal Air Conditioning System", *Advanced Materials Research*, Vols. 694-697, pp. 755-761 (2013).

[3] Yang Zeng, ZENG Xin-An, PENG Li. "Influence of Ice-temperature Storage on the Quality of Litchi Juice". *Food Science and Technology,* Vol.35,No.04,pp.51-55(2010)

[4] Yang Zeng, ZENG Xin-an. "Influence of Freeze Concentration Treatment on the Quality of Litchi Juice", *Food Science*, Vol.31,No.03,pp.91-95(2010)

[5] Yang Zeng, ZENG Xin-An, PENG Li. "Study on Rapid Measurement of the Freezing Point of Litchi Juice with Various Contents". *Science and Technology of Food Industry*, Vol. 30 (6), pp. 118-122. (2009)

[6] Yang Zeng, HUANG Kai, ZENG Xin-an. "Stability Research of the Nutritional Peanut Milk by Water Boiling". *Food Science and Technology*, Vol.34 (3), pp.89-91(2009).

[7] Yang Zeng, ZENG Xin-an, PENG Li. "Influence of Concentration on the Growth of Ice Crystals while Freezing Litchi Juice", *Food and Fermentation Industries*, Vol.35, No.11, pp.36-39 (2009)

[8]Yang Zeng, ZENG Xin-an. Juice Freeze Concentration Technology and Equipment by Cooperating with Ultrasound, Application No:200910192373.2

[9] ZHANG Xiaofeng, DAI Ya, XU Mingxi, Yang Zeng. "Characterization of the Cigarette Smoke Particulate with Scanning Election Microscope". *Modern Scientific Instruments*, Vol.1, pp.27-29(2008)

[10] Yang Zeng, ZENG Xin-an, PENG Li, HANG Zhong. Freeze Concentration of Lychee Juice and Evaluation of Products Quality. Revise.